CHANNEL ASSIGNMENT SCHEMES IN CELLULAR COMMUNICATION SYSTEMS

by

PETER H. J. CHONG

B.Eng. (Electrical Engineering), Technical University of Nova Scotia, Canada, 1993

M.A.Sc., The University of British Columbia, Canada, 1996

A THESIS SUBMITTED IN PARTIAL FULFILLMENT OF

THE REQUIREMENTS FOR THE DEGREE OF

DOCTOR OF PHILOSOPHY

in

THE FACULTY OF GRADUATE STUDIES

DEPARTMENT OF ELECTRICAL AND COMPUTER ENGINEERING

We accept this thesis as conforming

to the required standard

THE UNIVERSITY OF BRITISH COLUMBIA

September 2000

Department of Electrical and Computer Engineering

The University of British Columbia
Vancouver, Canada

Date Sept 28, 2000

Abstract

The demand for mobile cellular communications services is increasing rapidly. Much effort is being devoted to the design of techniques to support a large number of users in a limited radio frequency band. One approach is to employ a more efficient channel assignment scheme. Packet-switching will also be used in future mobile cellular systems since it is expected that most of the traffic sources carried in future systems will be very bursty due to the combination of voice, data and video communications services.

The objective of this thesis is to study various types of channel assignment methods, fixed channel assignment (FCA) and dynamic channel assignment (DCA), in order to improve capacity in *current* or *future* cellular systems. The performance of a Reuse Partitioning (RP) system using FCA (FRP) with and without handoff is first analyzed. RP uses n cluster sizes instead of one as used in a conventional FCA system. It is shown that the performance of FCA can be substantially improved by using RP. With mobile users, the capacity improvement of FRP relative to FCA decreases with the average handoff rate. A new distributed DCA scheme, known as DCA with interference information (DCA-WI), is then proposed and studied by computer simulation. In this scheme, a base station in a cell assigns a channel to a call based on the channel information in its neighboring cells. It is shown that DCA-WI outperforms previous channel assignment schemes in both uniform and nonuniform traffic distributions.

To support bursty traffic, FCA and DCA schemes used in conjunction with packet reservation multiple access (PRMA) and PRMA++ in a packet-switched voice cellular system are studied. Two measurement-based protocols, DCA/PRMA and DCA/PRMA++, are studied to cope with the highly unpredictable and time-varying microcellular environment. A channel

reassignment technique is suggested which reduces the number of packets lost due to out-of-cell interference during speech talkspurts. It is shown that channel reassignment can improve the performance significantly.

Table of Contents

List of Tables

List of Figures

Acknowledgment

I would like to thank my supervisor, Dr. C. Leung, for his continuous guidance and encouragement throughout my graduate studies in UBC. I feel also grateful to my industrial supervisor, Mr. W. Warner from Datum Telegraphic Inc., for his guidance and advice throughout the research work for this thesis. I would also like to thank Dr. A. Wright to provide me the financial support from Datum Telegraphic Inc.

This work was supported in part by the Natural Sciences and Engineering Research Council of Canada under Grant OGP0001731, by a British Columbia Science Council GREAT award and by a grant from Datum Telegraphic Inc.

Chapter 1 Introduction

The first-generation cellular communication systems, which used analog technology with FM modulation, were introduced in the world since early 1980s. Examples of first-generation cellular communication systems [1] include North American *advanced mobile phone service* (AMPS), British *total access communication system* (TACS), Japanese *mobile communication systems* (MCS) and Scandinavian *nordic mobile telephone* system (NMT). They all employ frequency division multiple access (FDMA) as the air interface access scheme.

Second-generation cellular communication systems, which use digital technology and more efficient air interface multiple access schemes (e.g., time division multiple access, TDMA, or code division multiple access, CDMA), were introduced in the early 1990's. The demand for mobile cellular communications services, i.e., voice, facsimile or low-bit-rate data, is increasing rapidly. The number of mobile subscribers worldwide is estimated to be currently around 400 million. By the year 2010, the Universal Mobile Telecommunications System (UMTS) Forum expects that the number of subscribers worldwide to be around 1800 million [2], with most of the growth occurring in Asia. In contrast, the number of subscribers for the first-generation systems is starting to decrease. The most common second-generation systems include the TDMA Global System for Mobile Communications (GSM) in Europe, TDMA IS-54/IS-136 and CDMA IS-95 in United States and TDMA Personal Digital Cellular (PDC) system in Japan [1].

Currently, the market demand for advanced wireless communications services [2], i.e., high-bit-rate data, multimedia or Internet, is very high. Research, standardization and development activities are ongoing worldwide for third-generation cellular communication systems - International Mobile Telecommunications in the year 2000 (IMT-2000) [3]-[7]. In Europe, IMT-

2000 is referred to as Universal Mobile Telecommunications System (UMTS). The major improved capabilities of third-generation cellular communication systems include:

- higher cellular system capacity, i.e., offered traffic load per unit area per unit bandwidth that can be supported at some minimum quality of service
- a wide range of services from voice to very high data rate services to support mobile multimedia applications
- evolution from mature second-generation systems in order to achieve the goal of universal access and global roaming
- support for circuit- and packet-oriented services

Three major proposals have been submitted and considered for the IMT-2000 [6]. They can be classified into two categories based on their air interface multiple access methods, i.e., wideband TDMA, namely Advanced TDMA (ATDMA), and wideband CDMA (WCDMA) [7]. One of the three proposals, Universal Wireless Communications (UWC-136), is proposed from TR45.3 in the United States and based on wideband TDMA for IS-136 evolution towards a third generation system. UWC-136 consists of a 30 kHz carrier for voice or low-speed data, a 200 kHz carrier for high-speed data, and a 1.6 MHz wideband TDMA carrier for very high-speed data, about 2Mb/s, in an indoor environment. The other two proposals are based on WCDMA. One of them is named UMTS Terrestrial Radio Access (UTRA) from Europe. In the paired band, the frequency-division duplexing (FDD) mode is employed whereas in the unpaired band, the time-division duplexing (TDD) is used, namely TD-CDMA. A WCDMA proposal similar to UTRA has been submitted by Japan. The other WCDMA proposal is cdma2000, which is backwards compatible with IS-95. Both WCDMA proposals use 5 MHz bandwidth for transmission. Details

of the above three major proposals and all other proposals for IMT-2000 are available in [5]-[7].

1.1 Motivations and Contributions of the Thesis

One of the major limitations to supporting a large number of users is the limited availability of radio frequency spectrum. Methods for increasing cellular system capacity are of great interest. One solution is to reduce the cell size (e.g., microcells or picocells) [8]-[9] which results in an increase in the number of base stations (BS's) and hence cost. It also increases the number of handoffs in a cellular system [10]. An alternative approach is to use a more efficient channel assignment scheme. There are two basic methods for assigning channels for use in cells. One is the conventional and widely used fixed channel assignment (FCA) [11] scheme, in which each cell is assigned a set of nominal channels (NC's) permanently. The second method is dynamic channel assignment (DCA) [12], in which all channels are potentially available in all cells, i.e., any channel can be used by any cell as long as a certain level of signal-to-interference power ratio (SIR) is maintained.

Two types of DCA schemes, cell-based and measurement-based schemes, have been studied for cellular communication systems. The applications of these two schemes for cellular communication systems are discussed in [13]. Cell-based DCA schemes are applicable in high-mobility systems and macrocellular systems in which shadow fading changes rapidly. Measurement-based DCA schemes may be used in low-mobility systems, fixed wireless access systems, packet-switched systems and microcellular systems. For third-generation cellular communication systems, ATDMA [7] and TD-CDMA [6], DCA schemes can be applied to improve the performance and have been studied in [14]-[15].

The objective of this thesis is to study different types of channel assignment methods

(FCA, cell-based and measurement-based DCA) in order to increase capacity in *current* or *future* cellular systems. Three topics are examined:

1. Analysis of the system performance of an enhanced FCA scheme which uses Reuse Partitioning (RP) [16], with and without handoff.
2. Design and evaluation of a new cell-based distributed DCA algorithm to enhance cellular system capacity.
3. Evaluation of measurement-based distributed DCA algorithms for packet voice in packet-switched cellular systems.

In the following subsections, the motivations and contributions for each of the above three topics are presented.

1.1.1 Analysis of RP using FCA (FRP)

In a conventional cellular communication system using FCA, a single cluster size is used [11]. The aim is to achieve a minimum target SIR at any point in the cell. For a system which does not employ power control (assuming no fading), the received signal power for a mobile close to its BS is generally higher than that for a more distant mobile. As a consequence, the signal from a close mobile can tolerate a higher interference level and the channel reuse distance may be smaller. In RP [16], this characteristic is exploited to increase the system capacity. RP is implemented by dividing the cell into two or more concentric regions. Each region has a different cluster size (and therefore a different reuse distance) and is assigned a set of channels according to the FCA scheme. In this thesis, the performances of FRP for stationary and mobile users are analyzed.

1.1.1.1 Stationary Users

The basic RP with FCA system, which does not incorporate channel rearrangement, has been studied in [17]-[22]. In [17] and [18], the call blocking probability, P_B, of a 2-region RP system was studied via computer simulation. In [19], the authors use a 2-dimensional Markov chain to model the basic 2-region RP system. However, the Markov chain used in [19] actually corresponds to a 2-region RP system with single channel rearrangement. Since RP introduces an unevenness in the P_B values experienced in the inner and outer regions, a control policy that can balance the P_B experienced in the two regions is studied by computer simulation in [20]. A similar problem but with two classes of calls, narrowband and broadband, is studied in [21] using a linear programming approach. The above-mentioned studies considered only 2-region RP systems. A simplified model is used to estimate the average blocking probability, $P_{B,av}$, of an n-region RP system in [22]. In this simplified model, it is assumed that the number of mobiles in each region is an independent Poisson random variable [23] and the channels are assigned so as to minimize $P_{B,av}$. This model tends to underestimate $P_{B,av}$ as shown in Chapter 3.

In this thesis, we develop a Markov chain model to examine the basic n-region RP scheme [16], with no channel rearrangement (NCR), assuming stationary users. The resulting n-dimensional Markov chain is used to evaluate the P_B in each region. A *modified* n-region RP scheme with optimal channel rearrangement (OCR) is then introduced. The basic idea in the modified scheme is to reallocate on-going calls to channels, whenever a channel is released due to a call completion, in such a way as to minimize $P_{B,av}$. A Markov chain model is obtained for the n-region RP scheme with OCR which yields a closed-form expression for P_B. The performance differences among the NCR, OCR and single channel rearrangement (SCR) alternatives are studied as are the capacity gains obtainable with RP.

1.1.1.2 Mobile Users

The call blocking probability of FRP for *stationary* users has been examined in [17], [18] and [20] by computer simulation. They show that RP can increase the capacity compared to conventional FCA with a single reuse distance. Other studies of FRP assuming stationary users include [19], [21] and [24]. The performance of an overlapping coverage scheme with RP for mobile users has been studied in [26]. However, since the inner and outer RP regions correspond to the non-overlapping and overlapping regions respectively, the effect of RP cannot be separated from that of overlapping.

In this thesis, an analytical traffic model is developed to study the impact of mobile users on the new call blocking probability, P_b, and the call dropping probability, P_d, in a 2-region FRP system [27]. This model allows P_b and P_d to be evaluated numerically. The influence of user speed and cell size on P_b and P_d is investigated. An approximate model which allows derivation of closed-form expressions for P_b and P_d in certain cases is also presented. The effect of a cutoff priority scheme for handoff calls on capacity is considered. The numerical results are compared with the simulation results for various mobility models.

1.1.2 A New Distributed DCA Scheme

FCA has been shown to be effective in systems with high and constant loads. However, it is inefficient in handling traffic which varies in time and space. More recently, some channel borrowing assignment (CBA) schemes [28]-[31] have been shown to perform better than FCA even at heavy traffic loads. In CBA, all available channels in the system are assigned to cells as NC's as in FCA. However, channels can be borrowed from neighboring cells according to some algorithm as long as the co-channel interference constraints are satisfied. One advantage of these

CBA schemes is that they do not require system-wide information.

A recent CBA [30] was shown to outperform those in [28] and [29]. The scheme uses an *impact-based borrowing* strategy which results in the least impact on the cells which have the same NC set as the lender cell and which are within the minimum cochannel reuse distance, D, of the borrower cell. However, the effect on the availability of channels in the *interfering* cells which are within D of the borrower cell, considered in [62] and [80], is not considered in the impact-based borrowing technique.

In this thesis, a new channel assignment scheme, DCA with interference information (DCA-WI), is proposed. Unlike many CBA schemes, pre-allocation of channels to cells is not required in DCA-WI. Each cell assigns a channel to a call from the central pool. DCA-WI is a distributed DCA scheme in which the channel to be used in a cell is selected by the local BS based on channel information in its neighboring cells. The channel assignment strategy attempts to minimize the effect on the availability of channels in interfering cells. Intra-cell channel reassignment and inter-cell single channel reassignment are used to further reduce the call blocking probability. The simulation results show that DCA-WI yields a lower blocking probability than previous channel assignment schemes [28]-[30]. Its performance is close to that of idealized DCA using Clique Packing method [32] and [33].

1.1.3 Measurement-based DCA for a Packet Voice System

In the above studies, a cell-based model (described in Chapter 2), which assumes a regular cell pattern for channel assignment and reuse, is used to study the performance of channel assignment schemes. If smaller cells are used to improve the capacity, it would be difficult to plan a regular pattern for channel reuse and the unpredictable traffic densities will result in inefficient

channel usage. For an example of a FCA system, once a frequency plan is adopted for a given service area, it will also be difficult to make future changes, e.g., adding or removing a base station (BS) or frequency spectrum. Besides, smaller cells will increase the number of handoffs and hence signalling information exchanges between BS's. One solution to these problems is to adopt a measurement-based dynamic channel assignment (DCA) strategy [34]-[38] which can adapt to the changing and unpredictable environment. In measurement-based DCA, the channel assignment decision is made dynamically by the local BS and/or (mobile or fixed) user terminal (UT) based on real-time measurements. Therefore, fewer signalling exchanges between BS's are required.

As the demand for wireless multimedia services grows, third-generation cellular communication systems will be required to support a combination of voice, data and video communications. It is expected that the sources of traffic will be very bursty. Current circuit-switched systems [41] which establish a dedicated connection for the entire duration of a call become inefficient because the time to set-up the connection might be longer than the transmission time of the data. An alternative is packet switching [41] in which no dedicated circuits are used. This technique can increase the spectrum efficiency for voice communications since speech consists of a sequence of talkspurt and silence periods which allows statistical multiplexing of many different speech users. The channel is reserved only during talkspurt period, leaving it free for use by other users during silence periods. Packet Reservation Multiple Access (PRMA) [42]-[45] is a simple and efficient multiple access scheme which allows for integration of speech and data packet transmissions. It is implemented on the uplink whereas on the downlink the BS broadcasts to all UT's. A modified version of PRMA, namely PRMA++, was proposed in [46]-[49].

For convenience, we will refer to the use of FCA with PRMA and PRMA++ as FCA/PRMA and FCA/PRMA++ and the use of DCA with PRMA and PRMA++ as DCA/PRMA and DCA/PRMA++. The performance of FCA/PRMA and FCA/PRMA++ schemes in a cellular environment has been studied in [50]-[52] but no direct comparison between FCA/PRMA and FCA/PRMA++ was made. The use of a channel segregation algorithm, which does not require power measurement at the UT or BS, with PRMA was proposed in [50]-[51]. It was found that the performance of this DCA/PRMA scheme is about the same as FCA/PRMA. This is because once a talkspurt starts experiencing high interference, the packets in the rest of the talkspurt will most likely be lost leading to very poor performance.

DCA/PRMA++ schemes based on power measurements being available at the BS have been proposed in [52]-[53]. In [52] one of the performance measures used is the probability that a talkspurt is interfered with, i.e., the SIR of any one of the packets falls below a certain threshold value, SIR_{min}. Based on this measurement, it was found that the performance of DCA/PRMA++ is about the same as that of FCA/PRMA++. However, a packet with an SIR below SIR_{min} is considered as a lost packet. Hence, the number of lost packets during a talkspurt should also be considered.

The performances of FCA/PRMA, FCA/PRMA++, DCA/PRMA and DCA/PRMA++ schemes for packet-switched cellular systems with and without channel reassignment (CR) are studied for packet voice in the uplink traffic. The performance for the downlink traffic which does not require contention has been studied in [38]-[40]. The CR technique, which has not been considered in the above studies [50]-[53], makes use of power measurements performed at the BS. It is found that the number of lost packets can be greatly reduced using CR. The DCA strate-

gies used in this study are Autonomous Reuse Partitioning (ARP) [34], Least Interfered Channel (LIC), [36]-[37] and [65], and Most Interfered Channel (MIC) [36].

1.2 Outline of the Thesis

The thesis is organized as follows: Chapter 2 contains a brief review of material related to topics discussed in later chapters. The analysis of n-region FRP system for stationary users is presented in Chapter 3. The results are compared with conventional FCA. In Chapter 4, we present the analysis of 2-region FRP system for mobile users. The results are verified with simulation in different mobility models. A new cell-based DCA scheme which uses interference information is proposed in Chapter 5. Results are given for both uniform and non-uniform traffic distributions and compared with those of some previously proposed DCA schemes. The performances of various measurement-based DCA algorithms with PRMA and PRMA++ schemes for packet voice system are studied in Chapter 6. The results for FCA/PRMA and FCA/PRMA++ are also provided for comparison. The main conclusions of the research work are summarized in Chapter 7 and some suggestions for future work are provided.

Chapter 2 Background

In this chapter, a brief review of previous studies related to the work presented in this thesis is provided. The two channel assignment schemes, FCA and DCA, are first described, followed by the basic idea of RP. Some of the previous work for cell- and measurement-based DCA are reviewed. System descriptions and operations of PRMA, PRMA++, DCA with PRMA and DCA with PRMA++ schemes are provided.

2.1 FCA and DCA

Two basic channel assignment methods, Fixed Channel Assignment (FCA) [11] and Dynamic Channel Assignment (DCA) [12], can be used for assigning channels in cells. In FCA, the entire service area is divided into clusters, each cluster consisting of N (cluster size) cells. The available channels in the system are divided into N nominal channel sets (NCS's), and one of the N NCS's is assigned permanently to each of the N cells in each cluster. The nominal channels (NC's) in each cell are used only for its local calls. The same set of channels can be reused with acceptable interference in cells which are at least a certain distance, D, apart. Frequency reuse is the main concept in cellular systems [11]. The cells allowed to use the same channels are called co-channel cells. The distance, D, is called the minimum co-channel reuse distance. The selection of N is determined by the co-channel reuse distance. The co-channel reuse distance depends on the minimum allowable SIR in the system. The number of NC's in each cell can be assigned uniformly or nonuniformly. The uniform channel assignment allocates the same number of channels to each cell regardless of the traffic load in the cells. The nonuniform channel assignment allocates NC's to each cell depending on the expected traffic load in each cell [54]. FCA has been shown to be effective in systems with high load and constant load. However, it is inefficient

in handling traffic which varies in time or space. To improve the efficiency, dynamic channel assignment (DCA) schemes have been proposed.

DCA is currently used in the digital European cordless telecommunication (DECT) system and cordless telephones known as CT2 [55]. In a DCA scheme, all channels are potentially available to all cells, i.e., any channel can be used by any cell as long as a certain level of SIR is maintained. Various DCA schemes have been proposed [28]-[30], [34]-[37] and [56]-[67]. They can be divided into *centralized* and *distributed* DCA schemes. In centralized DCA (CDCA) [56]-[60], a channel is assigned to a call by a central controller with global information. It has been shown that a CDCA scheme proposed in [59], called maximum packing (MP) DCA, uses the minimum number of channels required to carry the existing calls in each cell. In MP DCA, if a new call finds no free channel in a cell, the call is not blocked unless the system finds no possible reallocation of channels to accommodate the call. However, this scheme requires a high degree of centralization. In distributed DCA (DDCA) [28]-[30], [34]-[37] and [61]-[67], channel assignment decisions are made by either mobiles or their BS's without requiring global information. Therefore, the algorithms can be simpler and decisions can be made faster. DDCA schemes are more effective in microcellular systems because faster decisions are required in microcellular systems due to more frequent handoffs.

Two different models are used to study the performance of DCA schemes, namely *cell-based* DCA and *measurement-based* DCA [12]-[13]. The cell-based DCA schemes can be considered as traffic adaptation DCA schemes because the channel assignment in a cell is based on the traffic changes within the cell's boundary and the channel information of that cell and other cells. In cell-based DCA [28]-[30], [56]-[61], it is assumed that (1) each cell has a well-defined

coverage area, e.g., a regular hexagonal cell pattern, (2) each BS in a cell assigns a channel to a mobile within the boundary of the cell, i.e., a mobile can access a channel from a cell if the mobile is located anywhere within the cell's boundary and (3) the same channel can be reused in other cells which are at least distance D apart. The distance, D, is obtained based on worst case assumptions about the mobile location and propagation conditions [68]. This fixed D value may be too pessimistic. In some cases, the same channel may be able to be reused in another cell which is less than D away because the amount of interference may be acceptable. The measurement-based DCA schemes [34]-[37] and [63]-[67] are more effective because they take the actual propagation and interference conditions into account. In measurement-based DCA schemes, mobiles/BS's measure the interference strengths to determine the usability of channels. These schemes are DDCA because a BS or a mobile uses local measurement to make a channel assignment.

2.2 Reuse Partitioning using Fixed Channel Assignment

Reuse partitioning (RP) [16], which uses multiple reuse distances, can further improve traffic performance with FCA or DCA. RP is implemented by dividing the cell into two or more concentric cells as shown in Figure 2.1. These partitions are associated with different cluster sizes or reuse distances.

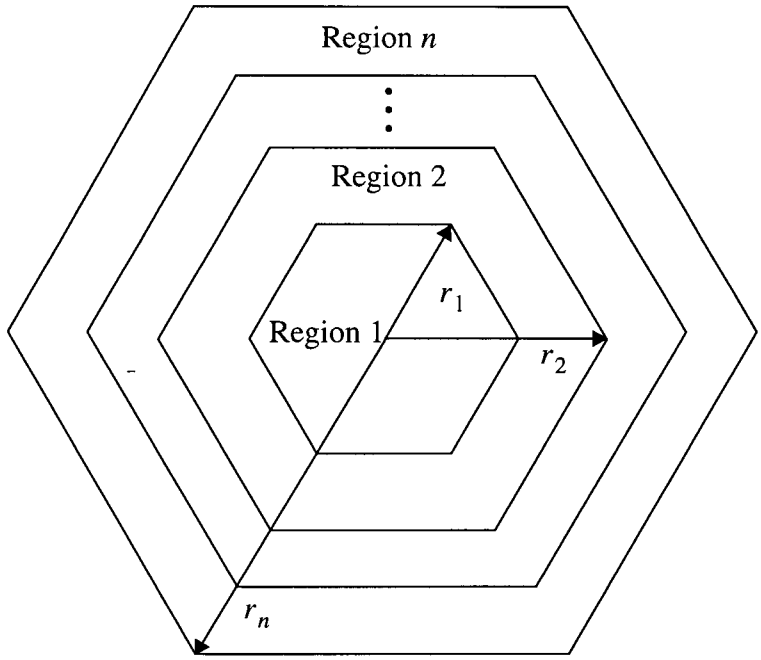

Figure 2.1 Cell reuse partitioning in a hexagonal cell.

For a conventional mobile cellular system with FCA [68] and [69], a cluster size of 7 is used. With RP, multiple cluster sizes can be used. An example of a two-region RP system is depicted in Figure 2.2. The cluster sizes N_A and N_B for the inner and outer regions are 3 and 7 respectively. Then, a set of NC's is assigned to each region. Since channels assigned to the inner region can be repeated more frequently than those assigned to the outer region, more channels can be assigned to a cell than in a conventional FCA system. It was shown [17] and [22] that a substantial increase in carried traffic can be achieved if the inner region calls can use (overflow into) the outer region channels. This can however result in unbalanced blocking to the subscribers in different regions. A control policy to address this problem is studied in [20] and [21].

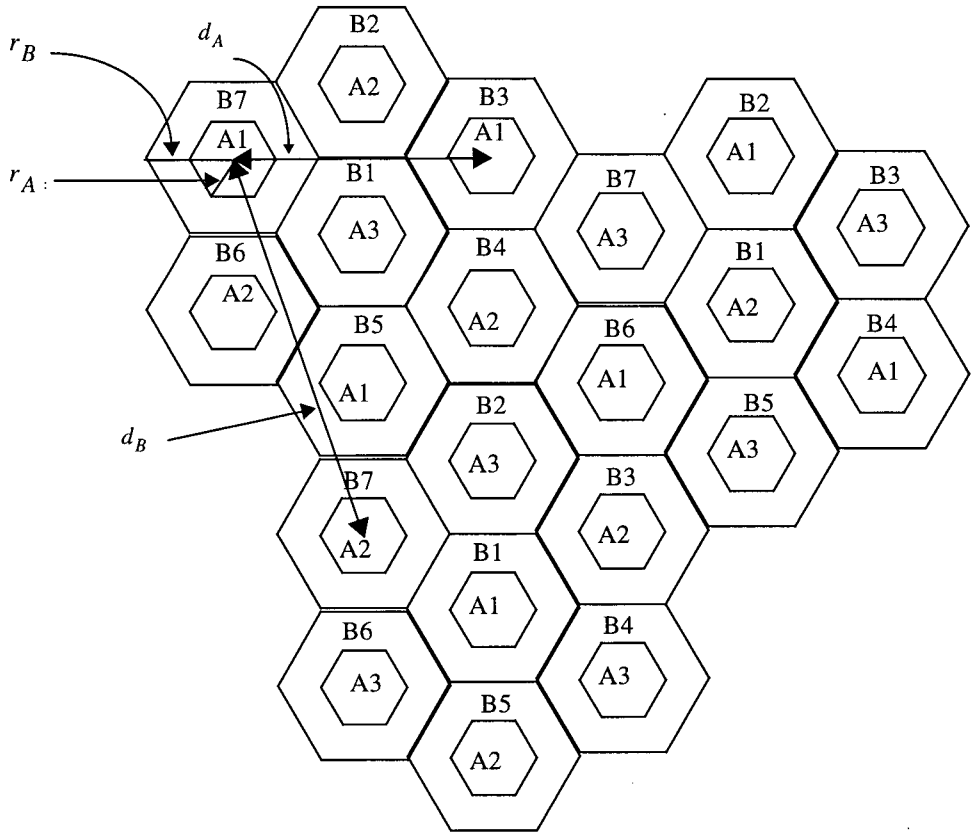

Figure 2.2 Cellular grid with reuse cluster sizes $N_A = 3$ and $N_B = 7$.

2.3 Cell-based DCA - Channel Borrowing Assignment

FCA is currently used in existing analog, AMPS [69], and digital, IS-54 [70], cellular systems. A disadvantage of FCA is that if a new call finds no free NC in its cell, the call is blocked even though there are NC's available in neighboring cells. This problem can be solved by using a DCA scheme such that a new call can use any free channel available in the system subject to co-channel interference constraints. Previous studies of DCA schemes [56]-[58] report that their performances are better than FCA at low to normal traffic loads, but at heavy traffic loads their performances are worse than FCA. The reason is that these DCA schemes provide a "short-term"

optimized channel assignment and the distance between any two cells using the same channel is normally larger than D. One type of cell-based DCA scheme, called channel borrowing assignment (CBA) [28]-[30] and [71]-[73], can have improved performance over FCA even at heavy traffic loads. In this section, some of the previous CBA schemes [28]-[30] and [71]-[73] are briefly reviewed. A comprehensive survey of other DCA schemes can be found in [12].

In CBA, all available channels are assigned to cells as NC's as in FCA [11], [54]. Channels can be borrowed from neighboring cells[1] based on some algorithm as long as the co-channel interference constraints are satisfied. CBA schemes in these papers are DDCA because they only require the local and surrounding cell[2] information and each BS makes its own channel assignment decision.

In early CBA scheme [71], when a new call finds no free NC[3] available in its own cell **A**, the BS will assign a channel borrowed from a neighboring cell **B** with the largest borrowable channel set which is not currently used by any of cell **A**'s *interfering* cells. The interfering cells of cell **A** are the cells within distance D of cell **A**. If the borrowable channel set contains more than one channel, a channel is randomly chosen. Since the NC or borrowed channel is chosen randomly, the distance between co-channel cells is generally greater than D and the performance is degraded.

A better CBA scheme, called borrowing with channel-ordering (BCO) [72], is proposed to maintain the average co-channel reuse distance minimum. In BCO, all NC's assigned to a cell are

---

1 Only the cells in the first tier are considered to be neighboring cells.

2 Surrounding cells can be any cells from the first, second, third,..., tier.

3 A free channel in a cell means that the channel is not used in the cell or its interfering cells so that it is available for use in the cell.

ordered. A new call will use the lowest numbered free NC from its cell **A**. If no free NC is found, the new call will borrow the highest numbered free NC from a neighboring cell **B** with the largest number of borrowable channels. A borrowable channel is a free channel in cell **B** and cell **B**'s nominal cells within distance D of cell **A**. Nominal cells are cells to which the same set of nominal channels are assigned. After cell **A** borrowing a channel, the borrowed channel is locked in cell **B** and cell **B**'s nominal cells within distance D of cell **A**. A channel being locked in cell **B** means that the channel cannot be used in cell **B** or be borrowed by a neighboring cell. For further packing the co-channel cells, channel reassignment is performed, i.e., reassignment of borrowed channel to NC, higher numbered NC to lower numbered NC or lower numbered borrowed channel to higher numbered borrowed channel from the lender cell.

An improved version of BCO is borrowing with directional channel-locking (BDCL) [28]. In BCO, when channel j is borrowed, channel j in the lender cell and its nominal cells within D of borrower cell are locked such that the channel j cannot be used in these cells locally or be borrowed by any of their neighboring cells. In fact, some of the neighboring cells of lender's nominal cells can borrow channel j if they are not within distance D of the borrower cell. Thus, BDCL allows channel j to be lent to some of the neighboring cells of the lender's nominal cells without violating the co-channel interference constraints. In other words, channel j in the lender's nominal cells is locked in certain direction. The rest of the procedures, such as channel ordering and channel reassignment, are as in BCO.

A more recent CBA scheme proposed by Chang, *et al.* [30] outperforms BDCL. In Chang's CBA, the NC's assigned to a cell are ordered. A new call will use the lowest numbered free NC from its own cell, say Cell **A**. If no free NC is available, the call will borrow a free NC

from a neighboring (lender) cell, say Cell **B**, using an *impact-based borrowing* strategy. Borrowing a channel from a neighboring cell, Cell **B**, has an impact on the nominal cells which are within D of the borrower cell, Cell **A**. The impact-based borrowing attempts to select a free channel from an neighboring cell which will have the least effect on its nominal cells which are within D of Cell **A**. If no free channel can be borrowed, a one-channel reassignment procedure is performed to release a locked channel[4], j, in cell **A** which is used by only one cell, the "locking" cell, Cell **C**, within distance D of the Cell **A**. The one-channel reassignment is to assign another free channel, k, to a call using the locked channel, j, in the locking cell, **C**. Therefore, channel j is released from Cell **C**. The locked channel, j, becomes available for use in Cell **A** and can be assigned to the new call. This scheme requires knowledge of the average traffic load in each cell in order to estimate the future channel availability rate.

In the above CBA schemes, channel locking is used to avoid violating the co-channel interference constraints. Another CBA called Channel Borrowing Without Locking (CBWL) is presented in [73]. In this scheme, a call with a borrowed channel reduces its transmission power and thus channel locking in other cells is not required. A disadvantage is that only users in a fraction of a cell area is allowed to borrow. This problem is solved by intra-cell channel reassignment.

2.4 Measurement-based DCA

In measurement-based DCA, channel assignment is based on signal strength measurements from mobiles or BS's which are used to estimate the SIR. A channel is assigned to a call if the estimated SIR of the channel is above the minimum acceptable SIR. Measurement-based

---

[4] Channel j is called a locked channel in cell i if channel j is used by any interfering cells of cell i.

DCA schemes have been proposed in [34]-[37] and [63]-[67]. The simplest scheme is to find the first channel which satisfies the minimum acceptable SIR level [63]. An improved version, called *Autonomous Reuse Partitioning* (ARP), is proposed in [34]. In ARP, all BS's have a list of ordered channels. When a call arrives, channels are viewed in the same order by all BS's, and the first channel which satisfies the minimum acceptable SIR level is assigned to the call. It is shown [34] that ARP can achieve "reuse partitioning" in that the lower numbered channels are reused at shorter distances. The lower numbered channels are assigned to the mobiles (close to their BS) with stronger received signal powers which can tolerate higher interference levels. In this scheme, BS's using the same channel are closely "packed" in order to support more traffic. One disadvantage is that this may cause many handoffs. Other schemes, least interfered channel (LIC) [36]-[37], flexible reuse (FRU) [64] or maximum signal-to-interference ratio (MSIR) [65], which selects a channel with highest SIR which is above the minimum acceptable SIR level, is studied to reduce the number of handoffs at the expense of an increased call blocking probability [65]. It is shown in [37] that the performance of ARP is better than that of LIC and ARP requires fewer SIR measurements to be performed. In [66], [67] and [81], fast algorithms to select channels are proposed. In these papers, each BS generates an ordered list of channels. The order of the channel is updated based on the history of how each channel was used in a cell. The lowest numbered channel has the highest priority to be used. A BS attempts to select the lowest numbered channel if the channel satisfies the minimum acceptable SIR level.

2.5 Packet Reservation Multiple Access (PRMA) and PRMA++

In this section, the frame structure for PRMA and PRMA++ protocols are described. The system operations for the two protocols are explained for speech users only.

2.5.1 PRMA

Packet Reservation Multiple Access (PRMA), proposed by Goodman, *et al.* [42] and [44], is a simple and efficient multiple access scheme which allows for integration of speech and data packet transmissions [43] and [45] for a local wireless network. This technique takes advantage of the nature of speech, which consists of a sequence of talkspurt and silence periods, to increase the spectrum efficiency by allowing statistical multiplexing of many different speech users. PRMA can be considered as a combination of slotted "reservation" ALOHA protocol [74] and time division multiple access (TDMA) [41]. One of its main features is a "*listen-before-you-send*" procedure which can properly control the user terminals (UT's) to send their message without collision. It is implemented on the uplink channel whereas on the downlink channel the BS broadcasts all the information to all UT's.

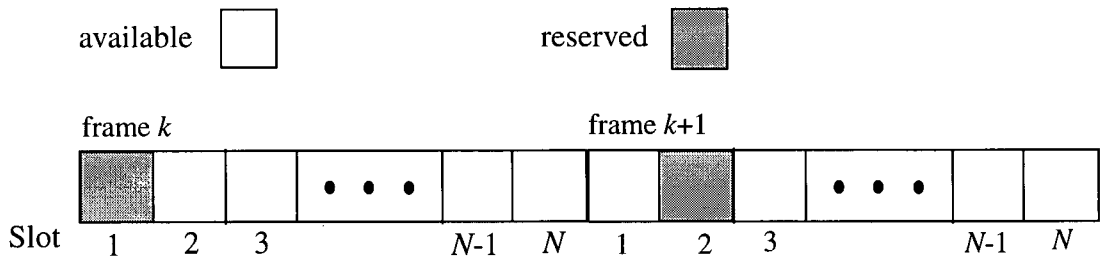

Figure 2.3 Frame structure of PRMA.

In PRMA, the uplink channel is divided into N time slots, each of duration of T_s, which are organized into frames as shown in Figure 2.3. The UT's recognize each time slot as "available" or "reserved" according to the feedback message broadcast from the BS at the end of each frame. With the implementation of speech activity detector (SAD), speech packets are only

generated within talkspurts at the frame rate and buffered at the UT for transmission during talkspurts. Each packet requires only one slot per frame. No packets are generated within a silence period.

When the first packet of a new talkspurt is generated at the UT, the UT contends for a reservation by sending the first packet in a "available" slot with a permission probability, p. If no other UT's contend for the same "available" slot, the reservation is successful. Then, the BS acknowledges the UT about its success on the downlink traffic at the end of the slot [42]-[45]. That slot is then reserved for the UT for the whole duration of its talkspurt. All other UT's are also informed about the status of the slot from the broadcast acknowledgment in the downlink traffic. Therefore, no other UT's attempt to send their packets in this "reserved" slot and the UT can get uncontended use of that slot. The UT continues to send its packets during the talkspurt in the "reserved" slot in subsequent frames until the talkspurt ends. When a BS detects no traffic on a previously "reserved" slot, it marks the status of the slot to be "available". At the end of the slot, the BS broadcasts to all other UT's that the slot is now "available" for contention.

If the contention is unsuccessful (due to packet collision), the UT attempts to send the same packet in the next "available" slot with probability p. Real-time speech packets can tolerate only a small delivery delay. Speech packets which have waited in the UT buffer for longer than the maximum acceptable delay, d_{max}, are dropped. The packet delay is measured from the time the packet is generated at the UT to the time the packet is successfully received at the BS. The value of d_{max} is usually set to be twice the frame time [42] and [43]. Hence, packets are dropped only at the beginning of the talkspurts during the contention process; this results in "front end clipping"[42].

In PRMA, one of the system design parameters is probability p. A low value of p reduces the chance of collision, but increases the waiting time for UT's to send their packets to contend for reservation which increases the number of dropped packets. If p is too high, it will increase the risk of collisions during the contention process so that the number of dropped packets will also be increased due to the excessive delay from the collision resolution process. The optimum value of p for different operating conditions is studied in [44].

2.5.2 PRMA++

PRMA++ [46]-[49] is a modified version of PRMA developed within the advanced TDMA (ATDMA) project [46] in Europe. In PRMA, any time slot can be used to contend for a reservation as long as the time slot is "available" on the uplink channel. The BS is required to broadcast the outcome of the contention corresponding to each of the "available" time slots on the downlink channel. In PRMA++, the uplink channel is divided into r reservation slots (R-slots) and $N - r$ information slots (I-slots) as shown in Figure 2.4. The R-slots are equally spaced in the frame. The UT's can send the access contention packets only in the R-slots for a reservation. The information packets can be sent to the I-slots. The downlink channel is similar to the uplink channel except that the R-slots are replaced by corresponding acknowledgment slots (A-slots) with a few slots delay as shown in Figure 2.4. The outcome of the contention process for each R-slot is acknowledged by its corresponding A-slot from the BS. There is also one fast acknowledgment slot and one fast paging slot in the uplink and downlink channel respectively which are not shown in Figure 2.4. Details of PRMA++ can be found in [48].

When a UT with a new talkspurt has generated the first packet, it sends the first packet in the first R-slot with probability p. If the contention on this R-slot is successful, the BS acknowl-

edges the UT in the corresponding A-slot on the downlink channel. If an I-slot is available, the BS makes an I-slot assignment for the UT and informs the UT of the assignment within the same corresponding A-slot. If no free I-slot is available, the reservation request from the UT is inserted into a *BS FIFO* buffer. Then, the BS will assign an I-slot to the first UT in the BS buffer when an I-slot becomes free. For a UT with an I-slot assignment, the UT sends its packets within the talkspurt in the "reserved" I-slot in all subsequent frames so that the UT has uncontended use of that I-slot. When the talkspurt ends, the BS releases the I-slot and reallocates it to another UT for use in the next transmission frame. If the contention on this R-slot is unsuccessful, the UT sends its packet in the next R-slot with probability p. The UT knows the contention has failed if no acknowledgment is received in the corresponding A-slot on the downlink channel.

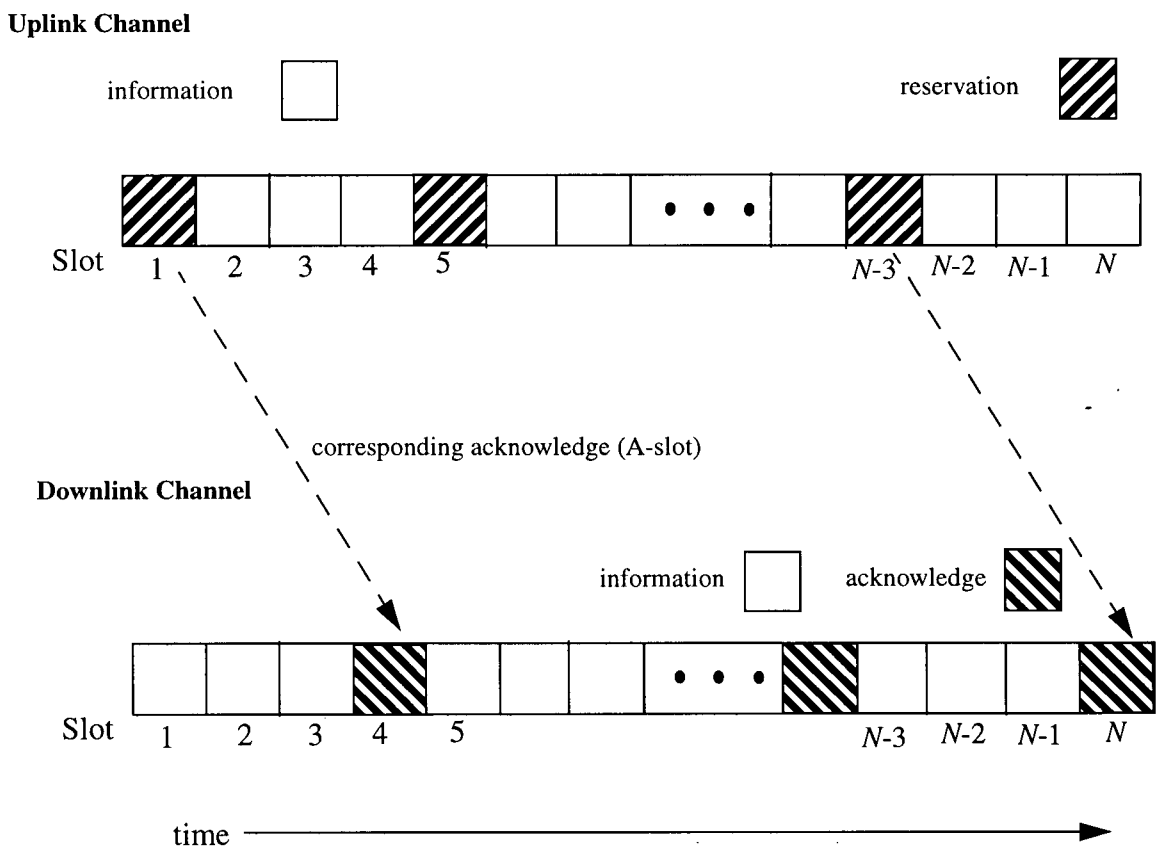

Figure 2.4 Frame structure of PRMA++.

In PRMA++, if the packets wait longer than d_{max} in the UT's buffer before the contention is successful, the packets are dropped. This packet loss phenomenon is similar to that in PRMA. After successful contention, a UT might not be assigned an I-slot immediately depending on the availability of the I-slots. If so, packets will be dropped if they wait in the UT buffer longer than d_{max}. The system design parameters p and r in PRMA++ have been studied in [46]-[49].

The advantages of PRMA++ over PRMA are discussed in [48]. However, no direct comparison between PRMA and PRMA++ has been made.

2.6 Previous Work on DCA/PRMA and DCA/PRMA++

The above-mentioned PRMA and PRMA++ studies do not consider co-channel interference. As long as a time slot has been reserved for a talkspurt, the packets will not be interfered with or dropped during that talkspurt period. However, in a cellular environment, the packets may be interfered with and dropped during a talkspurt even when transmitted in a "reserved" time slot due to co-channel interference from users in neighboring cells using the same time slot. Studies of both measurement-based and cell-based PRMA and PRMA++ in a cellular environment have been presented in [50]-[53] and [75]-[79]. These studies are considered for uplink traffic. In this section, the frame structure and system operation of DCA/PRMA [50]-[51] and DCA/PRMA++ [52]-[53] are described.

2.6.1 DCA/PRMA

In [50]-[51], the authors show that the power measurement technique used in current circuit-switched systems (e.g., GSM) at the BS/UT does not provide a fast and reliable quality measurement for packet-switched systems. Instead, the channel segregation algorithm [66] is

chosen as the DCA scheme used with the PRMA protocol in packet-switched systems. This algorithm assigns channels to calls based on previous performances of each channel and does not require real-time power measurement.

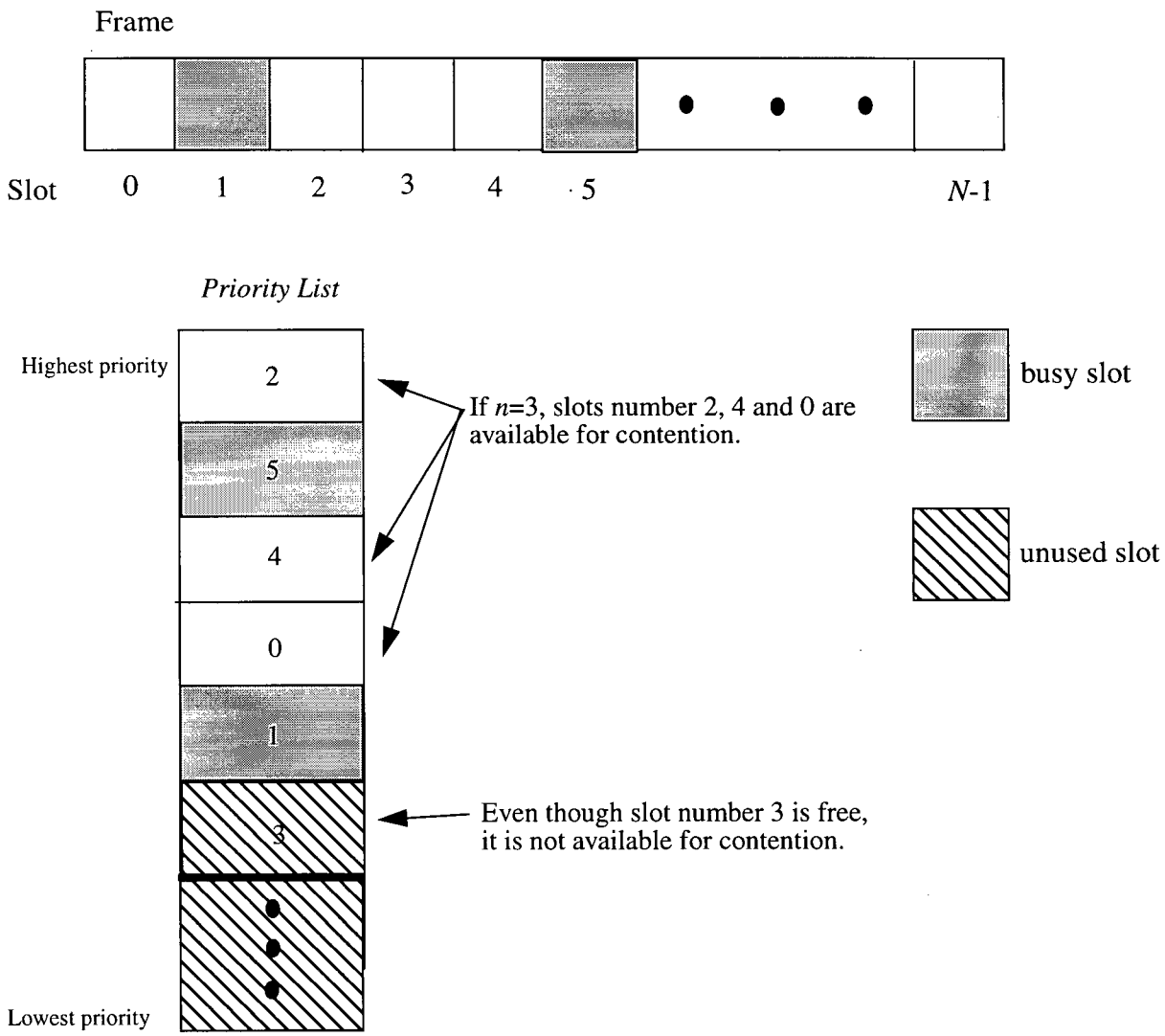

Figure 2.5 Channel segregation for PRMA system.

The frame structure and the procedure are depicted in Figure 2.5. Each BS creates its own priority list for all the time slots on a frame by frame basis and broadcasts the list to all its UT's.

Among all these free time slots, only a number, n, of time slots with highest priority are available for UT's to contend for a reservation. All other free time slots are considered as "unused". For example, in Figure 2.5, since $n = 3$, only slots number 2, 4 and 0 are available for contention. Even though slot number 3 is free, it cannot be used for contention. The order of each time slot in the list is formed according to the previous contention results in the contention process and the conversation quality during the current talkspurt. The hope is that a free time slot with higher priority in the list will provide a higher probability of successful contention and better speech quality.

When a UT has packets to send during a talkspurt, it sends the first packet to the first "available" time slot for contention. If it is successful, the time slot is reserved for the UT to transmit the rest of its packets in subsequent frames until the talkspurt ends. Otherwise, it will attempt to send the same packet in the next "available" time slot with permission probability, p, for contention. A packet will be dropped at the beginning of a talkspurt if it waits in the UT for longer than d_{max}. A packet will be lost within a talkspurt during the transmission in a "reserved" time slot, if it is interfered with, i.e., its SIR falls below a certain threshold value, SIR_{min}, due to co-channel interference.

The system design parameters for this scheme are p and n. A performance comparison between this scheme and FCA/PRMA is reported in [50]-[51] and shown to be about the same. The conclusion is that even though the performance of DCA/PRMA is close to that of FCA/PRMA, DCA/PRMA does not require frequency planning and can adapt to traffic fluctuations.

2.6.2 DCA/PRMA++

In a DCA/PRMA++ system [52] with M carriers and N time slots, there are a total of

$M \times N$ slots available in each cell. These are divided into r reservation slots (R-slots), which are used exclusively for contention, and $M \times N - r$ information slots (I-slots), which can be either "available" or "reserved" as shown in Figure 2.6. The R-slots are evenly placed in the M carriers. For example, if there are M R-slots, then each carrier has one R-slot at the beginning of a frame as shown in Figure 2.6. Two DCA algorithms are studied in [52], which are based on SIR measurement and a modified channel segregation algorithm to that used in [51].

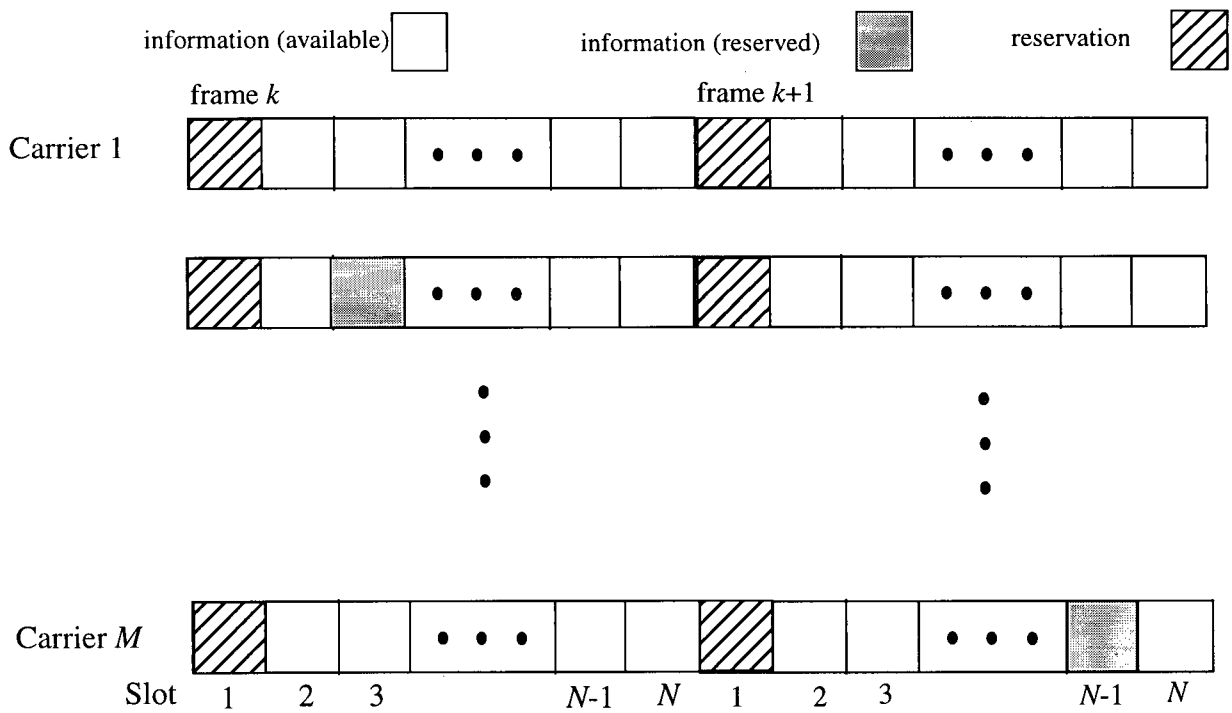

Figure 2.6 Frame structure of DCA/PRMA++.

A UT with a talkspurt sends the first packet in an R-slot on one of the M carriers. If the contention is successful, the BS assigns an "available" I-slot for the UT based on the particular DCA algorithm. If the contention fails, the UT tries the next R-slot on one of the M carriers. It was found that the performance of DCA/PRMA++ is comparable with that of FCA/PRMA++.

A similar DCA/PRMA++ is proposed in [53], in which minislots within the R-slot are used to improve the performance. The DCA algorithm used is ARP [34]. No comparison with FCA/PRMA++ is given. However, the performance will be improved, at least compared to DCA/PRMA++ without minislots, since the number of collisions can be reduced due to the use of minislots.

Chapter 3 Analysis of RP using FCA for Stationary Users

In this chapter, the performance of n-region reuse partitioning (RP) using fixed channel assignment (FCA), hereafter referred to FRP, for stationary users with no channel rearrangement (NCR) [16], single channel rearrangement (SCR) and optimal channel rearrangement (OCR) is analyzed. The basic idea behind channel rearrangement is to reallocate on-going calls using higher-numbered region channels to lower-numbered region channels, whenever a channel is released due to a call completion, in order to minimize the average blocking probability, $P_{B,av}$. The FRP systems with NCR and OCR can be represented by an n-dimensional Markov chain from which the blocking probability in each region can be obtained numerically.

The rest of the chapter is organized as follows. In Section 3.1 we describe the Markov model used for analyzing the n-region RP system using FCA. In Section 3.2 we present the analysis for n-region RP with NCR, OCR and SCR. Numerical results are presented and discussed in Section 3.3. The numerical results are also compared with the simulation results for slowly moving MS's.

3.1 System Model

In the design of a cellular system, it is convenient to divide the service coverage area into hexagonal cells, each of radius r_n. For a conventional FCA cellular system, a single cluster size, N_n, of 7 is commonly used. With RP, let the cluster size for region i, $1 \le i \le n$, be denoted by N_i and the radius of concentric hexagon i be denoted by r_i, as shown in Figure 2.1.

With a reuse cluster size of N_i, we have [11]

$$\frac{d_i}{r_n} = \sqrt{3N_i}\,, \quad i = 1, \ldots, n, \tag{3.1}$$

where d_i is the reuse distance associated with region i. In order to equalize the SIR's of mobile stations (MS's) close to the n region boundaries, we need

$$\frac{d_i}{r_i} = \sqrt{3N_n}\,, \quad i = 1, \ldots, n. \tag{3.2}$$

From (3.1) and (3.2), it follows that

$$\left(\frac{r_i}{r_n}\right)^2 = \frac{N_i}{N_n}. \tag{3.3}$$

An MS is served by the base station of the cell it is currently located in. We assume that the MS's move slowly enough that handoff issues can be neglected. This assumption is verified by comparing results from our analysis with simulation results obtained for slowly moving MS's and different mobility models [82]-[83]. An important example in which "MS's" can be considered stationary is a personal access communications system [90]. Calls are assumed to be uniformly distributed over the service area and arrive according to a Poisson process with per cell arrival rate, λ. The call arrival rate in region i of a cell can then be expressed as

$$\lambda_i = \lambda\left(\frac{r_i^2 - r_{i-1}^2}{r_n^2}\right), \tag{3.4}$$

where $r_0 = 0$. An arriving call which cannot be assigned a channel is blocked and departs the system, i.e. a blocked calls cleared model is assumed. Call durations are exponentially distributed with a mean of $1/\mu$. The offered traffic (in Erlangs) to MS's located in region i of a cell is defined as $\rho_i = \lambda_i/\mu$. Let C_i be the number of channels allocated to region i (hereafter referred to as region i channels) in each cell and $C = \sum_{i=1}^{n} C_i$ be the total number of channels available in

a cell. If a total of m channels are available to the system, we have

$$\sum_{i=1}^{n} N_i C_i \leq m. \tag{3.5}$$

3.2 Blocking Probability with RP

The evaluation of the blocking probability, $P_{B,i}$, for region i for various RP schemes is discussed in this section. In an RP scheme with no overflow, a call originating from or destined for an MS located in region i (hereafter referred to as a region i call) can *only* use one of the C_i region i channels. If all region i channels are busy, the call is blocked. Then, $P_{B,i}$ can be obtained using the Erlang B formula with C_i channels [25] and the average blocking probability, $P_{B,av}$, is given by

$$P_{B,av} = \sum_{i=1}^{n} \frac{\lambda_i}{\lambda} P_{B,i}. \tag{3.6}$$

We next consider RP schemes with overflow and different channel rearrangement algorithms.

3.2.1 RP With No Channel Rearrangement (RP-NCR)

In RP-NCR, a region i call is assigned, if possible, to an unused region i channel. If all region i channels are busy, an attempt is made to assign an unused channel from region $i+1, i+2, \ldots, n$ in this order. If no such unused channel is found, the call is blocked. Thus, region i calls can overflow into higher-numbered region j, $j > i$, channels.

A 2-region RP-NCR system can be represented by a two-dimensional Markov chain as shown in Figure 3.1. Each node represents a state (x_1, x_2) where x_i, $i = 1, 2$, is the number of

region i channels used. Since there are C_1 and C_2 channels allocated to regions 1 and 2 respectively, the set of allowable states is

$$S = \{(x_1, x_2) | 0 \le x_1 \le C_1, 0 \le x_2 \le C_2\}. \tag{3.7}$$

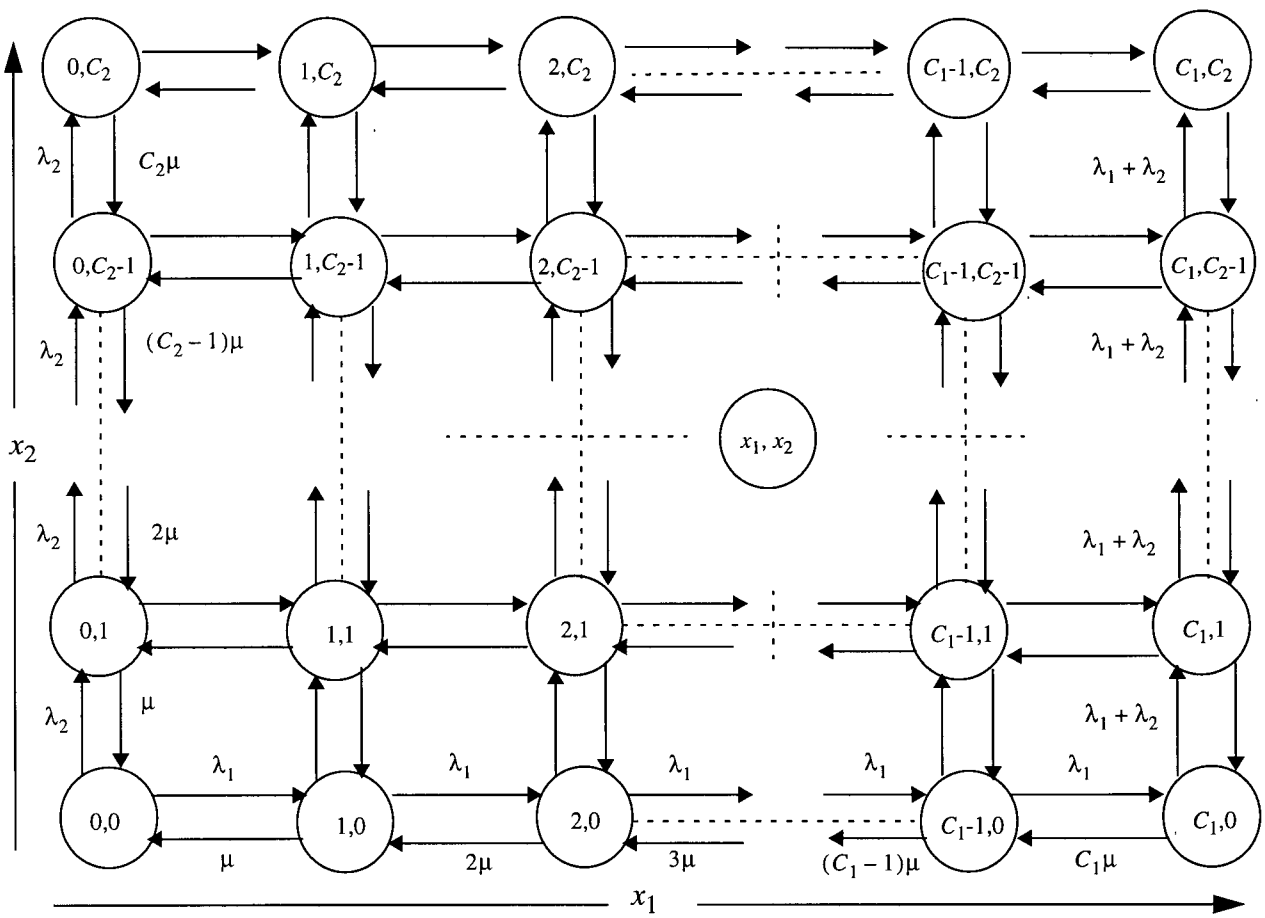

Figure 3.1 State-transition-rate diagram for a 2-region RP system with no channel rearrangement; $x_i, i = 1, 2$ denotes the number of region i channels used.

An assignment of a region 1 call to a region 1 channel corresponds to a transition from the current node to the node to its right with rate λ_1. If all region 1 channels are busy, a region 1 call can be assigned to a region 2 channel as shown by an upward rightmost transition with rate λ_1,

i.e. from nodes $(C_1, 0), (C_1, 1), \ldots, (C_1, C_2 - 1)$, in Figure 3.1. An arriving region 2 call can only be assigned to a region 2 channel as shown by an upward transition with rate λ_2 from any node (x_1, x_2) with $0 \le x_1 \le C_1, 0 \le x_2 \le C_2 - 1$. In Figure 3.1, the rate for an upward transition from nodes $(C_1, 0), (C_1, 1), \ldots, (C_1, C_2 - 1)$ is therefore $\lambda_1 + \lambda_2$.

The steady-state probabilities, $\pi(x_1, x_2)$, can be obtained by solving the set of equations [85]

$$\Pi Q = 0 \tag{3.8}$$

and

$$\sum_{x_1 = 0}^{C_1} \sum_{x_2 = 0}^{C_2} \pi(x_1, x_2) = 1. \tag{3.9}$$

In (3.8), $\Pi = \left[\pi(0, 0), \pi(0, 1), \ldots, \pi(0, C_2), \pi(1, 0), \pi(1, 1), \ldots, \pi(x_1, x_2), \ldots, \pi(C_1, C_2)\right]$ and Q is a $(C_1 + 1)(C_2 + 1) \times (C_1 + 1)(C_2 + 1)$ matrix whose elements are transition *rates* and are given as follows:

$$\begin{aligned}
q_{(x_1, x_2), (x_1 + 1, x_2)} &= \lambda_1, && \text{for } x_1 \in \{0, 1, \ldots, C_1 - 1\}, x_2 \in \{0, 1, \ldots, C_2\} \\
q_{(x_1, x_2), (x_1, x_2 + 1)} &= \lambda_2, && \text{for } x_1 \in \{0, 1, \ldots, C_1 - 1\}, x_2 \in \{0, 1, \ldots, C_2 - 1\} \\
q_{(x_1, x_2), (x_1, x_2 + 1)} &= \lambda_1 + \lambda_2, && \text{for } x_1 = C_1, x_2 \in \{0, 1, \ldots, C_2 - 1\} \\
q_{(x_1, x_2), (x_1 - 1, x_2)} &= x_1 \mu, && \text{for } x_1 \in \{1, \ldots, C_1\}, x_2 \in \{0, 1, \ldots, C_2\} \\
q_{(x_1, x_2), (x_1, x_2 - 1)} &= x_2 \mu, && \text{for } x_1 \in \{0, 1, \ldots, C_1\}, x_2 \in \{1, \ldots, C_2\} \\
q_{(x_1, x_2), (x_1, x_2)} &= - \sum_{i = 0, i \ne x_1}^{C_1} \sum_{j = 0, j \ne x_2}^{C_2} q_{(x_1, x_2), (i, j)}, && \text{for } x_1 \in \{0, \ldots, C_1\}, x_2 \in \{0, \ldots, C_2\} \\
q_{(., .), (., .)} &= 0, && \text{otherwise.}
\end{aligned} \tag{3.10}$$

It can be seen from Figure 3.1 that the call blocking probability for region 1 is given by

$$P_{B,1} = \pi(C_1, C_2), \tag{3.11}$$

and the call blocking probability for region 2 is given by

$$P_{B,2} = \sum_{x_1 = 0}^{C_1} \pi(x_1, C_2). \tag{3.12}$$

For $n \geq 3$, the system can be described by an n-dimensional Markov chain with each state denoted by an n-tuple $(x_1, x_2, \ldots, x_n)$. The set of allowable states is now given by

$$S = \{(x_1, x_2, \ldots, x_n) | 0 \leq x_i \leq C_i, 1 \leq i \leq n\}. \tag{3.13}$$

The square transition matrix Q is of size $\prod_{i=1}^{n} (C_i + 1)$ with elements

$$\begin{aligned}
&(1):\ q_{(x_1, \ldots, x_i, \ldots, x_n), (x_1, \ldots, x_i + 1, \ldots, x_n)} = \lambda_i, \\
&\quad \text{for } x_{i-1} \in \{0, \ldots, C_{i-1} - 1\},\ x_i \in \{0, \ldots, C_i - 1\},\ x_j \in \{0, \ldots, C_j\},\ j \neq i, i-1 \\
&(2):\ q_{(x_1, \ldots, x_i, \ldots, x_n), (x_1, \ldots, x_i + 1, \ldots, x_n)} = \lambda_i + \sum_{\substack{j,\, 1 \leq j \leq i-1 \\ k = i-1}} \lambda_k, \\
&\text{for } x_{i-1} = C_{i-1}, x_{i-2} = C_{i-2}, \ldots, x_j = C_j, x_i \in \{0, \ldots, C_i - 1\}, x_{j-1} \in \{0, \ldots, C_{j-1} - 1\}, \\
&\quad x_k \in \{0, \ldots, C_k\} \text{ where } k \neq i, i-1, \ldots, j-1 \text{ and } 1 \leq j \leq i-1 \\
&(3):\ q_{(x_1, \ldots, x_i, \ldots, x_n), (x_1, \ldots, x_i - 1, \ldots, x_n)} = x_i \mu, \\
&\quad \text{for } x_i \in \{1, \ldots, C_i\}, x_j \in \{0, \ldots, C_j\}, j \neq i \\
&(4):\ q_{(x_1, \ldots, x_i, \ldots, x_n), (x_1, \ldots, x_i, \ldots, x_n)} = - \sum_{j_1 = 0, j_1 \neq x_1}^{C_1} \cdots \sum_{j_n = 0, j_n \neq x_n}^{C_n} q_{(x_1, \ldots, x_i, \ldots, x_n), (j_1, \ldots, j_i, \ldots, j_n)}, \\
&\quad \text{for } x_j \in \{0, \ldots, C_j\}, j = 1, \ldots, n \\
&(5):\ q_{(., ., \ldots, .), (., ., \ldots, .)} = 0, \text{ otherwise.}
\end{aligned} \tag{3.14}$$

The steady-state probabilities can be solved using the same procedure as for $n = 2$. The blocking probability for region i is the sum of the probabilities of states for which

$x_1 \le C_1, \ldots, x_{i-1} \le C_{i-1}, x_i = C_i, \ldots, x_n = C_n$, i.e.

$$P_{B,i} = \sum_{x_1=0}^{C_1} \cdots \sum_{x_{i-1}=0}^{C_{i-1}} \pi(x_1, \ldots, x_{i-1}, C_i, \ldots, C_n) . \tag{3.15}$$

The average call blocking probability, $P_{B,av}$, is given by (3.6).

3.2.2 RP With Optimal Channel Rearrangement (RP-OCR)

One drawback of RP-NCR is that when a region i channel is released due to a call completion, an on-going region $k, k \le i$, call using a higher region $j, j > i$, channel is not switched to the just released lower region i channel. The release of a region i channel allows calls from regions 1 to i to use the channel. However, by releasing a higher region j channel, calls from regions 1 to j (with $j > i$) are allowed to use the channel. Thus, calls from a larger set of regions can access the released channel. In order to reduce the average call blocking probability, we need to rearrange channels so as to release a channel belonging to as high a numbered region as possible.

Consider the following example of a 2-region RP scheme with channel rearrangement. Let α_{xy} denote a region x call using a region y channel. If a call, α_{11}, completes and releases a region 1 channel, then an on-going call, α_{12}, can be switched to the released region 1 channel. The released region 2 channel is now available for use by either a region 1 or a region 2 call.

Such a 2-region RP system with channel rearrangement can be represented by the two-dimensional Markov chain shown in Figure 3.2. The state of the system is described by the pair (x_1, x_2), where $x_i, i = 1, 2$, is the number of channels used by region i calls. Note that this meaning of x_i is different from that in Section 3.2.1. The maximum number of channels that is

available for use by region 1 calls is C since these calls can overflow into region 2 channels whereas the maximum number of channels available to region 2 calls is C_2. Since the number of channels in a cell is C, we must have $x_1 + x_2 \leq C$.

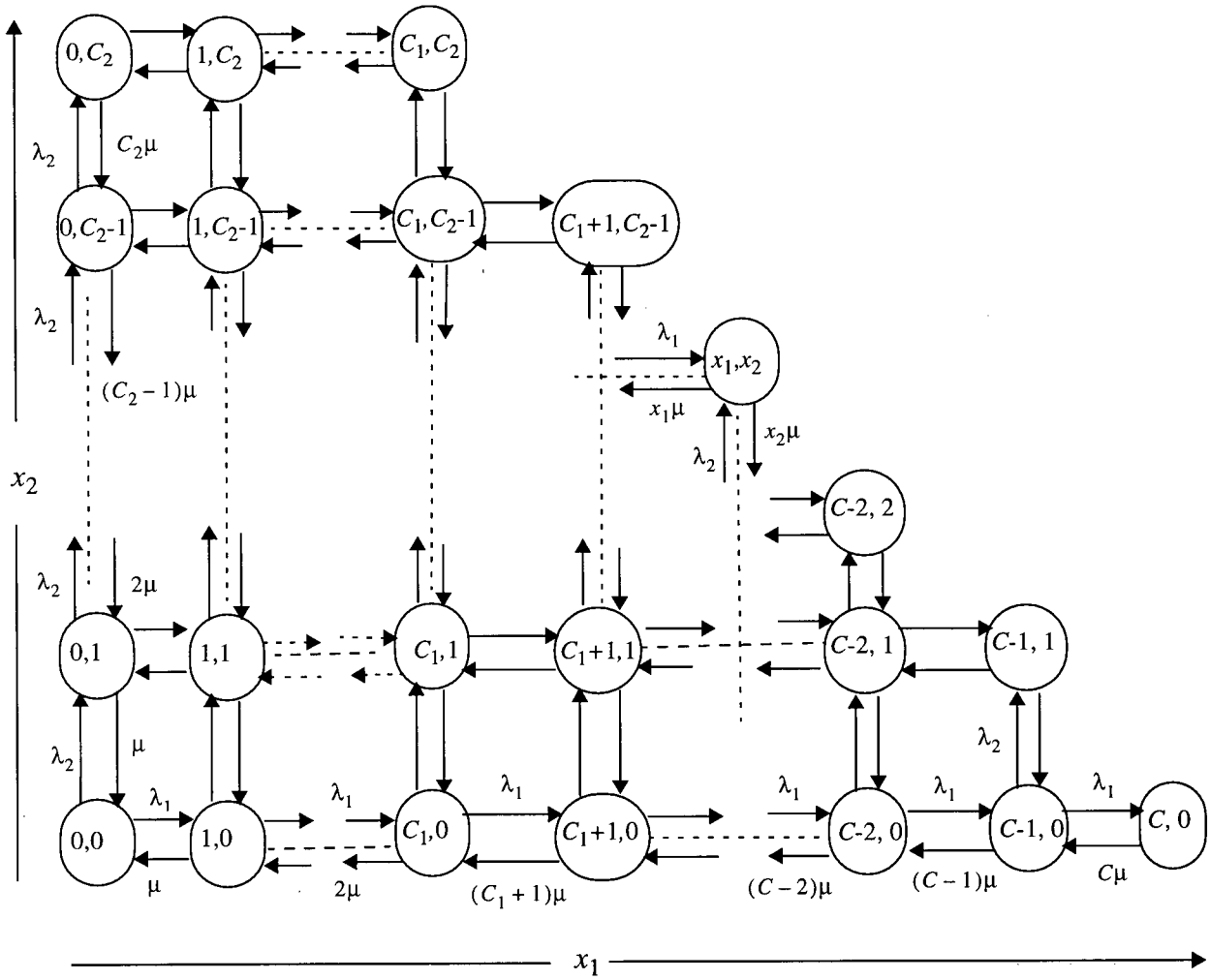

Figure 3.2 State-transition-rate diagram for a 2-region RP system with channel rearrangement; $x_i, i = 1, 2$ denotes the no. of channels used by region i calls.

As an example, for state $(C, 0)$, there are C channels used by region 1 calls and no region 2 call. There are C_1 region 1 calls using region 1 channels, C_2 region 1 calls using all region 2 channels. If a region 1 call using a region 1 channel completes, the state changes from $(C, 0)$ to

$(C-1, 0)$. Because of channel rearrangement, a region 1 call using a region 2 channel is switched to the just released region 1 channel and thus, a region 2 channel is released. The system can now accept either a new region 1 call as shown by the transition with rate λ_1 from $(C-1, 0)$ to $(C, 0)$ or a new region 2 call as shown by the transition with rate λ_2 from $(C-1, 0)$ to $(C-1, 1)$.

The call blocking probability for region 1 is the sum of the probabilities of states for which $x_1 + x_2 = C$, i.e.

$$P_{B,1} = \sum_{x_1 = C_1}^{C} \pi(x_1, C - x_1). \tag{3.16}$$

The call blocking probability for region 2 is given by

$$P_{B,2} = \sum_{x_1 = 0}^{C_1 - 1} \pi(x_1, C_2) + \sum_{x_1 = C_1}^{C} \pi(x_1, C - x_1). \tag{3.17}$$

The average call blocking probability, $P_{B,av}$, is given by (3.6).

For 2-region RP-OCR, at most a *single* channel rearrangement is required following the release of a channel by a completing call. For $n \geq 3$, $n-1$ channel rearrangements may be required so as to release a channel in the highest numbered region possible. When a region n channel becomes available (due either to a call completion or a call being switched to another channel), no rearrangement of on-going calls is necessary. On the other hand, when a region i, $i < n$, channel becomes available, the following rearrangement algorithm is performed.

Step 1. Set $k = 0$.

Step 2. Determine if a region j, $1 \leq j \leq i$, call is currently using a region $(n-k)$ channel? If so,

go to step 4.

Step 3. Is $k = n - i - 1$? If so, stop. Otherwise, increment k by one and go to step 2.

Step 4. Switch this call to the released region i channel. Note that this causes the release of a region $(n-k)$ channel. If $k = 0$, stop. Otherwise, set $i = n - k$ and go to step 1.

An n-region RP-OCR system can be described by a Markov chain with an n-dimensional state vector $(x_1, x_2, \ldots, x_n)$, where x_i is the number of channels used by region i calls. This Markov chain, as shown in Figure 3.2, corresponds to a truncation of n independent M/M/m/m queues and thus satisfies the detailed balance equations [25], i.e.

$$\lambda_i \pi(x_1, \ldots, x_{i-1}, x_i, x_{i+1}, \ldots, x_n) = \mu_i \pi(x_1, \ldots, x_{i-1}, x_i + 1, x_{i+1}, \ldots, x_n) \tag{3.18}$$

for all pairs of adjacent states

$\pi(x_1, \ldots, x_{i-1}, x_i, x_{i+1}, \ldots, x_n)$ and $\pi(x_1, \ldots, x_{i-1}, x_i + 1, x_{i+1}, \ldots, x_n)$.

The stationary distribution for such a n-dimensional Markov chain can be written as [25]

$$\pi(x_1, x_2, \ldots, x_n) = \pi(0) \prod_{j=1}^{n} \frac{\rho_j^{x_j}}{x_j!}, \tag{3.19}$$

where

$$\pi(0) = \frac{1}{\sum\limits_{(x_1, x_2, \ldots, x_n) \in S} \left(\prod\limits_{j=1}^{n} \frac{\rho_j^{x_j}}{x_j!} \right)}. \tag{3.20}$$

In (3.20), S is the set of all states $(x_1, x_2, \ldots, x_n)$ such that

$$x_i \leq \min_{j = 1, 2, \ldots, i} \left\{ \sum_{l=j}^{n} C_l - \sum_{k=j}^{i-1} x_k \right\}. \tag{3.21}$$

As an example, for a 2-region RP system, i.e. $n = 2$,

$$S = \{(x_1, x_2) | 0 \leq x_1 \leq C_1 + C_2, 0 \leq x_2 \leq \min\{C_1 + C_2 - x_1, C_2\}\}, \tag{3.22}$$

as depicted in Figure 3.2.

The blocking probability, $P_{B,i}$, for region i is obtained by summing the probabilities of all states for which

$$\sum_{k=i}^{n} x_k = \min_{j = 1, 2, \ldots, i} \left\{ \sum_{l=j}^{n} C_l - \sum_{k=j}^{i-1} x_k \right\}. \tag{3.23}$$

The average blocking probability, $P_{B,av}$, can then be obtained using (3.6).

3.2.3 RP With Single Channel Rearrangement (RP-SCR)

The RP-OCR scheme of Section 3.2.2 may involve up to $n - 1$ channel rearrangements. We now investigate a simpler method which uses a single rearrangement. In this method, when a region i channel is released, an on-going region k, $k \leq i$, call using the highest numbered region j, $j > i$, channel is switched to the released region i channel. If there are several calls currently using a region j channel, the call in the lowest-numbered region is switched. The just-released region j channel is then available to any new call in regions 1 to j.

The following example illustrates the difference between the single and optimal rearrangement methods. Assume that the system has two on-going calls, α_{13} and α_{34}. If a region 2 channel

is released due to a call completion, then in single rearrangement, call α_{13} is switched to the region 2 channel and a region 3 channel is released. But call α_{34} cannot be switched to the released region 2 channel because α_{34} is a region 3 call and so cannot use a region 2 channel. In optimal channel rearrangement, α_{13} is first switched to the released region 2 channel. This frees up a region 3 channel to which call α_{34} can be switched. In so doing, the region 3 call is switched from a region 4 channel to a region 3 channel and a region 4 channel is released. In this example, the single rearrangement method frees up a region 3 channel whereas the optimal rearrangement method is able to free up a region 4 channel.

3.3 Numerical Results

In this section, the numerical results obtained from the analysis of n-region RP system are first presented. Numerical results for a 2-region RP system are then compared with simulation results for slowly moving MS's in order to determine the range of parameter values over which the assumption of stationary MS's is valid.

3.3.1 Analysis Results for n-region FRP

For the numerical results, we consider a system with $m = 140$ channels. A cluster size of $N = 7$ is used for the (conventional FCA) system without RP (i.e. $n = 1$) so that each cell has 20 channels. Hence, the cluster size, N_n, for the outermost region is 7. Figures 3.3 and 3.4 show the average blocking probability, $P_{B,av}$, of 2- and 3-region RP systems with no channel rearrangement for different combinations of reuse cluster sizes, RC(N_1, ..., N_n). For a given RC(N_1, ..., N_n), the number of channels, CA(C_1, ..., C_n), allocated to each region was chosen to be proportional to the traffic load. The channel allocations for the cluster combinations used are as follows: RC(1,7) → CA(7,19), RC(3,7) → CA(11,15), RC(4,7) → CA(14,12), RC(1,3,7) →

CA(4,8,16), RC(1,4,7) → CA(4,13,12), RC(3,4,7) → CA(12,5,12). In both figures, it can be seen that at $P_{B,av} = 0.01$, conventional FCA has the lowest capacity. In Figure 3.3, $P_{B,av}$ for RC(3,7) and RC(4,7) are similar and lower than that for RC(1,7). Figure 3.4 shows that RC(1,3,7) outperforms RC(1,4,7) and RC(3,4,7). To verify the analysis, a few computer simulation results are also included in both figures. The 99% confidence intervals for the simulation results are within $\pm 1\%$ of the average values shown. It can be seen that the simulation results closely match the results from the analysis.

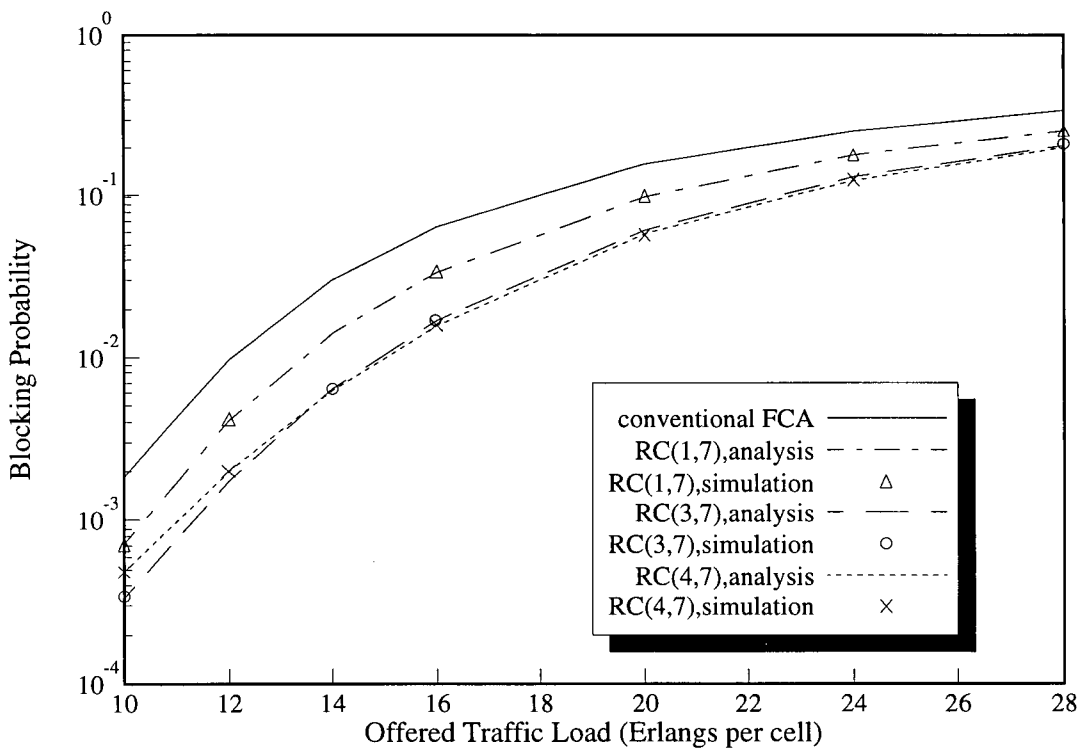

Figure 3.3 Average call blocking probability for conventional FCA and a 2-region RP system with no channel rearrangement for different RC(N_1,N_2).

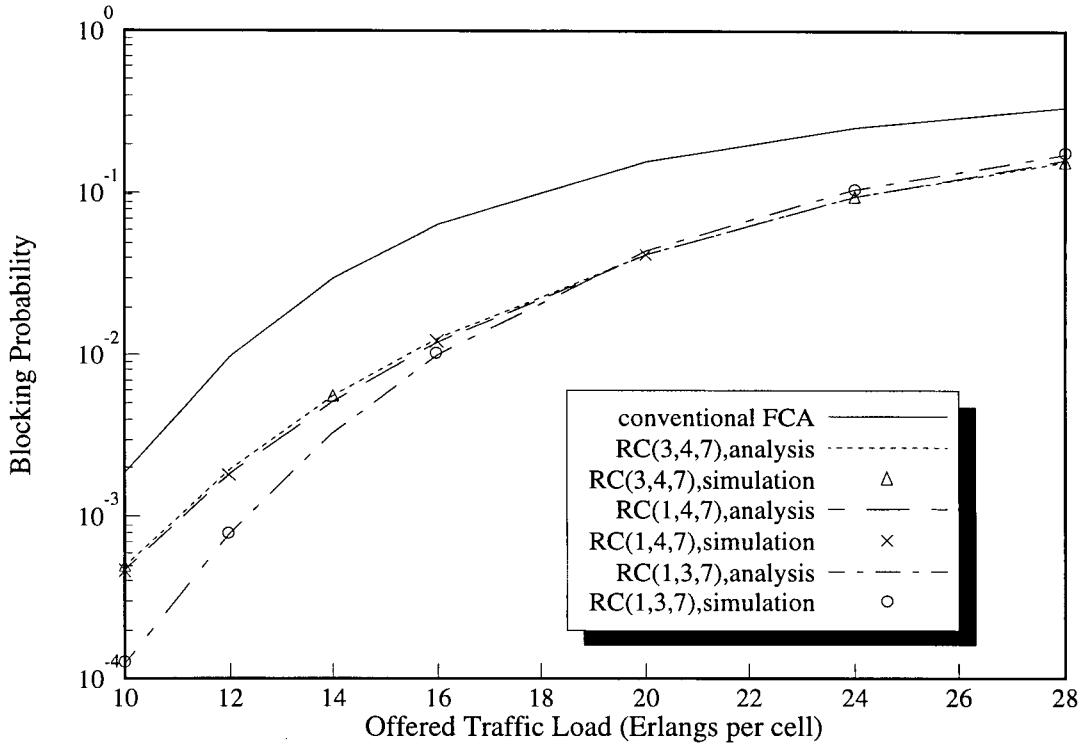

Figure 3.4 Average call blocking probability for conventional FCA and a 3-region RP system with no channel rearrangement for different RC(N_1,N_2,N_3).

The $P_{B,av}$ values for 2, 3 and 4-region RP-OCR are shown in Figure 3.5. The cluster sizes used for the 2, 3 and 4-region RP-OCR systems are RC(3,7), RC(1,3,7) and RC(1,3,4,7) respectively. The number of channels allocated to each region for 4-region RP system with RC(1,3,4,7) is CA(5,8,5,13). It can be seen that the performance of RP-OCR is substantially better than that of conventional FCA. For $P_{av} = 0.01$, the traffic capacity improvements for 2, 3 and 4-region RP-OCR relative to conventional FCA are about 25%, 36% and 43% respectively. Some simulation points are also plotted in Figure 3.5 and agree closely with the results from the analysis.

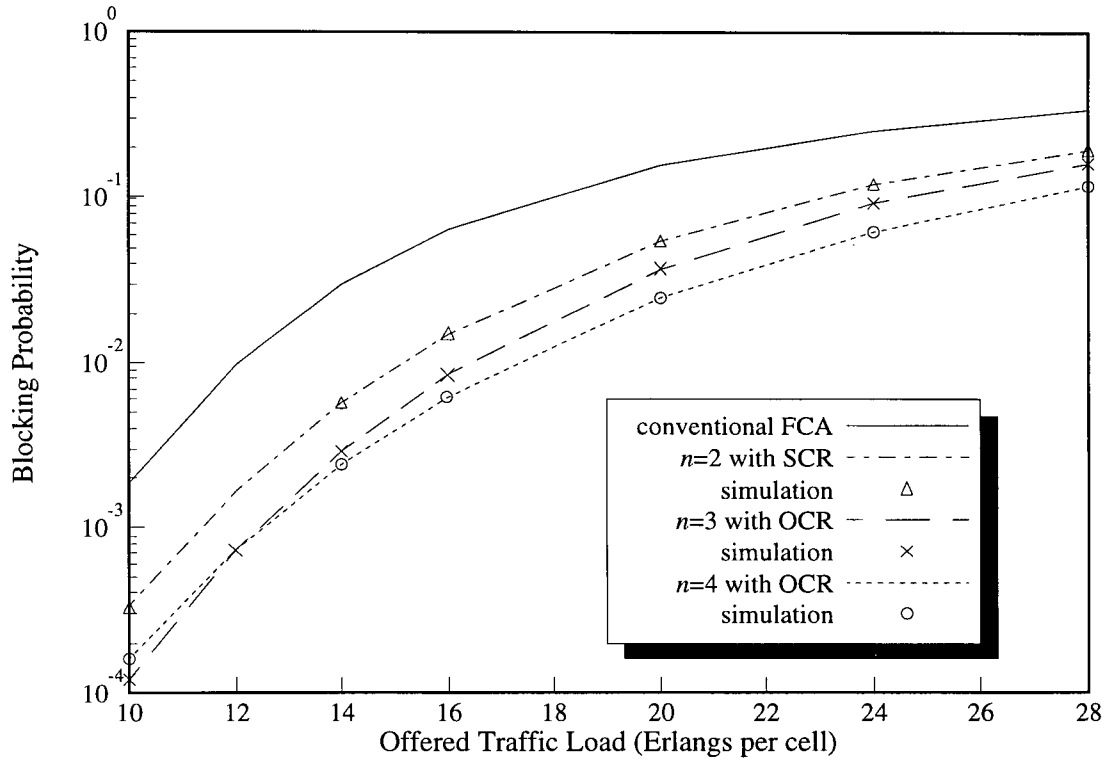

Figure 3.5 Average blocking probability for conventional FCA and 2, 3 and 4-region RP with channel rearrangement.

At light traffic loads, the inner region calls seldom need to use the outer region channels and there is little overflow. In this case, the blocking probability, $P_{B,n}$, for the outermost region can be approximated by the Erlang B formula with C_n channels. This is illustrated in Figure 3.6 for 4-region RP system. Using the Erlang B formula with C_i channels to calculate $P_{B,i}$, $i < n$, results in overly pessimistic values. In Figure 3.5, the performance of 4-region RP is slightly worse than that of 3-region RP for $\rho < 12$ because the $P_{B,n}$ for 4-region RP is higher than that for 3-region RP due to an insufficient number of channels being allocated to the outermost region. The $P_{B,n}$ values obtained from the analysis in Section 3.2.2 at $\rho = 10$ for 2, 3 and 4-region RP-

OCR are 5.747×10^{-4}, 2.065×10^{-4} and 3.689×10^{-4} respectively. The $P_{B,n}$ values obtained from the Erlang B formula at ρ = 10 for 2, 3 and 4-region RP-OCR are 5.707×10^{-4}, 2.038×10^{-4} and 3.638×10^{-4} respectively, confirming the close agreement between the analysis and the Erlang B results.

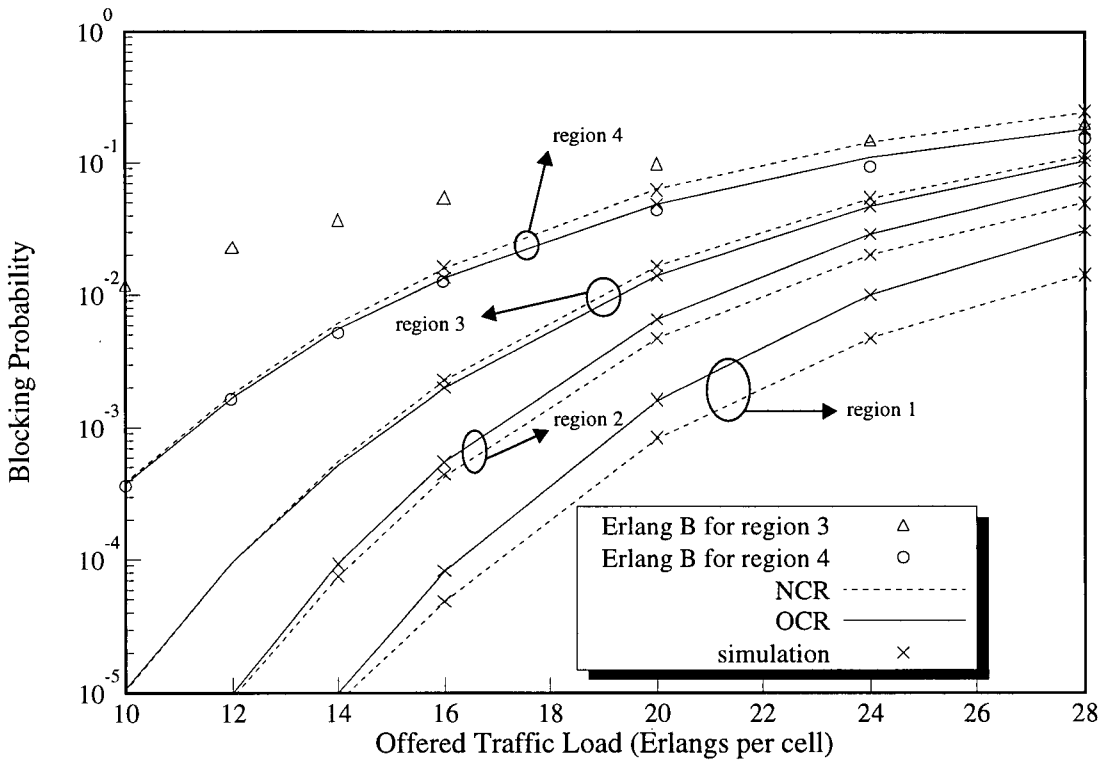

Figure 3.6 Blocking probability of each region for 4-region RP without and with channel rearrangement.

The blocking probabilities, $P_{B,i}$, for each region i for a 4-region RP system with and with no channel rearrangement are presented in Figure 3.6. With no channel rearrangement, there can be a large difference in the blocking probabilities for different regions. Some control policies to alleviate this problem for 2-region RP has been studied in [17], [20] and [21]. It can be seen that when channel rearrangement is employed, the blocking probabilities, $P_{B,3}$ and $P_{B,4}$, of the

higher-numbered regions are decreased whereas the blocking probabilities, $P_{B,1}$ and $P_{B,2}$, of the lowered-numbered regions are increased. This is due to the fact that channel rearrangement tends to release higher-numbered region channels which favors higher-numbered region calls at the expense of lower-numbered region calls. As a consequence, the use of channel rearrangement tends to decrease the blocking probability difference between lower- and higher-numbered regions. From Figure 3.6, it can be seen that the results from analysis agree closely with the simulation points.

The $P_{B,av}$ values for conventional FCA and a system using 2-region RP without or with overflow are plotted in Figure 3.7. For $P_{B,av} = 0.01$, the 2-region RP system with (without) overflow can carry about 25% (10%) more traffic than the FCA system. The $P_{B,av}$ values for RP-NCR and RP-SCR are also shown in Figure 3.7. It can be seen that the $P_{B,av}$ with no rearrangement is slightly higher than that with single rearrangement. The capacities for both no and single rearrangement at $P_{B,av} = 0.01$ are about the same.

The $P_{B,av}$ values for conventional FCA and a system using 4-region RP without or with overflow and NCR, SCR and OCR are plotted in Figure 3.8. The $P_{B,av}$ values for SCR were obtained by computer simulation. The $P_{B,av}$ with NCR is slightly higher than that with SCR or OCR. For $P_{B,av} = 0.01$, the traffic capacity with NCR is higher than with FCA by about 38%. The capacity improvement over FCA with SCR or OCR is about 43%. There is little difference between the performance with SCR and that with OCR. For $P_{B,av} = 0.01$, the traffic capacity for RP with no overflow is about the same as that for the FCA system. Also plotted in Figures 3.7 and 3.8 are the $P_{B,av}$ curves obtained using the simplified model in [22] for a system using RP with overflow. The figures show that the simplified model can significantly underestimate $P_{B,av}$.

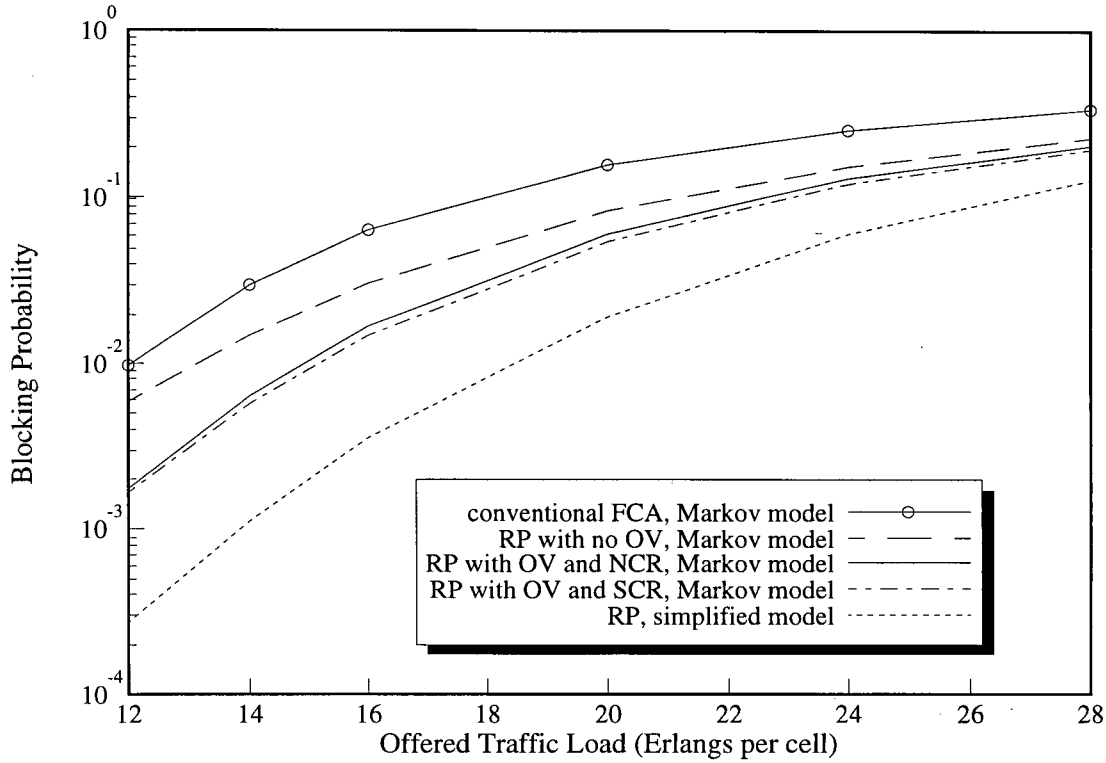

Figure 3.7 Average blocking probability for conventional FCA and a 2-region RP system: OV - overflow.

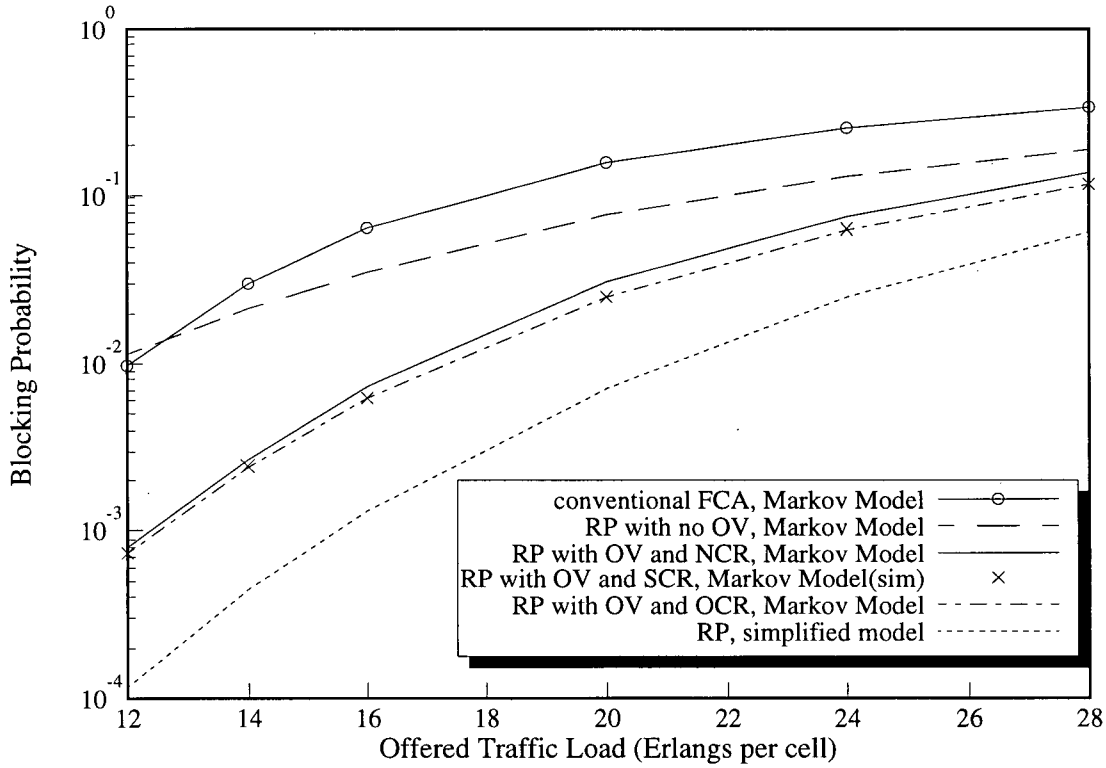

Figure 3.8 Average blocking probability for conventional FCA and a 4-region RP system.

The capacity at $P_{B,av} = 0.01$ for FCA, 2, 3 and 4-region FRP with channel rearrangement for larger numbers, m, of available system channels is shown in Figure 3.9. It can be seen that RP systems perform better than FCA for any value of m. The relative capacity improvement for RP systems over conventional FCA system is about the same for any values of m.

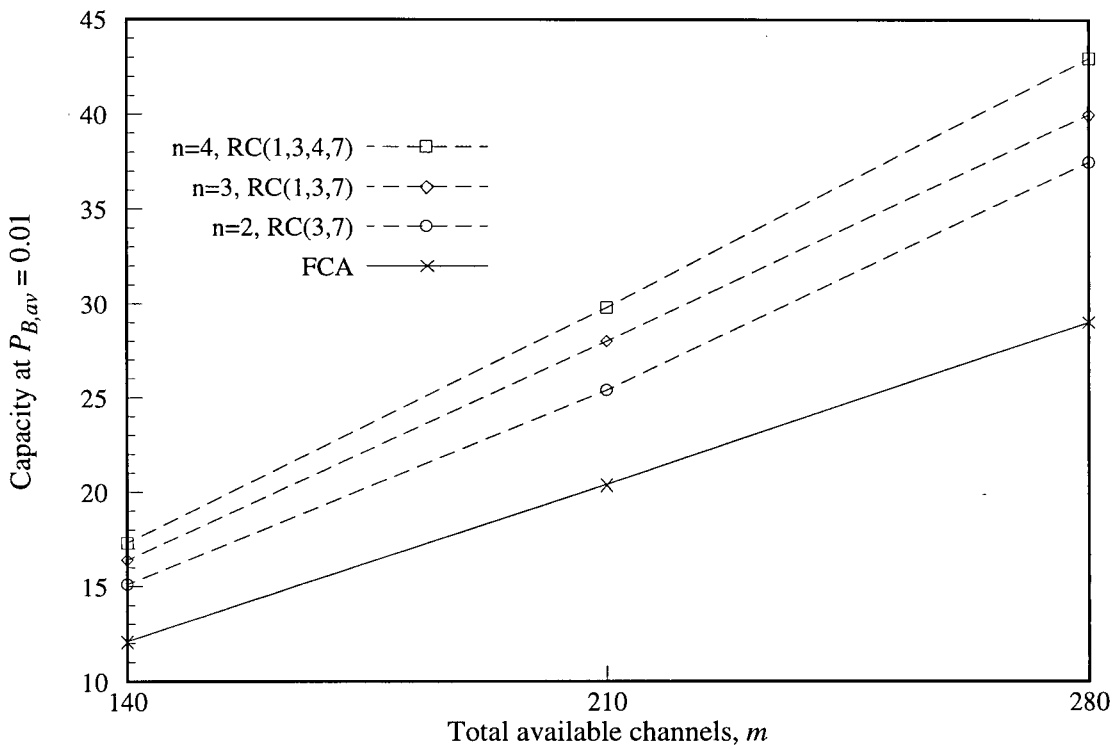

Figure 3.9 Traffic load at $P_{B,av} = 0.01$ for FCA, 2, 3 and 4-region RP with channel rearrangement with different m.

3.3.2 Simulation Results for Slow Moving MS's

In this section, the simulation results for slowly moving MS's in a 2-region RP system are compared with our analysis results. Several mobility models have been proposed for use in cellular systems [82]-[84]. Two mobility models, Model A and Model B, illustrated in Figure 3.10 are used in the simulation.

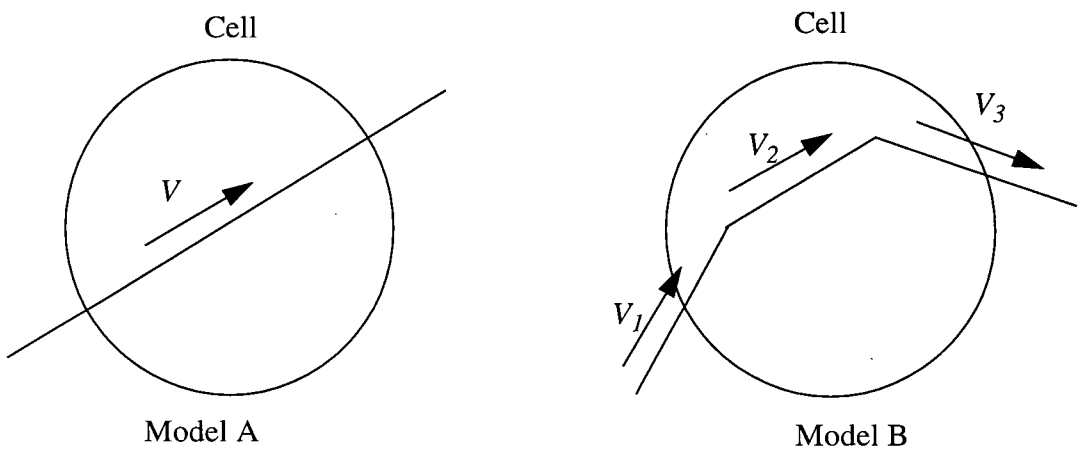

Figure 3.10 Illustration of the two Mobility Models.

(1) Model A

In this model [83], the MS moves in a straight line without changing its speed and direction which are independent random variables. The speed and direction of an MS are uniformly distributed in $(\overline{V}/2, 3\overline{V}/2)$ and $[0, 2\pi)$ respectively where $\overline{V}$ is the mean speed of the MS.

(2) Model B

In this model [82], the speed and direction of an MS are independent random variables, uniformly distributed in $(\overline{V}/2, 3\overline{V}/2)$ and $(0, 2\pi)$ respectively. An MS changes its speed and direction after some random time interval which is exponentially distributed with a mean of T seconds. Model A can be viewed as a special case of Model B with $T = \infty$. As T decreases, MS's tend to stay in a cell longer.

The simulated area consists of 49 hexagonal cells with radius R, with each cell divided

into two concentric regions. The cluster sizes used are RC(3,7) and the channel allocation to each cell is CA(11,15). The simulation results are collected from the central 7 cells to avoid edge effects. When an MS reaches the system boundary, it is assumed that the MS returns to the system with an angle which is uniformly distributed in $(-\pi/4, \pi/4)$ relative to the normal direction of the cell boundary as shown in Figure 3.11. No channel rearrangement is used in the simulation.

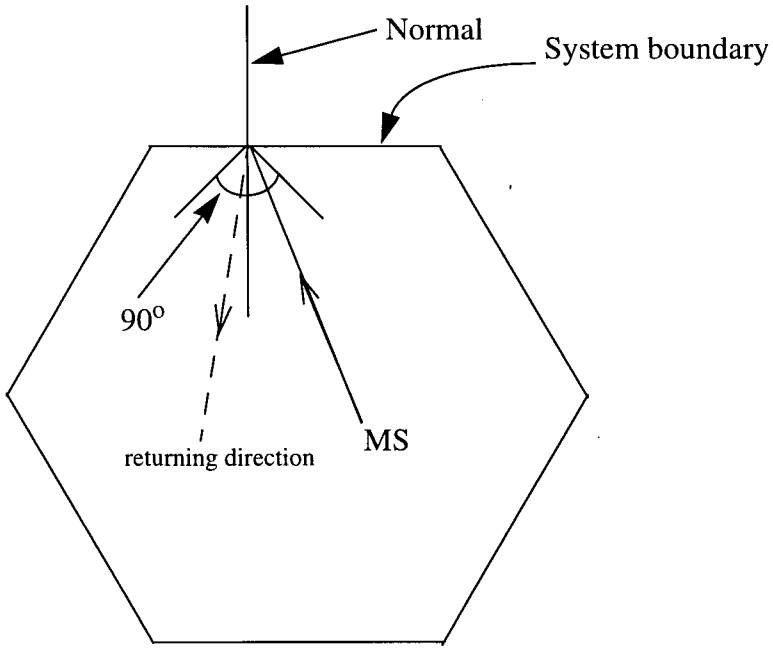

Figure 3.11 Illustration of returning direction of a MS which reaches the system boundary.

The system model used in the simulation is as follows: If a new call arrives in the inner region and cannot be assigned a (inner or outer region) channel, the call is blocked. If a new call arrives in the outer region and cannot find a free outer channel, it is blocked. When an MS using an inner region channel moves from the inner region to the outer region of its cell, it requests an intracell handoff. In this case, its call will release the inner region channel and be assigned an available outer-region channel. If no outer region channel is available, the call is dropped. For an

MS using an outer region channel crossing from inner to outer region, no intracell handoff is needed because the outer region channel can be used within the whole cell. If an MS (using an outer region channel) crosses its cell boundary, it will request an intercell handoff. If no outer region channel is available in the new cell, the call is dropped.

A mean of slow MS speed of 3 Km/hr, corresponding to typical pedestrian speeds [10], and a cell radius of 2 Km are used in the simulation. The simulation results depend on the ratio, h, of the mean speed to the cell radius, i.e.,

$$h = \frac{\overline{V}}{R} = \frac{3 \text{ Km/hr}}{2 \text{ Km}} = 1.5 \text{ hr}^{-1}. \tag{3.24}$$

The case of $h = 0$ corresponds to stationary MS's which do not require handoffs. The handoff activity and dropping probability increase with h.

Simulation results for blocking, P_b, and dropping, P_d, probabilities for slow MS's (with different values of h) and mobility models A and B are shown in Figure 3.12 (a) and (b) respectively. For Model B, T was chosen as 30 seconds. It can be seen that the blocking probabilities in both figures are close to the blocking probability obtained from the analysis. This is because for a slowly moving MS, the probability of a handoff is low and thus, the handoff call arrival rate is small compared to the new call arrival rate. As expected, the dropping probability increases with h. The dropping probability is about 20 times and 5 times less than the blocking probability for $h = 0.75$ and $h = 3$ respectively. In general, the dropping probability in mobility Model A is slightly higher than that in mobility Model B because in Model A, the duration of a MS staying in a cell tends to be shorter and thus, the number of handoff attempts becomes higher.

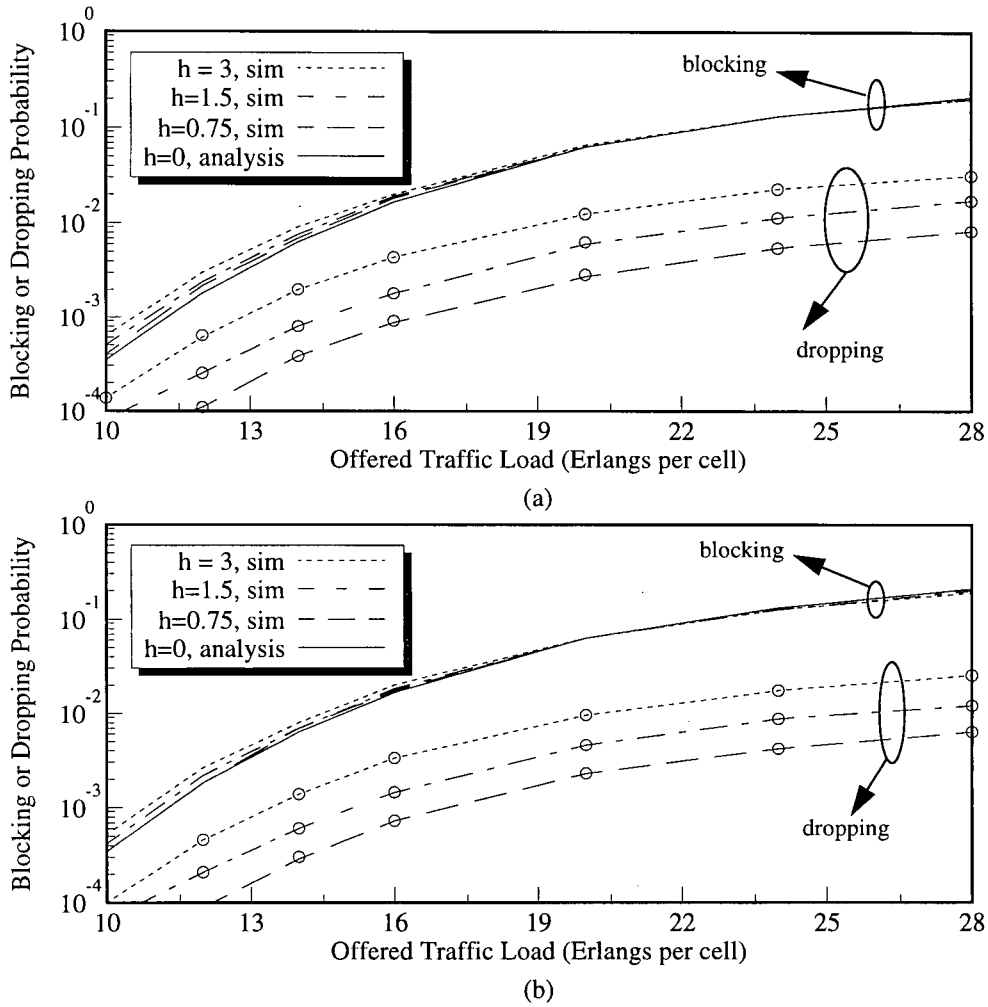

Figure 3.12 Call blocking or dropping probability for slow MS's for (a) mobility Model A and (b) mobility Model B.

Since our analysis does not consider handoff, there are no dropped calls. In order to compare our analysis results with the simulation results for slow MS's, we use the noncompleted call probability [86], P_{nc}, which is defined as probability that a new call is not successful due to either being blocked or dropped, i.e.

$$P_{nc} = P_b + P_d(1 - P_b). \tag{3.25}$$

In our analysis, P_{nc} is simply equal to $P_{B,\,ave}$. The P_{nc} curves for slow MS's with mobility models A and B are shown in Figure 3.13. In both mobility models, the P_{nc} for slow MS's, i.e., $h = 0.75$ or 1.5, is well approximated by our analysis. At $P_{nc} = 0.01$, the offered traffic load for $h = 3$ is about 1 Erlang less than that from our analysis.

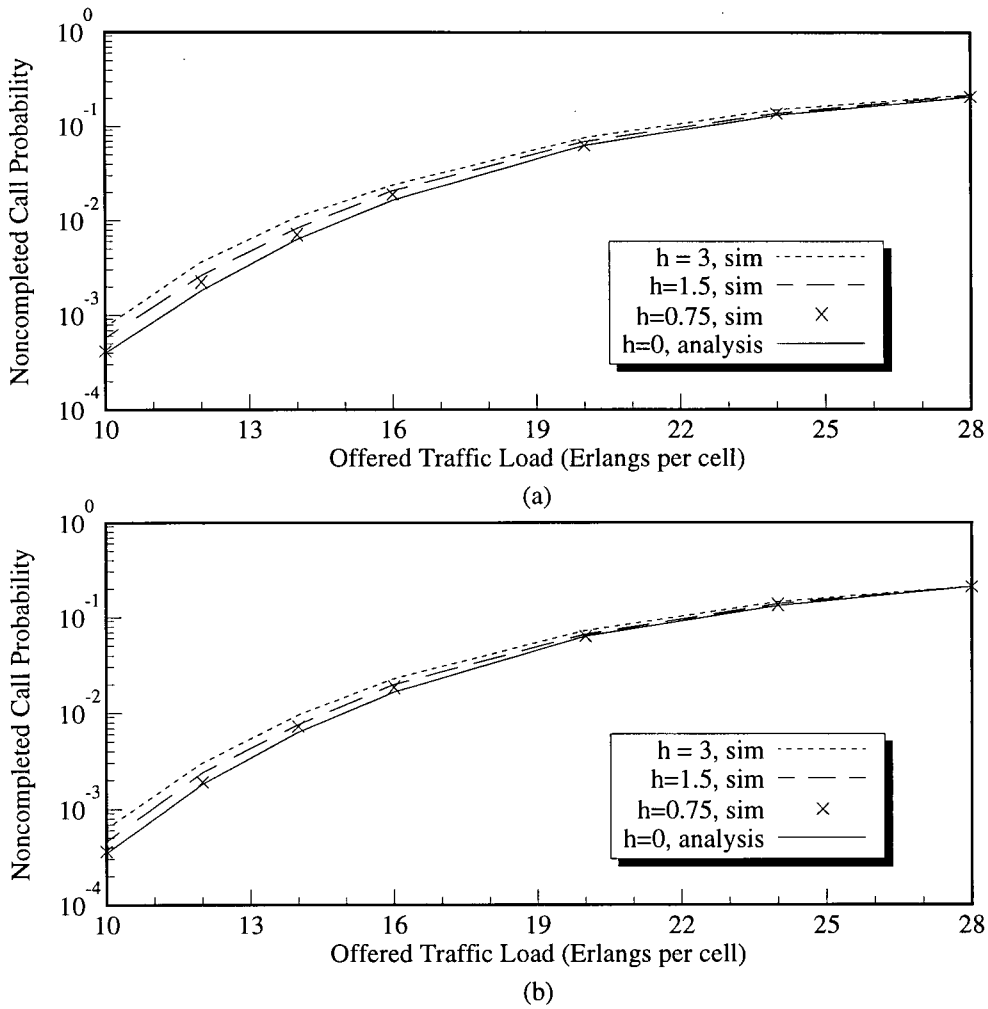

Figure 3.13 Noncompleted call probability in mobility (a) Model A and (b) Model B.

3.4 Summary

A performance analysis for the n-region reuse partitioning (RP) scheme with no channel rearrangement and fixed channel allocation (FCA) was presented. A closed-form expression for the call blocking probability of an n-region RP scheme with optimal channel rearrangement is given. The analysis results agree closely with the simulation results. Results show that a 2, 3 and 4-region RP scheme can improve the system capacity by about 25%, 36% and 43% compared to a conventional FCA system without RP. The effects of allowing no, single or optimal channel rearrangement were studied. As expected, RP with optimal rearrangement provides the best performance. The performance difference between single rearrangement and optimal rearrangement is quite small indicating that single rearrangement is a good choice for the RP system. The performance difference between the no rearrangement and optimal rearrangement schemes increases slightly with n. For $n = 2$, the capacity of RP with no rearrangement is about same as that with optimal rearrangement so that the derived closed-form expression can be used to approximate the performance of RP with no rearrangement. For $n = 4$, the capacity of RP with no rearrangement is about 5% less than that of RP with optimal rearrangement. Simulation results were used to examine the effect of mobility on the call blocking and dropping probabilities for slowly moving MS's. It is shown that the blocking probability for slowly moving MS's is well approximated by our analytic results.

Chapter 4 Analysis of RP using FCA for Mobile Users

In this chapter, a traffic model is developed to study the impact of mobile users on the new call blocking probability, P_b, and the call dropping probability, P_d, in a 2-region RP using FCA (FRP) system. This model allows P_b and P_d to be evaluated numerically. A simplified model which allows derivation of closed-form expressions for P_b and P_d in certain cases is also presented. The effect of a cutoff priority scheme for handoff calls on capacity is considered, with the capacity defined as the total offered traffic that can be supported in a cell at a certain value of Grade of Service (*GOS*) as given by [86]

$$GOS = (1-\alpha)P_b + \alpha P_d \tag{4.1}$$

where $\alpha \in [0, 1]$ is the *GOS* parameter and indicates the relative importance of P_b and P_d in a given system.

This chapter is organized as follows. A review of the analysis of FCA with mobile users is provided in Section 4.1 and the analytic results are compared with simulation in different mobility models in Section 4.2. The traffic model for a 2-region FRP system is formulated in Section 4.3. The channel assignment scheme is described in Section 4.4, followed by the performance analysis of the 2-region FRP system for both stationary and mobile users. The model which yields approximate closed form results is discussed in Section 4.5. Numerical results are provided in Section 4.6, and the main findings are summarized in Section 4.7.

4.1 Review of the Analysis of FCA with Mobile Users

Analysis of FCA with mobile users appear in [86]-[88]. In a FCA system, each cell has n channels. New calls and handoff calls arrive in a cell according to a Poisson process with arrival

rate, λ_n and λ_h per cell respectively. Channel holding times are exponentially distributed with a mean of $1/\mu_c$. The channel service rate, μ_c, is defined as the rate of which an assigned channel becomes free, i.e. a call using that channel is completed or handed off to other cells and given by

$$\mu_c = \mu + \mu_h \tag{4.2}$$

where $1/\mu$ is the mean call duration and assumed to be exponentially distributed and μ_h is mean handoff rate per calling mobile. The residual time of a *calling* MS using a channel is defined as the time that a MS with a new or handoff call stays in a cell as shown in Figure 4.1.

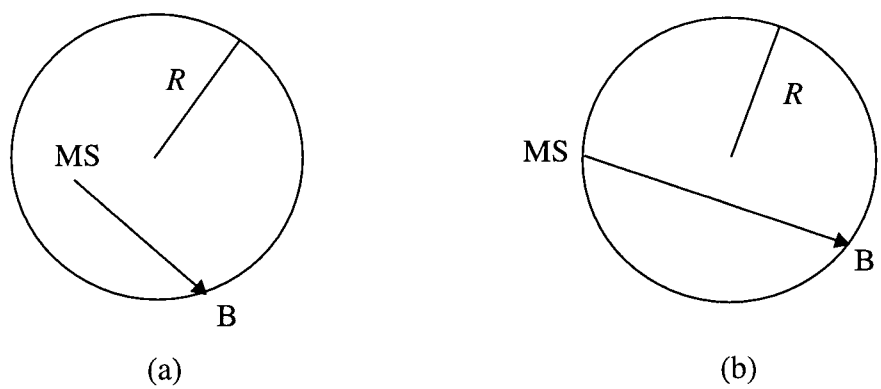

Figure 4.1 Residual time of a calling mobile with a (a) new call and (b) handoff call.

In [83], [84], [87] and [88], the residual time of a *calling* MS (with a new or handoff call) is assumed to exponentially distributed with the same mean of $1/\mu_h$. In a FCA system, a new call is blocked if the number of free channels is less than or equal to m where m is the number of reserved channels to be used for handoff calls only. A handoff call is dropped if no free channel is found. With the blocked-calls-cleared (BCC) model, the FCA system can be modeled as an $(n+1)$ state Markov chain as shown in Figure 4.2.

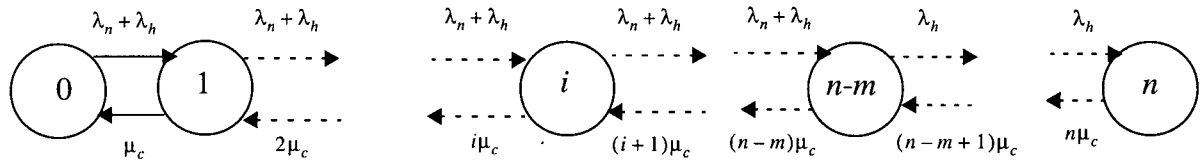

Figure 4.2 Markov chain state diagram for FCA System.

In Figure 4.2, the state i represents the number of channels in use in a cell. It can be seen that a new call is blocked if $i \geq n-m$ whereas a handoff call is blocked if $i = n$. The total arrival rate is $\lambda_n + \lambda_h$ for $i < n-m$ whereas the total arrival rate is λ_h for $i \geq n-m$. The steady-state probability, $p(i)$, of state i is given by

$$p(i) = \begin{cases} \dfrac{p(0)(\lambda_n + \lambda_h)^i}{\mu^i i!} & \text{if } i \leq n-m \\ \dfrac{p(0)(\lambda_n + \lambda_h)^{n-m}\lambda_h^{i-(n-m)}}{\mu^i i!} & \text{if } i > n-m \end{cases} \tag{4.3}$$

where

$$p(0) = \left[\sum_{i=0}^{n-m} \frac{(\lambda_n + \lambda_h)^i}{\mu^i i!} + \sum_{i=n-m+1}^{n} \frac{(\lambda_n + \lambda_h)^{n-m}\lambda_h^{i-(n-m)}}{\mu^i i!} \right]^{-1}. \tag{4.4}$$

To evaluate $p(i)$, we need to find the values of μ_h and λ_h. In [83], [84], [87] and [88], it is assumed that the speed and direction of a MS remain constant in a given cell. The mean handoff rate per calling mobile, μ_h, can be then approximated by the mean boundary crossing rate per mobile, μ_b, and given by [83]

$$\mu_h \approx \mu_b = \frac{E[V]L}{\pi S} \tag{4.5}$$

where V is the random variable denoting the speed of the MS, $E[V]$ is the mean speed of the MS, L is the length of the perimeter of the cell and S is the area of the cell. The handoff call arrival rate, λ_h, per cell is equal to the mean handoff rate, μ_h, from the k neighboring cells[1] and each MS is moving to one of the k neighboring cells with equal probability. Hence,

$$\lambda_h \approx k \times \frac{1}{k} \times E[I]\mu_b \tag{4.6}$$

where $E[I]$ is the mean number of calling mobiles in a cell and is given by

$$E[I] = \sum_{i=0}^{n} ip(i). \tag{4.7}$$

The steady-state probability $p(i)$ can be obtained numerically by an iterative process using Equations (4.3)-(4.7).

From Figure 4.2, the new call blocking probability, P_b, is

$$P_b = \sum_{i=n-m}^{n} p(i), \tag{4.8}$$

and the handoff call blocking probability, P_h, is

$$P_h = p(n). \tag{4.9}$$

The call dropping probability, P_d, is the probability that a nonblocked call is dropped due to

[1] Applies only for a cell with a full complement of neighbors.

handoff failure and given by [89]

$$P_d = \frac{qP_h}{1 - q(1 - P_h)} \tag{4.10}$$

where q is the probability that handoff occurs before call completion. Because of the exponential assumptions, q is given by

$$q = \frac{\mu_h}{\mu + \mu_h}. \tag{4.11}$$

The handoff activity, H_n, defined as the expected number of handoff call attempts for a nonblocked call, is another system parameter of interest [26] and is given by [89]

$$H_n = \frac{q\{P_h + (1 - P_h)p\}}{\{1 - q(1 - P_h)\}^2} \tag{4.12}$$

where p is the probability that the call completes before the next handoff. Because of the exponential assumptions, p is given by

$$p = \frac{\mu}{\mu + \mu_h}. \tag{4.13}$$

4.2 Comparison of Analytic and Simulation Results for FCA

In this section, the analytic results obtained from the previous section are now compared with the simulation results for different mobility models [82]-[84] and [86] which have been used in the performance study of mobile cellular systems. Three mobility models are described and shown in Figure 4.3:

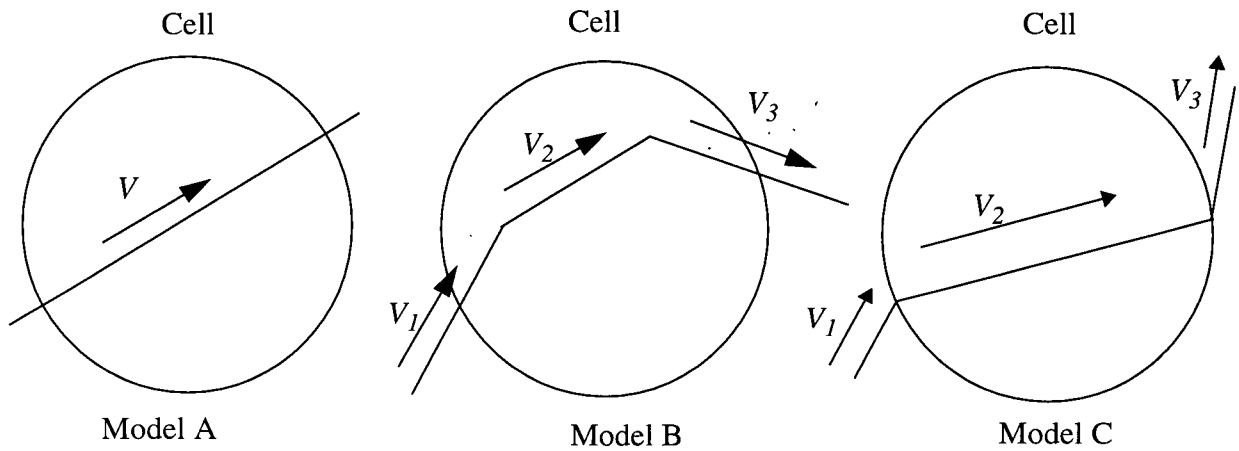

Figure 4.3 Three Mobility Models.

(1) Model A [83]

In this model, the MS moves in a straight line without changing its speed and direction which are independent random variables. The speed and direction of an MS are uniformly distributed in $[E[V]/2, 3E[V]/2]$ and $(0, 2\pi]$ respectively.

(2) Model B [82]

The speed and the direction of an MS are independent random variables, uniformly distributed in $[E[V]/2, 3E[V]/2]$ and $(0, 2\pi]$ respectively. The MS changes its speed and direction after a random time interval which is exponentially distributed with a mean of T seconds. Model A can be a special case of Model B with $T = \infty$.

(3) Model C [86]

The speed and the direction of an MS are independent random variables uniformly distributed in $[E[V]/2, 3E[V]/2]$ and $(0, 2\pi]$ respectively. The MS changes its speed and direction

whenever it crosses a cell boundary. The new speed is uniformly distributed in $[E[V]/2, 3E[V]/2]$ and the new direction is uniformly distributed in $(-\pi/2, \pi/2)$ relative to the normal direction of the boundary through which the MS enters the cell.

Models A and C satisfy the assumption in (4.5) since in these two models the MS's do not change speed and direction within a cell. In Model B, the MS's change speed and direction within a cell depending on the value of T. If T is small, the MS's change speed and direction more frequently within a cell. If T is large, the MS's are less likely to change speed and direction within a cell. As T decreases, the MS's tend to stay in a cell longer.

The simulated area consists of 49 hexagonal cells, each with radius $R = 2$ Km. The cluster size used is 7 and the channel allocation to each cell is $n = 20$. The simulation results are collected from the central 7 cells to avoid the edge effect. When the MS reaches the system boundary, it is assumed that the MS will return to the system with an angle which is uniformly distributed in $(-\pi/4, \pi/4)$ relative to the normal direction of the cell boundary as shown in Figure 3.11. The mean speed, $E[V]$, of the MS is assumed to be 50 Km/hr. Mobility Model A and B will be used to simulate the FCA system with mobile users. The value of T for Model B is 5 seconds. This value was chosen so that the MS changes its speed and direction often within a cell and Model B is used to check the sensitivity of the assumption in (4.5). The 99% confidence intervals of the simulation results are within ± 5 % of the values plotted.

The new call blocking probability for $m = 0$ and $m = 2$ obtained from the analysis and the simulation are shown in Figure 4.4 (a) and (b) respectively. It can be seen that the simulation results agree closely with the analytic results even for Model B.

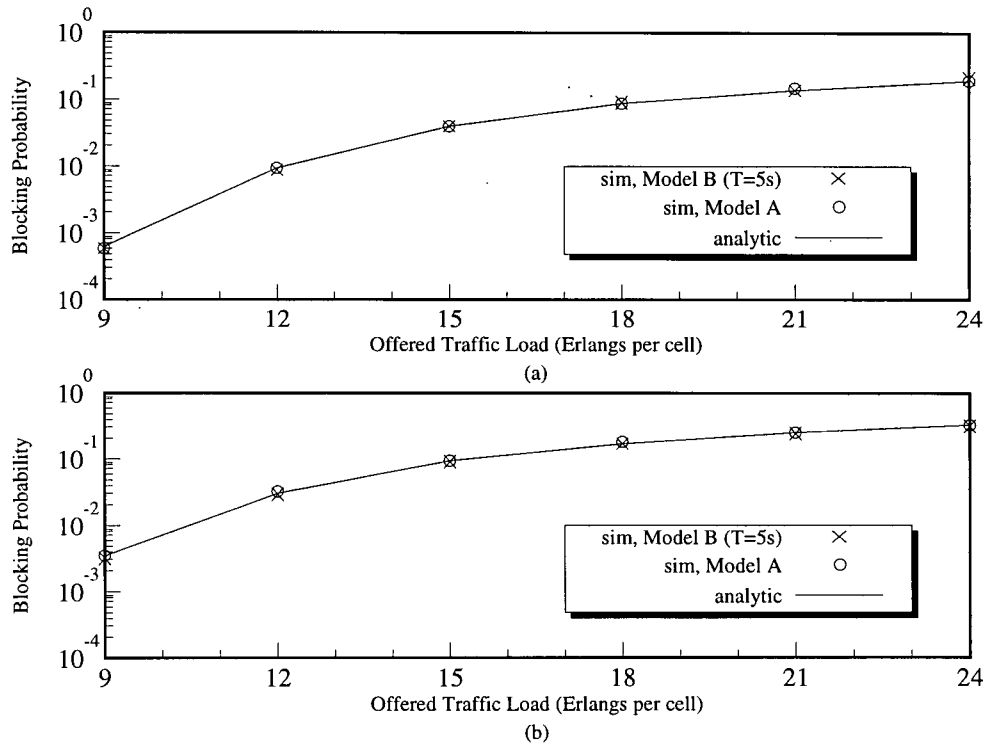

Figure 4.4 Comparison of blocking probability for FCA from the analysis and the simulation in different mobility models with (a) $m = 0$, (b) $m = 2$.

The call dropping probability for $m = 0$ and $m = 2$ obtained from the analysis and the simulation are shown in Figure 4.5 (a) and (b) respectively. The simulation results for Model A agree closely with the analysis. The simulation results for Model B are slightly lower because in Model B the MS's change speed and direction within a cell and thus the residual time for MS's within a cell are somewhat longer than indicated using the assumption in (4.5). The number of handoff attempts using Model B is expected to be lower than that using (4.5). To verify this, the handoff activity for $m = 0$ and $m = 2$ obtained from the analysis and the simulation are shown in Figure 4.6 (a) and (b) respectively. The handoff activity for Model A is close to the analytic results whereas the handoff activity for Model B is slightly lower than the analytic results.

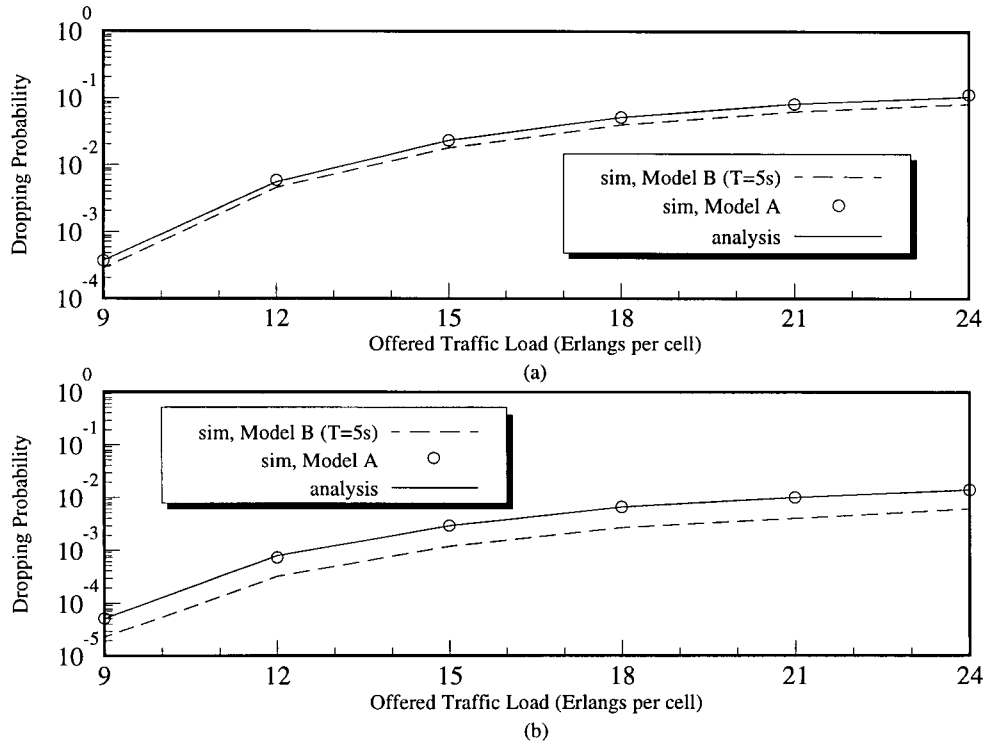

Figure 4.5 Comparison of dropping probability for FCA from the analysis and the simulation in different mobility models with (a) $m = 0$, (b) $m = 2$.

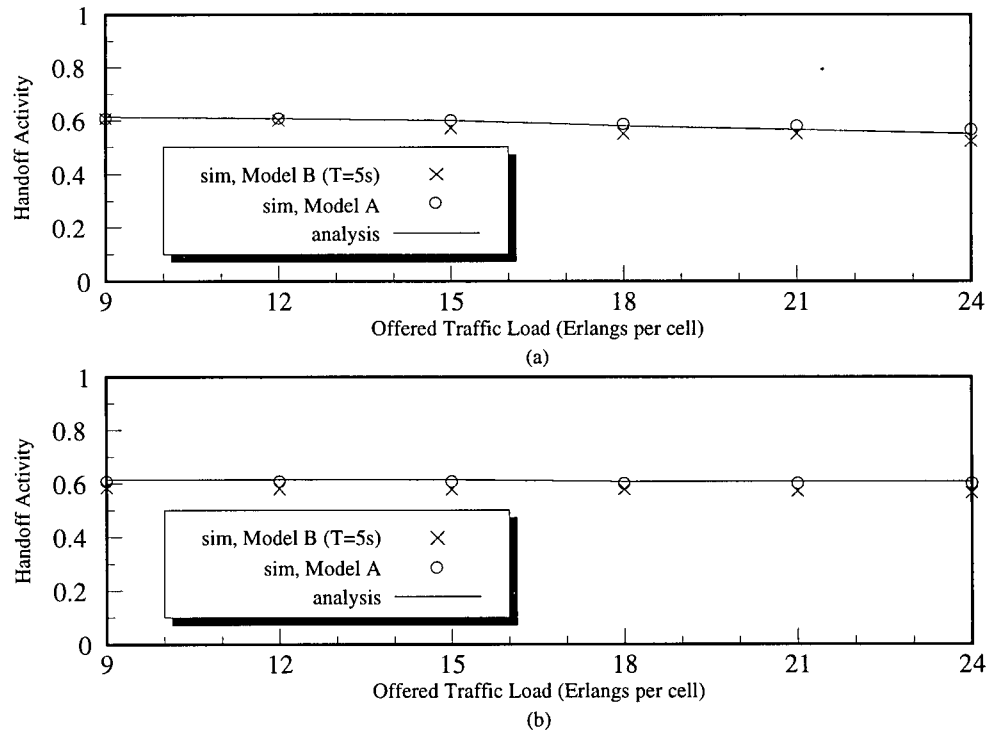

Figure 4.6 Comparison of handoff activity for FCA from the analysis and the simulation for different mobility models with (a) $m = 0$, (b) $m = 2$.

4.3 Traffic Model for a 2-region FRP System

In the analytic model, a two-region FRP system with hexagonal cells and omnidirectional BS antennas are assumed. An example with an inner region cluster size, $N_A = 3$, and outer region cluster size, $N_B = 7$, is shown in Figure 4.7.

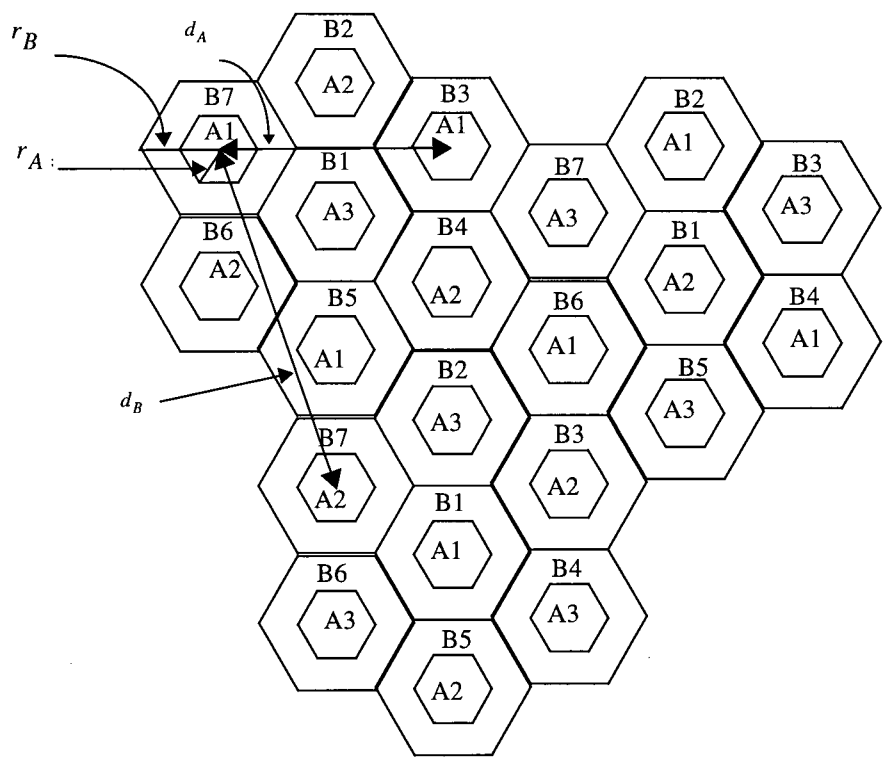

Figure 4.7 Cellular grid with reuse cluster sizes $N_A = 3$ and $N_B = 7$.

With a reuse cluster size of N_A, we have [11]

$$\frac{d_A}{r_B} = \sqrt{3N_A} \tag{4.14}$$

where d_A is the reuse distance associated with inner region and r_B is the radius of the cell as shown in Figure 4.7. Since the target SIR for both inner and outer region calls are the same, we

have

$$\frac{d_A}{r_A} = \frac{d_B}{r_B} = \sqrt{3N_B} \tag{4.15}$$

where r_A is the radius of the inner region. From (4.14) and (4.15), it follows that

$$\left(\frac{r_A}{r_B}\right)^2 = \frac{N_A}{N_B} \tag{4.16}$$

Note that $N_B = N$, the cluster size for the conventional FCA.

Let C_A and C_B be the number of channels allocated to the inner and outer regions respectively and $C = C_A + C_B$ be the total number of channels available in a cell. If a total of M channels are available to the cellular system, the parameters N_A and N_B must satisfy

$$N_A C_A + N_B C_B \leq M. \tag{4.17}$$

It is assumed that a MS is served by the base station of its current cell and that new call arrivals are uniformly distributed over the service area. A blocked-calls-cleared (BCC) model [41] is used. New calls arrive in a cell according to a Poisson process with arrival rate, λ, per cell. Call durations are exponentially distributed with a mean of $1/\mu$. Since new call arrivals are uniform throughout the service area, the new call arrival rates in the inner and outer regions are proportional to the region's area and given by

$$\lambda_A = \lambda \frac{r_A^2}{r_B^2}; \quad \lambda_B = \lambda - \lambda_A. \tag{4.18}$$

The offered traffic to each region of a cell is denoted by

$$\rho_A = \frac{\lambda_A}{\mu}\ ;\ \rho_B = \frac{\lambda_B}{\mu}. \tag{4.19}$$

To study the effect of mobile users, it is convenient to define the *residual time* as the time that a MS stays in a given region. The residual time of a *calling* MS using an inner (outer) region channel within the inner region (cell) is assumed to be negative exponentially distributed with a mean of $1/\mu_A$ $(1/\mu_B)$. The parameter μ_A is the mean outgoing handoff rate per calling mobile using an inner region channel crossing from inner region to outer region and μ_B is the mean outgoing handoff rate per calling mobile using an outer region channel crossing from cell to cell.

Since the MS uses an inner region channel only when the MS originates or receives a new call inside the inner region (described in the next section), Equation (4.5), which is used for MS with a new or handoff call, cannot be applied. The residual time of a *calling* mobile **M** in a cell **A** is defined as the time duration between a new call arrival for mobile **M** and its departure from cell **A** and is illustrated in Figure 4.1 (a). The mean, $1/\mu_x$, of this residual time is given by [88]

$$\frac{1}{\mu_x} = \frac{8R}{3\pi V_f} \tag{4.20}$$

where the fixed mobile speed V_f is assumed and R is the radius of a circular cell. Thus, the mean outgoing handoff rate, μ_A, per calling mobile using an inner region channel is given by μ_x. Equation (4.20) is derived for a circular cell. Since we assume the hexagonal cell in this model, (4.20) is modified by replacing the circular radius R with a hexagonal radius of $0.91 r_A$ in order to have the same perimeter length of the cell, i.e.,

$$\mu_A = \frac{3\pi V_f}{8 \times 0.91 r_A}. \tag{4.21}$$

The MS using an outer region channel can carry a new call or handoff call as shown in Figure 4.1. This situation is similar to FCA system in Section 4.1. Therefore, the mean outgoing handoff rate per calling mobile, μ_B, using an outer region channel crossing from cell to cell can be approximated by the mean boundary crossing rate per mobile in a given cell (4.5), i.e.

$$\mu_B \approx \frac{E[V]L_B}{\pi S_B} \tag{4.22}$$

where $L_B = 6r_B$ is the length of the perimeter of the cell and $S_B = 3r_B^2(\sqrt{3})/2$ is the area of the cell. Since we assume fixed mobile speed, V_f, for μ_A, (4.22) becomes

$$\mu_B \approx \frac{V_f L_B}{\pi S_B}. \tag{4.23}$$

The assumptions of an exponential pdf for the *calling* mobile residual time and a fixed mobile speed, V_f, within an inner region and a cell in (4.21) and (4.23) respectively are used to analyze the performance of mobile users in a 2-region FRP system. The first assumption is valid if MS's do not change speed and direction within a cell. The analytic results are verified by simulation for different mobility models with uniformly distributed mobile speeds in Section 4.6.

4.4 Analysis of 2-region FRP

In this section, the channel assignment scheme to be used for a 2-region FRP system is described. The resulting Markov chain model is derived. We outline the procedure used to obtain the steady state probabilities which are then used to evaluate P_b and P_d for stationary and mobile users.

4.4.1 Markov Chain Model for a 2-region FRP System

Let $i_A(i_B)$ be the number of inner (outer) region channels used. When a new call arrives for a MS located in the inner region, the call is assigned an inner channel if $i_A < C_A$ or an outer channel if $i_A = C_A$ and $i_B < C_B - C_h$ where C_h is the number of reserved channels to be used for handoff calls only. Thus, inner region calls, i.e. calls of mobiles located in the inner region, can use (overflow into) outer region channels. If no channel is available, the new call is blocked. A call currently using an inner region channel requires a handoff when its MS exits the inner region. At that time, the handoff call (or outer region call) is assigned an outer region channel if $i_B < C_B$. Otherwise, the handoff call is dropped. A call using an outer region channel is kept on the same channel as long as its MS remains within the cell.

There are four situations in which a call might use an outer region channel in a cell: (1) a new call arrives in the inner region, (2) a call moves from the inner region to the outer region (intracell handoff), (3) a new call arrives in the outer region or (4) a call moves from a neighboring cell into the outer region (intercell handoff). The first two situations are described in the previous paragraph. When a new call arrives in an outer region, the call is assigned an outer region channel if $i_B < C_B - C_h$. Otherwise, the call is blocked. When a MS with a call crosses the cell boundary to one of the six neighboring cells, the call requires a handoff. This intercell handoff call is assigned an outer region channel if $i_B < C_B$. Otherwise, the handoff call is dropped. The 2-region FRP system with mobile users can be represented by the two-dimensional state-transition diagram shown in Figure 4.8.

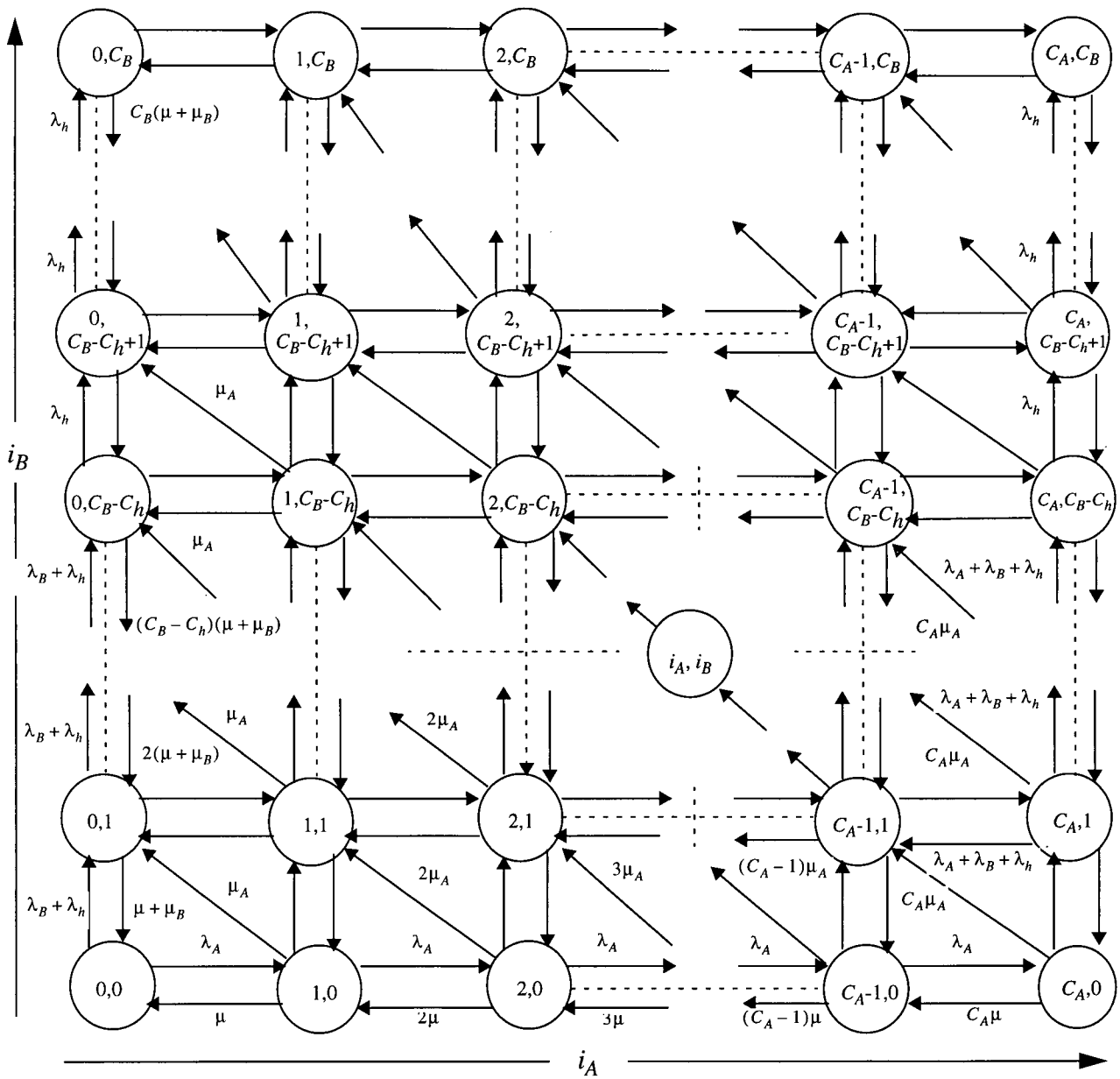

Figure 4.8 State-transition diagram for 2-region FRP with mobile users.

In Figure 4.8, the pair (i_A, i_B) denotes the state of the system. Since there are C_A and C_B channels allocated to the inner and outer regions respectively, the set of allowable states is

$$S = \{(i_A, i_B) | 0 \le i_A \le C_A, 0 \le i_B \le C_B\}. \tag{4.24}$$

The assignment of an inner region call to an inner region channel corresponds to a transition from the current node to the node to its right with rate λ_A. If all inner region channels are busy, an inner region call can be assigned to an outer region channel as represented in Figure 4.8 by an upward transition with rate λ_A for nodes $(C_A, 0), (C_A, 1), \ldots, (C_A, C_B - C_h - 1)$. A new outer region call can only be assigned to an outer region channel, as shown by an upward transition with rate λ_B from any node (i_A, i_B) with $0 \le i_A \le C_A, 0 \le i_B \le C_B - C_h - 1$. The intracell handoff rate per calling mobile is μ_A from nodes (i_A, i_B) to $(i_A - 1, i_B + 1)$ for $1 \le i_A \le C_A, 0 \le i_B \le C_B - 1$ so that the total intracell handoff rate is $i_A \mu_A$. For intracell handoffs, the total number of channels used, i.e. $i_A + i_B$, in a cell remains the same. The intercell handoff calls are assumed to arrive in a cell according to a Poisson process with rate λ_h per cell which is equal to the average outgoing handoff rate, μ_B, from the six neighboring cells. An intercell handoff call can only be assigned to an outer region channel, as shown by an upward transition with rate λ_h from any node (i_A, i_B) with $0 \le i_A \le C_A, 0 \le i_B \le C_B - 1$. In 2-region FRP, an intercell handoff call originates from a mobile using an outer region channel in one of the six neighboring cells. Hence,

$$\lambda_h = 6 \times \frac{1}{6} \times E[I_B]\mu_B \tag{4.25}$$

where $E[I_B]$ is the mean number of MS's using outer region channels in a cell and is given by

$$E[I_B] = \sum_{i_A = 0}^{C_A} \sum_{i_B = 0}^{C_B} i_B p(i_A, i_B). \tag{4.26}$$

In Figure 4.8, the term λ_h is initially unknown. The state probabilities, $p(i_A, i_B)$, can be solved by estimating λ_h using an iterative procedure as follows. First, an initial value is assigned to λ_h, e.g. $\lambda_h \approx 0.1\lambda_B$. The Markov chain in Figure 4.8 can then be solved numerically [85] to obtain an

estimate of $p(i_A, i_B)$. Following this, we use (4.25) and (4.26) to obtain a new estimate, $\hat{\lambda}_h$, of the average outgoing handoff rate. If $|\lambda_h - \hat{\lambda}_h|$ is less than some small specified value, the procedure is ended. Otherwise, the new estimate, $\hat{\lambda}_h$, is used to obtain new estimates of $p(i_A, i_B)$ and the procedure continues.

4.4.2 FRP with Stationary Users

The new call blocking probabilities, $P_{b,A}(\rho_A, C_A)$ and $P_{b,B}(\rho_B, C_B)$, for the inner and outer regions of a 2-region FRP system with no overflow and stationary users are given by the Erlang B formula [25]. The average new call blocking probability, P_b, can then be obtained as

$$P_b = \frac{\rho_A}{\rho} P_{b,A}(\rho_A, C_A) + \frac{\rho_B}{\rho} P_{b,B}(\rho_B, C_B) \tag{4.27}$$

where $\rho_A = \frac{\lambda_A}{\mu}$, $\rho_B = \frac{\lambda_B}{\mu}$ and $\rho = \rho_A + \rho_B$ is the total offered traffic in a cell.

The 2-region FRP system with overflow for stationary users can be represented by a two-dimensional state-transition diagram as in Figure 4.8 with μ_A, μ_B, λ_h and C_h set to zero. The new call blocking probability for the inner region is given by

$$P_{b,A} = p(C_A, C_B), \tag{4.28}$$

and the new call blocking probability for the outer region is given by

$$P_{b,B} = \sum_{i_A = 0}^{C_A} p(i_A, C_B). \tag{4.29}$$

The average new call blocking probability, P_b, is given by

$$P_b = \frac{\rho_A}{\rho} P_{b,A} + \frac{\rho_B}{\rho} P_{b,B}. \tag{4.30}$$

4.4.3 FRP with Mobile Users

For mobile users, the new call blocking probability for the inner region is the sum of the probabilities of states for which $i_A = C_A$ and $i_B \geq C_B - C_h$, i.e.

$$P_{b,A} = \sum_{i_B = C_B - C_h}^{C_B} p(C_A, i_B). \tag{4.31}$$

The new call blocking probability for the outer region is the sum of probabilities of states for which $i_B \geq C_B - C_h$, i.e.

$$P_{b,B} = \sum_{i_A = 0}^{C_A} \sum_{i_B = C_B - C_h}^{C_B} p(i_A, i_B). \tag{4.32}$$

The average new call blocking probability, P_b, is given by (4.30).

The handoff call blocking probability for a call using an inner region channel, i.e. $i_A \geq 1$ and $i_B \geq 0$, is the sum of the probabilities of states for which $i_A \geq 1$ and $i_B = C_B$, i.e.

$$P_{h,A} = \frac{\sum_{i_A = 1}^{C_A} p(i_A, C_B)}{\sum_{i_A = 1}^{C_A} \sum_{i_B = 0}^{C_B} p(i_A, i_B)}. \tag{4.33}$$

The handoff call blocking probability for a call using an outer region channel is the sum of probabilities of states for which $i_B = C_B$, i.e.

$$P_{h,B} = \sum_{i_A = 0}^{C_A} p(i_A, C_B). \tag{4.34}$$

The call dropping probability, P_d, is the probability that a nonblocked call is dropped due to handoff failure. A nonblocked call at the first handoff could be using an inner region channel or an outer region channel. Hence, the probability that a nonblocked call does not complete before the first handoff and is dropped at the first handoff is $P_{h1}(1) = \eta_A h_A P_{h,A} + \eta_B h_B P_{h,B}$ where η_A and η_B are the probabilities that a new nonblocked call uses an inner region and an outer region channel respectively and are given by

$$\eta_A = \frac{\lambda_A \sum_{i_A=0}^{C_A-1} \sum_{i_B=0}^{C_B} p(i_A, i_B)}{\lambda_A \sum_{i_A=0}^{C_A-1} \sum_{i_B=0}^{C_B} p(i_A, i_B) + \lambda_A \sum_{i_B=0}^{C_B-C_h-1} p(C_A, i_B) + \lambda_B \sum_{i_A=0}^{C_A} \sum_{i_B=0}^{C_B-C_h-1} p(i_A, i_B)} \tag{4.35}$$

$$\eta_B = 1 - \eta_A.$$

The terms h_A and h_B are the probabilities that handoff occurs before call completion for a nonblocked call using an inner region channel and an outer region channel respectively. Because of the exponential assumption for residual times and call durations, h_A and h_B are given by

$$h_A = \frac{\mu_A}{\mu + \mu_A}; \quad h_B = \frac{\mu_B}{\mu + \mu_B}. \tag{4.36}$$

A nonblocked call at the ith, $i = 2, 3, 4, \ldots$, handoff can only be using an outer region channel since a call using an outer region channel does not switch back to an inner region channel. A nonblocked call is dropped at the ith handoff if the previous $(i-1)$ handoffs were successful, the call does not complete before the ith handoff and the ith handoff is unsuccessful. Hence, the

probability that a nonblocked call is dropped at the ith handoff is $P_{h1}(i) = s_1(h_B(1-P_{h,B}))^{i-2}h_B P_{h,B}$ where $s_1 = (h_A\eta_A(1-P_{h,A}) + h_B\eta_B(1-P_{h,B}))$ is the probability that a nonblocked call does not complete before the first handoff and is successful at the first handoff. Therefore, the average call dropping probability is

$$\begin{aligned} P_d &= \sum_{i=1}^{\infty} P_{h1}(i) \\ &= P_{h1}(1) + s_1 \sum_{i=2}^{\infty} h_B^{i-1}(1-P_{h,B})^{i-2}P_{h,B} \\ &= P_{h1}(1) + s_1 \frac{h_B P_{h,B}}{1-h_B(1-P_{h,B})}. \end{aligned} \tag{4.37}$$

The handoff activity, H_n, defined as the expected number of handoff call attempts for a nonblocked call, is another system parameter of interest [26]. A nonblocked call has i handoff attempts if (1) the call is dropped at ith handoff or (2) the call completes after ith handoff. The probability that a nonblocked call does not complete before the first handoff and is dropped at the first handoff is $P_{h1}(1)$. The probability that a nonblocked call does not complete before the ith handoff and is dropped at the ith, $i = 2, 3, 4, \ldots$, handoff is $P_{h1}(i)$. The probability that a nonblocked call does not complete before the first handoff and completes before the second handoff is $P_{h2}(1) = s_1(1-h_B)$ where $(1-h_B)$ is the probability that a nonblocked call using an outer region channel completes before it is handed off. The probability that a nonblocked call does not complete before the ith, $i = 2, 3, 4, \ldots$, handoff and completes before the $(i+1)$th handoff is $P_{h2}(i) = s_1(h_B(1-P_{h,B}))^{i-1}(1-h_B)$. The handoff activity can then be obtained as

$$
\begin{aligned}
H_n &= \sum_{i=1}^{\infty} i(P_{h1}(i) + P_{h2}(i)) \\
&= \left[P_{h1}(1) + s_1 \frac{P_{h,B}(1-(1-h_B(1-P_{h,B}))^2)}{(1-P_{h,B})(1-h_B(1-P_{h,B}))^2} \right] \\
&\quad + \left[\frac{s_1(1-h_B)}{(1-h_B(1-P_{h,B}))^2} \right].
\end{aligned}
\tag{4.38}
$$

4.5 An Approximate Method

In Section 4.4, the state probabilities $p(i_A, i_B)$ for a 2-region FRP system was obtained by iteratively solving the 2-dimensional Markov chain of Figure 4.8. As the number of states increases, the computation becomes very time-consuming. We now present an approximate method for analyzing the performance of the 2-region FRP system with no reserved channels for handoff calls, i.e. $C_h = 0$. This method allows the state probabilities to be expressed in closed form.

The system can be represented approximately by the two-dimensional Markov chain shown in Figure 4.9. The pair (i_a, i_b) denotes the state of the system, where i_a is the number of (inner or outer region) channels used by new calls of MS's which were located in the inner region at the time of the call arrival and which have not yet exited the inner region (for convenience, such calls are referred to as type 1 calls); i_b is the number of channels used by all other calls in a cell, i.e. an intracell handoff call, an intercell handoff call or a new outer region call, (for convenience, such calls are referred to as type 2 calls). Note that $i_a(i_b)$ is different from $i_A(i_B)$ used in Section 4.4. The maximum number of channels that is available for use by type 1 calls is C since these calls can overflow into outer region channels whereas the maximum number of channels available to type 2 calls is C_B. Since the number of channels in a cell is C, we must have $i_a + i_b \leq C$. The

residual time within the inner region (cell) of a MS with a type 1 (2) call is assumed to be exponentially distributed with a mean of $1/\mu_A$ and $1/\mu_B$ as given by (4.21) and (4.23) respectively. The parameters, λ_a and λ_b, are the mean intracell and intercell handoff call arrival rates. The intracell handoff calls come from MS's located in the inner region of the cell. Thus,

$$\lambda_a = E[I_a]\mu_A. \tag{4.39}$$

The intercell handoff calls come from MS's located in the outer regions of neighboring cells, i.e.

$$\lambda_b = E[I_b]\mu_B. \tag{4.40}$$

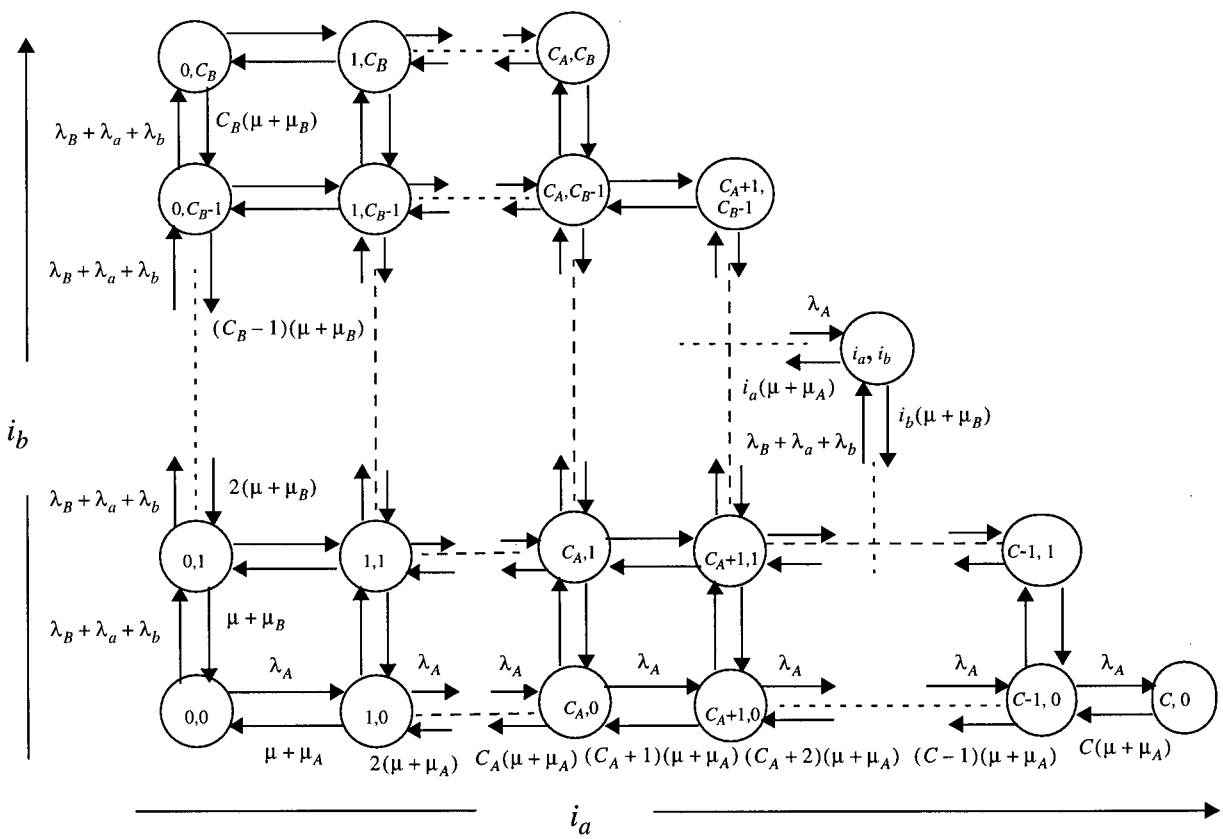

Figure 4.9 State-transition diagram for the approximate model for 2-region FRP with mobile users.

The model in Figure 4.9 is approximate because it does not correspond exactly to the actual system behavior. In particular, if a call arriving to the outer region results from an intracell handoff call, $i_a + i_b$ should remain the same. But, in our approximate model, $i_a + i_b$ is increased by 1 as shown in Figure 4.9 corresponding to the upward transition rate contribution of λ_a. However, the approximate method still provides fairly accurate results. Since the Markov chain represented in Figure 4.9 is reversible, the stationary distribution has a product form solution [25] as follows

$$p(i_a, i_b) = p(0)\frac{\rho_a^{i_a}\rho_b^{i_b}}{i_a!\,i_b!} \tag{4.41}$$

where $p(0) = \left(\sum_{i_a=0}^{C_A}\sum_{i_b=0}^{C_B}\frac{\rho_a^{i_a}\rho_b^{i_b}}{i_a!\,i_b!} + \sum_{i_a=C_A+1}^{C}\sum_{i_b=0}^{C-i_a}\frac{\rho_a^{i_a}\rho_b^{i_b}}{i_a!\,i_b!}\right)^{-1}$, $\rho_a = \frac{\lambda_A}{\mu+\mu_A}$ and $\rho_b = \frac{\lambda_B+\lambda_a+\lambda_b}{\mu+\mu_B}$.

In Figure 4.9, the new call blocking probability for the inner region is the sum of the probabilities of states for which $i_a \geq C_A$ and $i_a + i_b = C$, i.e.

$$P_{b,a} = \sum_{i_a=C_A}^{C} p(i_a, C-i_a). \tag{4.42}$$

The new call blocking probability for the outer region is the sum of the probabilities of states for which $i_b = C_B$ or $i_a + i_b = C$, i.e.

$$P_{b,b} = \sum_{i_a=0}^{C_A-1} p(i_a, C_B) + \sum_{i_a=C_A}^{C} p(i_a, C-i_a). \tag{4.43}$$

The average new call blocking probability, P_b, is given by

$$P_b = \frac{\rho_A}{\rho} P_{b,a} + \frac{\rho_B}{\rho} P_{b,b}. \tag{4.44}$$

For the approximate model in Figure 4.9, the handoff call blocking probabilities for the inner and outer regions are also given by $P_{b,b}$. The call dropping probability and handoff activity are obtained from (4.37) and (4.38) with the replacement of $P_{h,A}$ and $P_{h,B}$ by P_h, η_A by η_a and η_B by η_b; η_a and η_b are the probabilities that a new nonblocked call originates from an inner and an outer region respectively and are given by

$$\begin{aligned} \eta_a &= \frac{\lambda_A(1-P_{b,a})}{\lambda_A(1-P_{b,a}) + \lambda_B(1-P_{b,b})} \\ \eta_b &= 1-\eta_a. \end{aligned} \tag{4.45}$$

For stationary users, $P_{b,a}$ and $P_{b,b}$ are given by (4.42) and (4.43) respectively, with $\mu_A = \mu_B = \lambda_a = \lambda_b = 0$.

4.6 Numerical Results and Discussions

In this section, the numerical results obtained from the analysis for 2-region FRP with mobile users are provided first. Then, the simulation results for different mobility models with fixed mobile speed as well as uniform mobile speed are obtained for comparison purposes.

4.6.1 Analytic Results

To provide numerical results, we assume that a total of $M = 140$ channels are available in the system and an average call duration, $1/\mu$, of 120 sec. The capacity is taken to be the offered traffic that can be supported at $GOS = 0.01$. For stationary users, GOS is equal to P_b.

A cluster size, $N = 7$, is used for the conventional FCA. Hence, each cell will have 20 channels and the cluster size, N_B, for the outer region is 7.

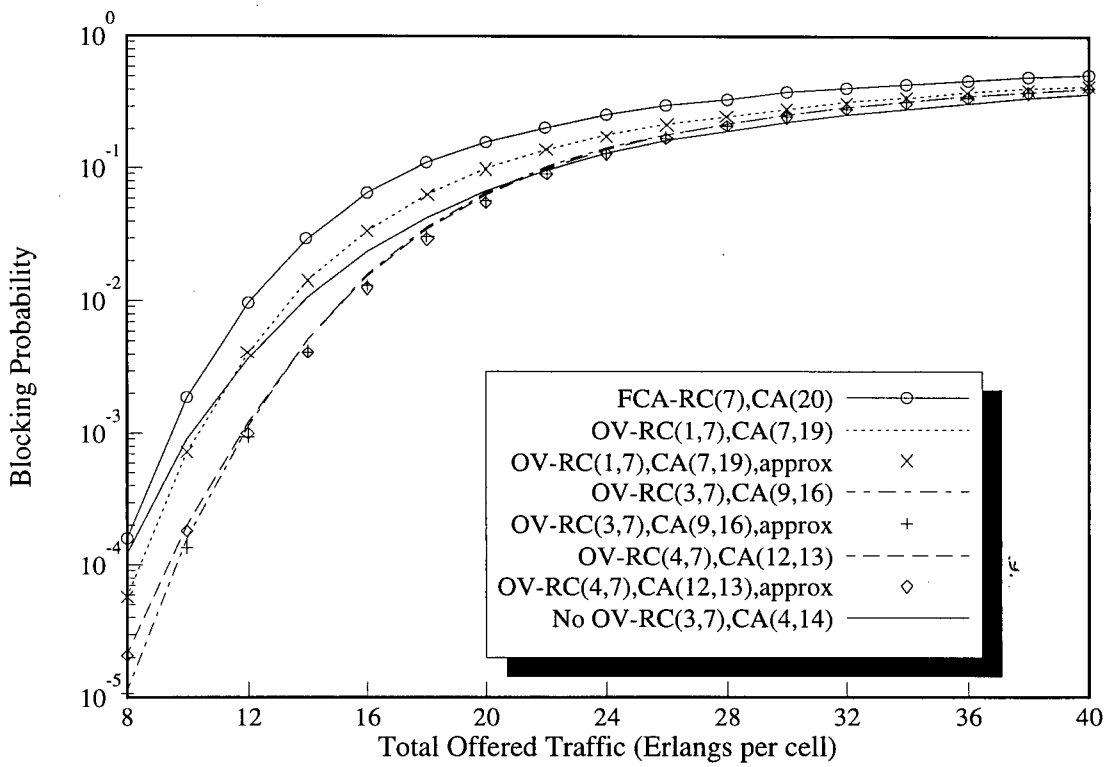

Figure 4.10 Average new call blocking probability for stationary users for different RC(N_A,N_B): OV-overflow.

Figure 4.10 shows the average new call blocking probability, P_b, of a 2-region FRP system with stationary users and different combinations of reuse cluster sizes, RC(N_A, N_B), for inner and outer regions. In Figure 4.10, for a given RC(N_A, N_B) the number of channels, CA(C_A, C_B), allocated to each region (subject to the constraint in (4.17)) has been chosen so as to provide the highest capacity at $P_b \approx 0.01$. It can been seen that conventional FCA has the lowest capacity. The average new call blocking probabilities, P_b, for RC(3,7) and RC(4,7) are better than P_b for RC(1,7). RC(3,7) is slightly better than RC(4,7) for $P_b < 0.01$. At $P_b = 0.01$,

FRP using RC(3,7) without overflow can carry about 15% more traffic than conventional FCA. FRP using RC(3,7) with overflow can carry about 12% more traffic than FRP using RC(3,7) without overflow. Results obtained using the simple product form solution of (4.41) are also plotted in Figure 4.10. It can be seen that they agree closely with the exact results.

To study the effect of mobility on the 2-region FRP system, we compare the numerical results for three cases with different values for the system parameters V_f, r_A and r_B: Case 1: $V_f = 50$ Km/hr and $r_B = 2$ Km; Case 2: $V_f = 25$ Km/hr and $r_B = 2$ Km; Case 3: $V_f = 50$ Km/hr and $r_B = 10$ Km. In all three cases, r_A is given by (4.16). The mean outgoing handoff rates, μ_A or μ_B, per calling mobile for Case 1, Case 2 and Case 3 are in decreasing order. The new call blocking probability, P_b, and call dropping probability, P_d, using RC(3,7) for Case 1 with different CA(C_A, C_B) are shown in Figure 4.11 (a) and (b) respectively. For stationary users at $GOS \approx 0.01$, CA(9,16) gives the best performance for RC(3,7) as shown in Figure 4.10. When mobile users are assumed, there is more traffic to be carried in the outer region channels (compared to the stationary user case) due to the handoff calls from a cell's inner region and neighboring cells. In Figure 4.11 (a) and (b), CA(9,16) no longer provides the best performance because more channels should be allocated to the outer region to handle the increased traffic in the outer region. It can be seen that both P_b and P_d decrease as C_B increases. It means that more channels should be assigned to the outer region with mobile users. In Figure 4.11 (a) and (b), P_b and P_d for CA(4,18) and CA(2,19) are very close. It was found that CA(4,18) gives the best overall performance among all CA(C_A, C_B) for $GOS \approx 0.01$. For Case 2 and Case 3, the best performance is obtained with CA(7,17) for RC(3,7).

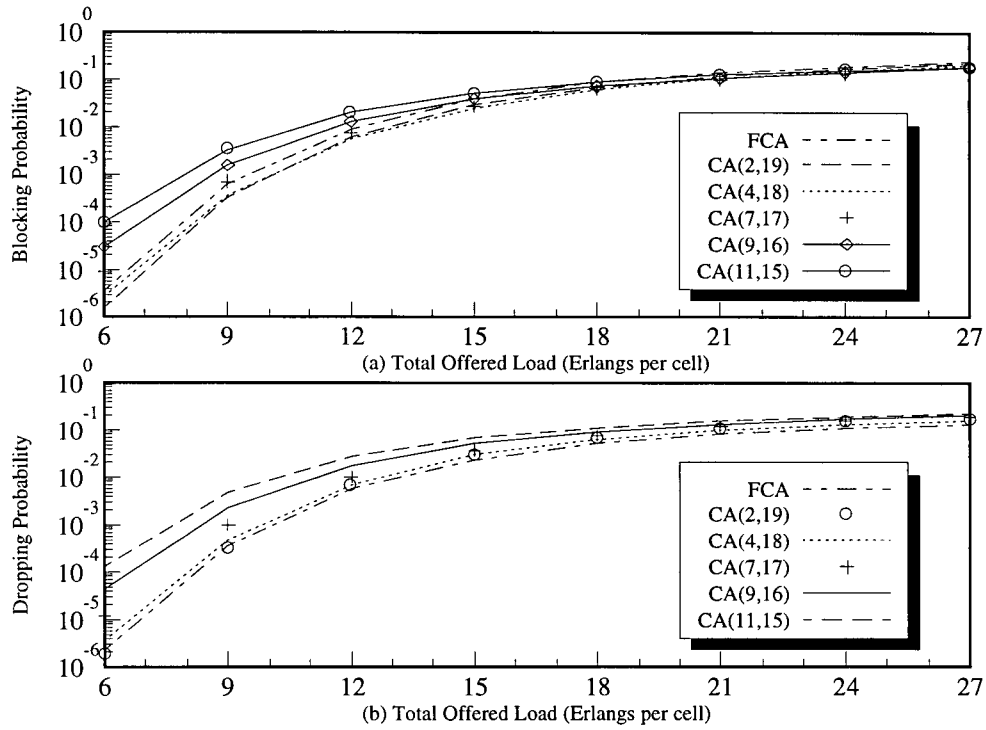

Figure 4.11 (a) Average new call blocking and (b) call dropping probabilities for Case 1 with C_h =0 and different CA(C_A,C_B) for Case 1.

The average new call blocking probability, P_b, and call dropping probability, P_d, with no reserved handoff channels for Cases 1, 2 and 3 are shown in Figure 4.12. For case 1, P_d is slightly higher than P_b at low traffic load due to the high handoff rate. In cases 2 and 3, P_d is lower than P_b. Both P_b and P_d increase with μ_A (or μ_B), because the traffic load is increased in the outer region due to more frequent handoff calls. For a given offered traffic load, P_d increases faster with μ_A (or μ_B) than P_b. This is because the handoff call arrival rate increases significantly whereas the new call arrival rate remains the same. For low μ_A (or μ_B) in Case 3, P_d is much lower than P_b, e.g. P_d = 0 for μ_A and μ_B = 0. But, the difference between P_b and P_d decreases with μ_A (or μ_B) as evidenced by the P_b and P_d curves for Case 1 being close due to higher handoff rate. The handoff activity curves for conventional FCA and RC(3,7) with no

reserved handoff channel for the three cases are shown in Figure 4.13. As expected, the handoff activity of 2-region FRP is higher than that of FCA because in 2-region FRP there are handoff attempts for calls moving from the inner region to the outer region. Also, handoff activity increases with μ_A (or μ_B) due to MS's crossing region or cell boundaries more frequently. In both figures, the approximate results for P_b, P_d and H_n obtained using the product form solution in (4.41) are reasonably good.

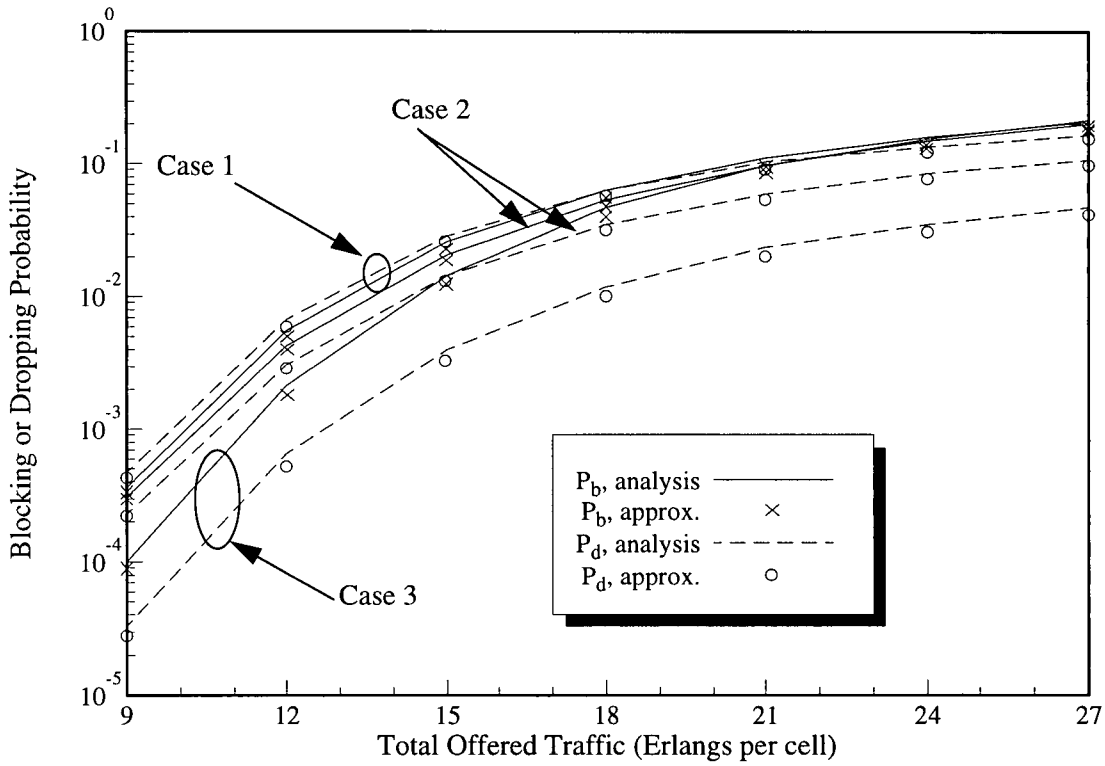

Figure 4.12 Average new call blocking and call dropping probabilities with $C_h = 0$ for Cases 1, 2 and 3.

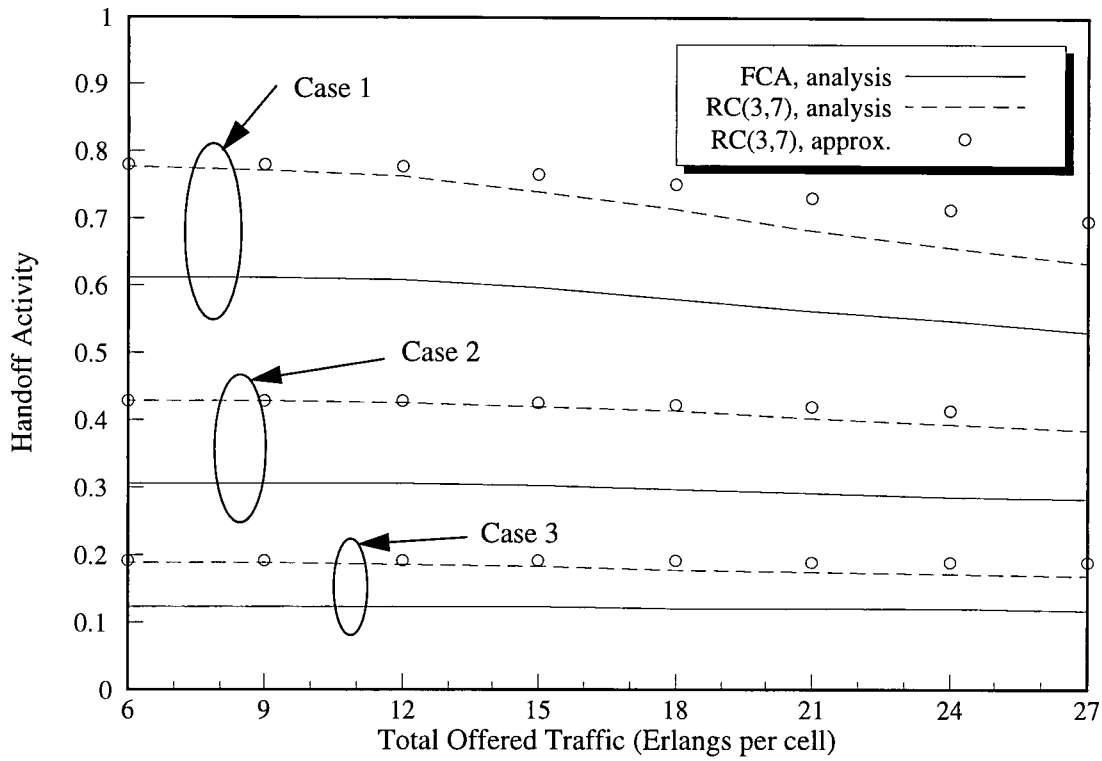

Figure 4.13 Handoff activity with $C_h = 0$ for Cases 1, 2 and 3.

The effect of C_h on P_b and P_d for Case 1 is shown in Figure 4.14. It can be seen that as C_h increases, P_d decreases whereas P_b increases. Similar observations were made for Cases 2 and 3. To determine the value of C_h to be used for a given system, we can maximize the system capacity at a given GOS value. The capacity for Case 1 with different C_h values at $GOS \approx 0.01$ for α ranging from 0.1 to 0.9 is shown in Figure 4.15. The capacity for $C_h = 0$ is slightly decreasing with α because P_d is slightly higher than P_b as shown in Figure 4.14 for $GOS \approx 0.01$. For $0.1 \leq \alpha \leq 0.65$, the maximum capacity is obtained with $C_h = 0$ and thus the optimum number, C_{opt}, of reserved channels for handoff calls is 0. For $0.65 \leq \alpha \leq 0.8$ and $0.8 \leq \alpha \leq 0.9$, C_{opt} is 1 and 2 respectively. For $C_h = 3$ or 4, P_d is reduced as shown in Figure 4.14 but so is the capacity.

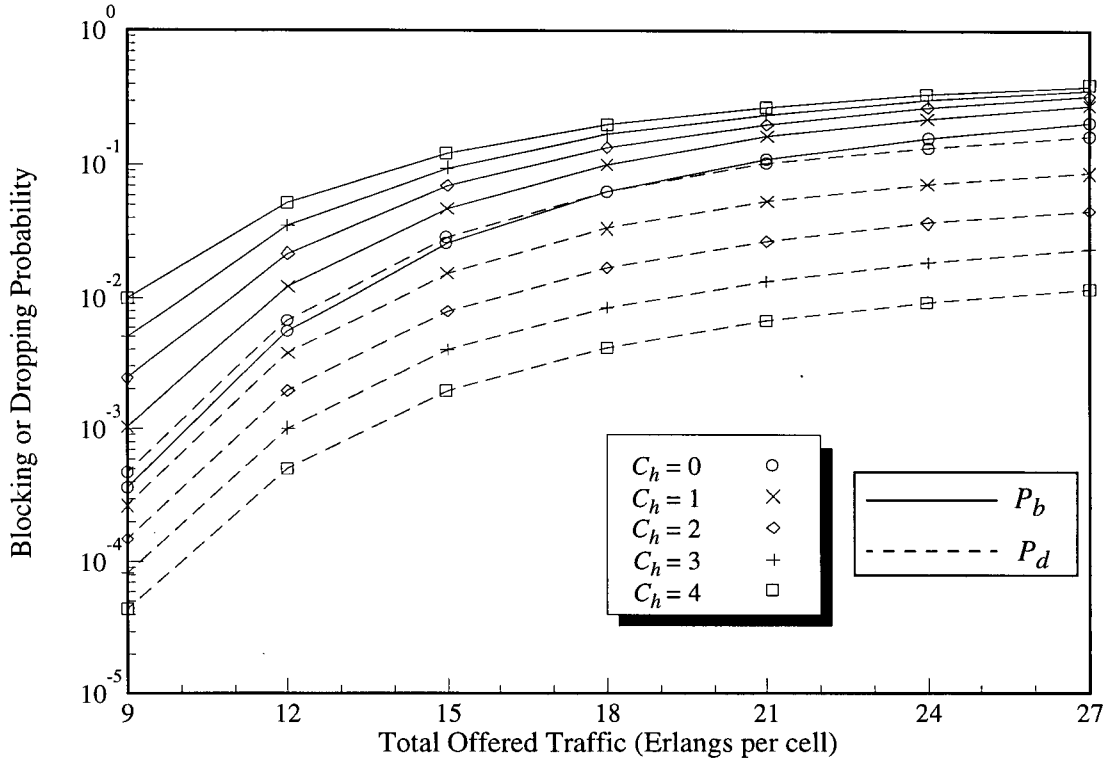

Figure 4.14 Average new call blocking and call dropping probabilities for Case 1 and different values of C_h.

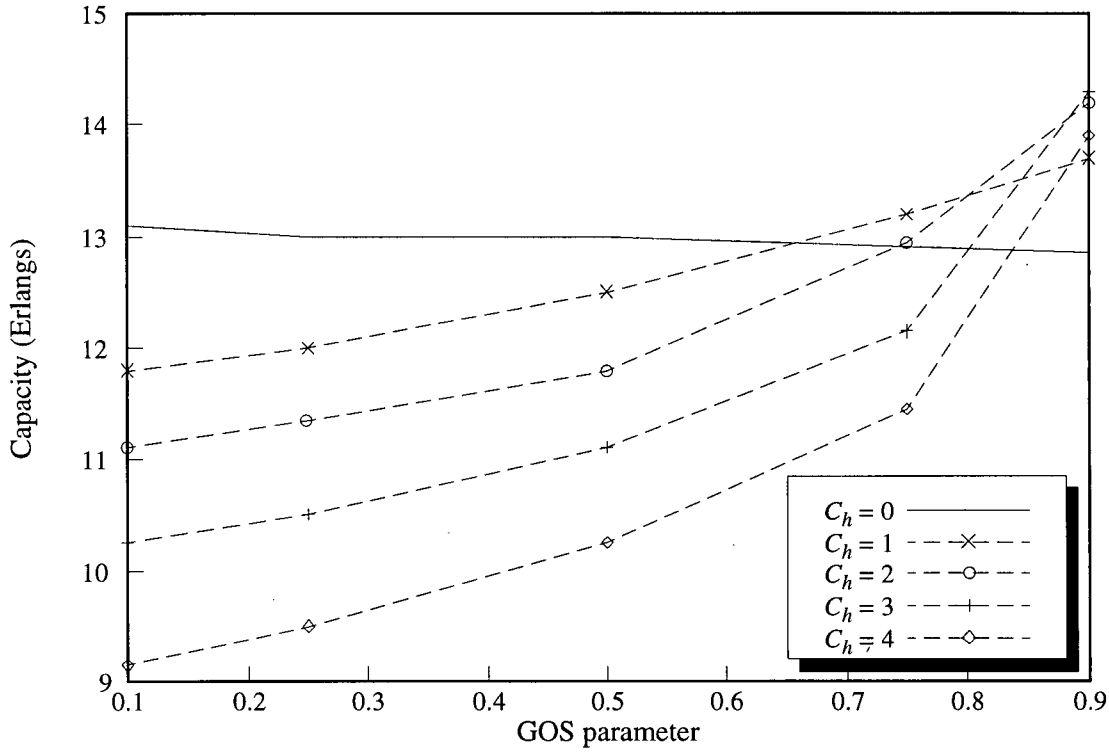

Figure 4.15 Capacity of 2-region FRP system with different C_h values at $GOS = 0.01$ for Case 1.

The maximum capacities (in Erlangs) and C_{opt} of FRP and FCA for all three cases for $\alpha = 0.1, 0.5$ and 0.9 at $GOS = 0.01$ are shown in Tables 4.1, 4.2 and 4.3 respectively. The capacities for both FRP and FCA increase as μ_A (or μ_B) decreases. This is because the number of handoffs increases and it degrades the performance. For $\alpha = 0.1$ and 0.5, C_{opt} is zero, i.e., no channels should be reserved for handoff calls. A low value of α corresponds to P_b being more important than P_d. In this case, C_{opt} should be small so as to keep P_b low. For $\alpha = 0.9$, the values of C_{opt} are non-zero and increase with μ_A (or μ_B). This is because for large α, C_{opt} should be higher to favor the handoff call in order to keep P_d low. The capacity improvement for FRP relative to FCA is also shown in the tables. The capacity improvements for Cases 1, 2 and 3 are 6%, 12% and 19% at $\alpha = 0.1$, which are smaller than the improvements with stationary users. The capacity improvement decreases with μ_A (or μ_B) because in 2-region FRP, the number of intra-cell handoffs of MS's moving from inner to outer region increase. In FCA, no intra-cell handoff occurs. Therefore, FRP will be less effective in a system with high handoff rates. For Case 1 and $\alpha = 0.9$, the capacity of FRP is even less than that of FCA.

The capacities of FRP and FCA at $GOS = 0.01$ and $\alpha = 0.5$ for Case 1 with different number of available system channel, M, are shown in Table 4.4. The number of channels assigned to 2-region FRP shown in the table gives the best overall performance among all $\mathrm{CA}(C_A, C_B)$ for $GOS \approx 0.01$. The value of C_{opt} is equal to 0 for all cases in the table. As expected, both capacities increase with M. It is found that the capacity improvement of FRP relative to FCA is about 4% even for large values of M.

Table 4.1 Capacity (Erlangs) and C_{opt} of $RC(3, 7)$ and FCA at $GOS \approx 0.01$ and $\alpha = 0.1$.

Case	1	2	3
FRP	13.0, $C_{opt} = 0$	13.7, $C_{opt} = 0$	14.6, $C_{opt} = 0$
FCA	12.3, $C_{opt} = 0$	12.3, $C_{opt} = 0$	12.3, $C_{opt} = 0$
Improvement	5.7%	11.4%	18.7%

Table 4.2 Capacity (Erlangs) and C_{opt} of $RC(3, 7)$ and FCA at $GOS \approx 0.01$ and $\alpha = 0.5$.

Case	1	2	3
FRP	13.1, $C_{opt} = 0$	14.0, $C_{opt} = 0$	15.2, $C_{opt} = 0$
FCA	12.6, $C_{opt} = 0$	13.0, $C_{opt} = 0$	13.2, $C_{opt} = 0$
Improvement	4.0%	7.7%	15.2%

Table 4.3 Capacity (Erlangs) and C_{opt} of $RC(3, 7)$ and FCA at $GOS \approx 0.01$ and $\alpha = 0.9$.

Case	1	2	3
FRP	14.3, $C_{opt} = 3$	16.0, $C_{opt} = 2$	18.4, $C_{opt} = 1$
FCA	14.5, $C_{opt} = 2$	15.3, $C_{opt} = 1$	16.4, $C_{opt} = 1$
Improvement	-1.4%	4.6%	12.2%

Table 4.4 Capacity (Erlangs) comparison for $RC(3, 7)$ and FCA at $GOS \approx 0.01$ and $\alpha = 0.5$ for Case 1 with different M.

M	140	210	280
FRP	13.1, CA(4,18)	22.0, CA(4,28)	31.1, CA(4,38)
FCA	12.6, CA(20)	21.0, CA(30)	29.8, CA(40)
Improvement	4.0%	4.8%	4.4%

4.6.2 Simulation Results

Simulation results for the three mobility models described in Section 4.2 are obtained for Case 1, i.e., $V_f = 50$ Km/hr and $r_B = 2$ Km, which has the highest handoff rate. For mobility Model A, a fixed mobile speed, $V_f = 50$ Km/hr as well as a uniformly distributed mobile speed in $[E[V]/2, 3E[V]/2]$ with $E[V] = 50$ Km/hr are considered. For mobility Models B and C, a uniformly distributed mobile speed is assumed. The random time used in Model B is $T = 5$ seconds so that the MS's are expected to change speed and direction frequently within a cell. The simulated area consists of 49 2-region hexagonal cells. The cluster sizes choice is RC(3,7) and the channel allocation to each cell is CA(4,18). The simulation results are collected from the central 7 cells to avoid the edge effect. When the MS reaches the system boundary, it is assumed that the MS will return to the system with an angle which is uniformly distributed in $(-\pi/4, \pi/4)$ relative to the normal direction of the cell boundary as shown in Figure 3.11. All the simulation results shown have 99% confidence intervals which are within ±5 % of the values plotted.

The blocking probabilities obtained from the analysis and simulation for three mobility models with $C_h = 0$ and $C_h = 2$ are shown in Figure 4.16 (a) and (b). It can be seen that the simulation results for Model A and Model C are very similar and are close to those obtained from the analysis. This is because the Models A and C agree with our assumptions that MS's do not change speed and direction within an inner region or a cell. The blocking probability for Model B is slightly lower than that for other models.

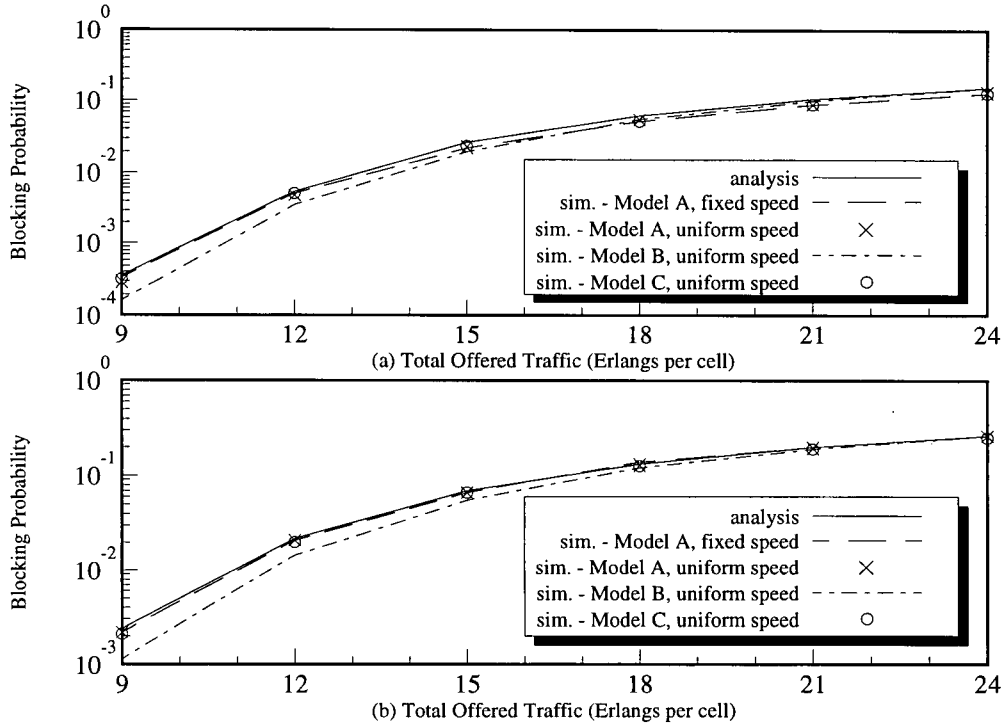

Figure 4.16 Blocking probabilities obtained from the analysis and simulation for different mobility models for (a) $C_h = 0$ and (b) $C_h = 2$.

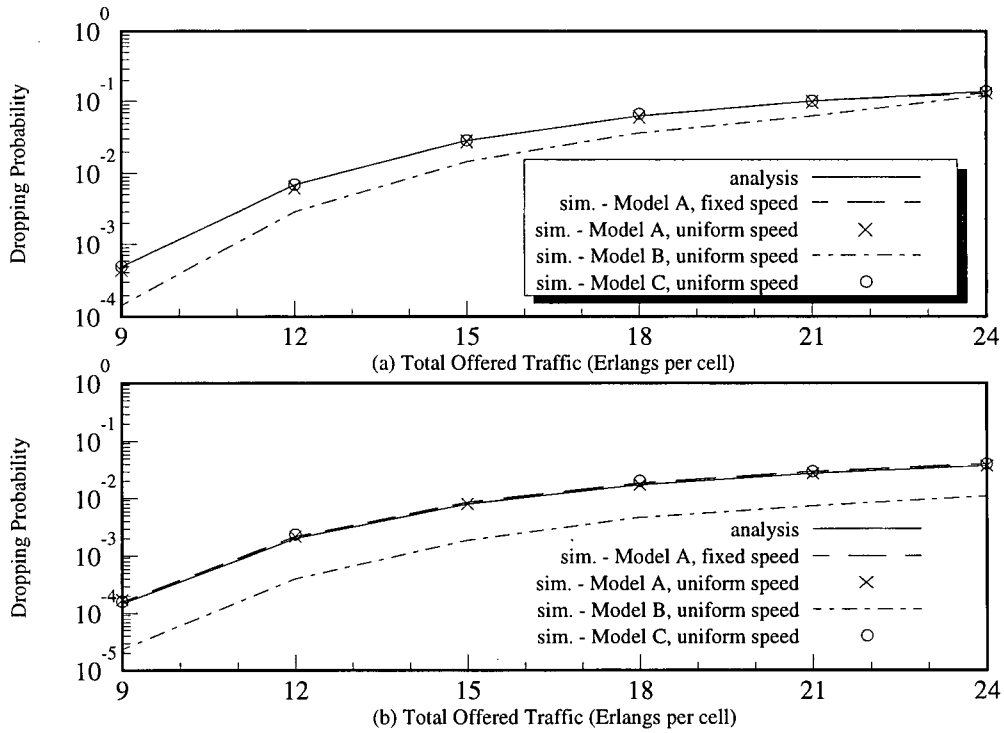

Figure 4.17 Dropping probabilities obtained from the analysis and simulation for different mobility models for (a) $C_h = 0$ and (b) $C_h = 2$.

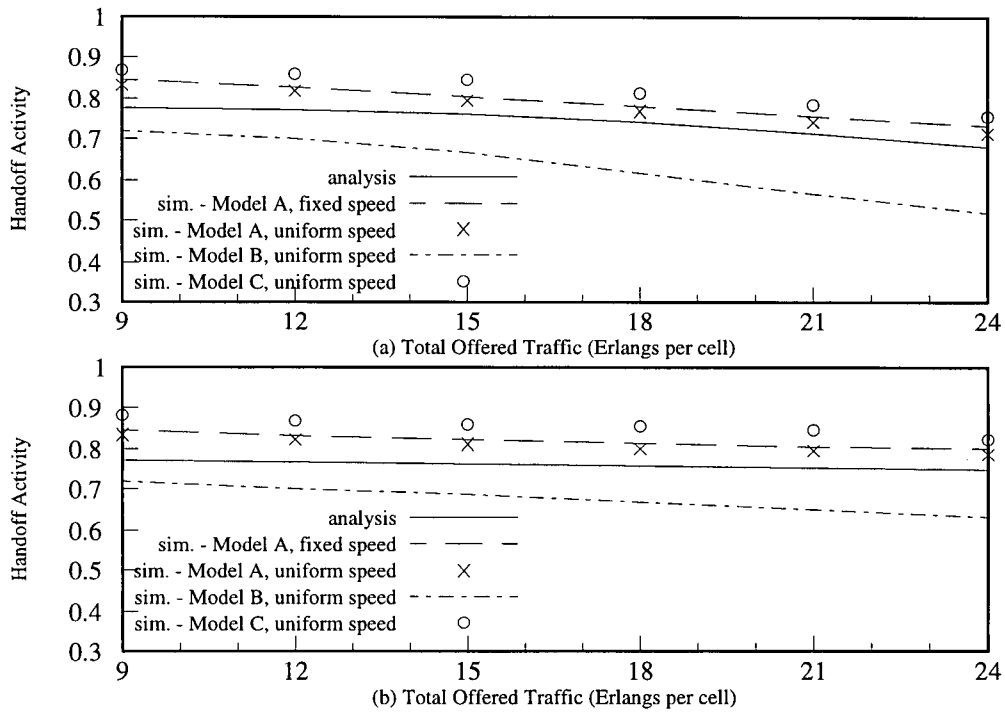

Figure 4.18 Handoff activities obtained from the analysis and simulation for different mobility models for (a) $C_h = 0$ and (b) $C_h = 2$.

The dropping probabilities obtained from the analysis and simulation for the three mobility models for $C_h = 0$ and $C_h = 2$ are shown in Figure 4.17 (a) and (b). The simulation results for Model A and Model C are very close to those obtained from the analysis due to the agreement of the assumptions. The dropping probability for Model B is lower because the MS's tend to stay longer in a cell and thus require fewer handoffs as evidenced in Figure 4.18. This figure shows that the handoff activity for Model A and Model C are similar and slightly higher than the analytic results. The difference is about 5 to 10%. Model B has the lowest handoff activity due to the longer residual time in a cell.

In Figure 4.19, three handoff cases, H1, H2 and H3, are illustrated when a new call arrives in the inner region. The higher handoff activities for the simulations with Model A and Model C

in Figure 4.18 are due to the higher handoff rate for handoff H2. From the analysis in Section 4.3, it is assumed that the mean residual time for a calling MS using an outer region channel within a cell is $1/\mu_B$. Therefore, in Figure 4.19, the mean *travelling* time for a calling mobile from inner region boundary to cell boundary or from cell boundary to cell boundary is assumed to be $1/\mu_B$ in the analysis. However, the actual mean travelling time for a calling mobile to go from the inner region boundary to the cell boundary is shorter as shown in Figure 4.19. Therefore, the handoff rate for H2 should be higher than that in the analysis. However, the higher handoff rate for H2 does not much affect the dropping probability as shown in Figure 4.17 because (1) the number of handoffs for H2 are small compared to the total number of handoffs and (2) when a mobile makes a handoff, H2, it first releases a channel and then requests a new channel from the cell; these two actions tend to offset each other.

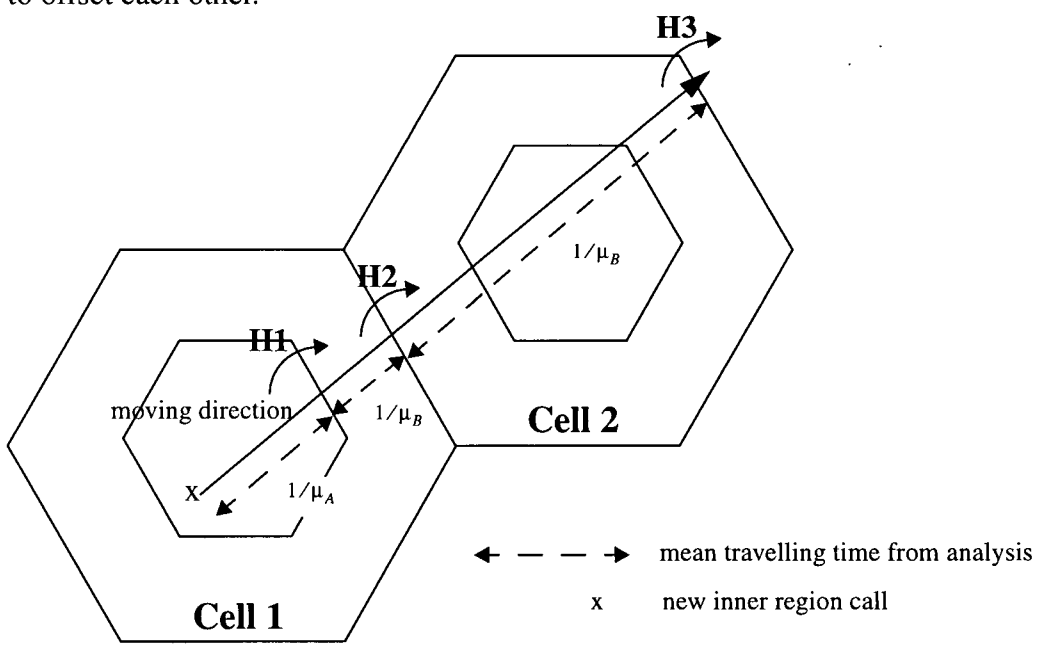

Figure 4.19 Illustration of the handoff activity for an inner region call.

4.7 Summary

The impact of mobile users in a 2-region FRP system was studied. With no channels

reserved for handoffs, the new and handoff call blocking probabilities can be approximated using a product form solution. With stationary users, the capacity can be increased by about 30% compared to conventional FCA. With mobile users, the capacities for both FRP and FCA decrease with average handoff rates. It is found that FRP outperforms FCA at the expense of an increase in average number of handoffs per call. This is due to the intra-cell handoffs of MS's crossing from inner to outer region in FRP system. However, the average number of handoffs is quite low for both systems. The capacity improvement of FRP relative to FCA is reduced as the average handoff rates increase. The results show that more channels should be assigned to the outer region as average handoff rates increase. It is found that even though prioritized handoff can reduce the call dropping probability, in some cases it may also degrade the capacity. The choice of the number of channels reserved for handoffs which maximizes the capacity was also examined. The analytic results are verified with simulation for different mobility models and agree closely with the simulation results.

The performance analyses with mobile users for FCA systems [83], [84] and [86]-[88], overlapping systems [26], [89], and 2-region FRP system [27] assume that the channel holding time is exponentially distributed. One reason is to keep the analysis tractable. Another reason is that the exponential distribution yields accurate results with certain mobility models [82]-[83] and [91]. However, the channel holding time may not be exponentially distributed for other mobility models [92]. Other distributions have been used to model channel holding times [93]-[94]. Some measurements on cellular communication systems in [95]-[96] suggest that the channel holding time can be modeled by a log-normal distribution. Even though an exponential channel holding time distribution is assumed in this study, it is expected that FRP will still outperform FCA for other distributions.

Chapter 5 A New DCA Scheme for Cellular Systems

In the channel borrowing assignment (CBA) scheme [72], the ordered channel assignment method, in which channels in a cell are numbered and assigned to a call in an ordered basis, is proposed to maintain the average co-channel reuse distance minimum. This method has been widely used in [28], [30] and [97]. In these CBA schemes, channels are permanently assigned to each cell as nominal channels as in the FCA scheme. A channel can be borrowed by a neighboring cell according to some rules. In this chapter, an ordered dynamic channel assignment scheme which does not require pre-allocation of channels to cells, DCA with interference information (DCA-WI), is presented. In this scheme, all the system channels are numbered and each BS assigns a channel to a call from the central pool. The channel assignment, inter-cell and intra-cell channel reassignment are performed in an ordered basis and attempt to minimize the effect on the interfering cells [97] and [98]. To achieve this, an Interference Information Table (IIT) is proposed for use in each cell.

In a cellular system with a given cluster size, each cell has a certain number of interfering cells. For example, with a cluster size of 7, each cell has 18 interfering cells. If the BS of cell **A** assigns channel j to a call, then channel j cannot be reused in the interfering cells of cell **A** due to co-channel interference constraints, thereby affecting the channel availability of the interfering cells. In DCA-WI, the BS of cell **A** chooses a channel j which is locked in the largest number of interfering cells of cell **A**. We say that a channel j is *locked* in a cell k if channel j cannot be used in cell k because it is being used in some interfering cells of cell k. We also refer to cell k as a *locked* cell for channel j. In other words, channel j is chosen for use in cell **A** if channel j cannot be used in the largest number of interfering cells of cell **A**. The channel assignment attempts to

minimize the effect on channel availability in all the interfering cells of cell **A**. Information about whether channel j is locked or not locked in an interfering cell of cell **A** is provided by its (cell A's) IIT. DCA-WI is a distributed DCA scheme in which the channel to be used in a cell is selected by the local BS based on information provided by its IIT. Simulation results show that DCA-WI yields a lower blocking probability than previous channel assignment schemes [28]-[30]. Its performance is close to that of idealized DCA using the Clique Packing method [32], [33].

This chapter is organized as follows: Section 5.1 describes the functions and channel updating procedures in the IIT. The DCA-WI scheme is described in Section 5.2. Simulation results for this scheme and some previously studied DCA schemes are presented in Section 5.3. The main conclusions are summarized in Section 5.4.

5.1 Interference Information Table (IIT)

The IIT contains information about the status of channels in each interfering cell. In its IIT, each cell lists all the interfering cells. As an example, consider a cellular system with a cluster size, N, of 7 as shown in Figure 5.1. In this system, the same channel cannot be reused in the cells located in the first or second tiers. Referring to Figure 5.1, there are 18 interfering cells for cell 25. If channel i is used in cell 25, then channel i cannot be used in any one of the 18 interfering cells of cell 25 due to co-channel interference constraints. The IIT for cell 25 is shown in Table 5.1. The first column lists the local cell, cell 25, and all its interfering cells in some order. The first row lists all available channels in the system. In this example, there are a total of $M = 70$ channels in the system and the channels are numbered from 1 to M as shown in Table 5.1.

The information provided by the IIT can be described as follows:

(i) A letter U in a cell's row indicates that the corresponding channel is a ***used channel** in that cell.* For example, in Table 5.1, channels 2 and 4 are used in cell 25 and channels 3, 68, 69 and 70 are used in cell 17. Table 5.2 shows a compatible IIT for cell 17.

(ii) A letter L in an interfering cell's row indicates that the corresponding channel is a ***locked channel** in the interfering cell* and that interfering cell is a ***locked cell***. For example, in Table 5.1, channel 4 is a locked channel in cell 17 with a label of 2L because two interfering cells of cell 17, namely cells 3 and 22 which are not interfering cells of cell 25, use channel 4 as can be seen in Table 5.2. Even though there is 2L in the box of (cell 17, channel 4), this is still considered as one locked cell for channel 4. Thus, in Table 5.1, channel 4 has 3 locked cells, cells 17, 32 and 33.

(iii) An empty box in a local cell's row indicates an unused channel which can be either a ***free channel** in the local cell* (if there is no letter U in the channel's column) or a ***locked channel** in the local cell* (if there is at least one letter U in the channel's column; an interfering cell in which the channel is being used is called a ***locking cell***). A free channel in a cell is a channel which is available for use in that cell. For example, in Table 5.1, channel 1 is a free channel in cell 25. Channel 3 is a locked channel in cell 25 with one locking cell, cell 17. Channel 3 cannot be used in cell 25 because cell 17 is already using that channel. A locked channel in the local cell cannot be used in the local cell unless an inter-cell channel reassignment is performed.

(iv) An empty box in an interfering cell's row means a ***free channel** in the interfering cell* if the interfering cells of that interfering cell has no U in the channel column. For example, in Table 5.1, channel 3 is a free channel in cell 33 because the interfering cells of cell 33

have no U in channel 3's column in Table 5.1. But channel 70 is not a free channel in cell 33 because cell 32 which is an interfering cell of cell 33 has a letter U in channel 70's column in Table 5.1. This requires cell 25 to know the interfering cells of its interfering cells. The free channel information about the interference cells is used in the inter-cell channel reassignment algorithm discussed in Section 5.2.2.

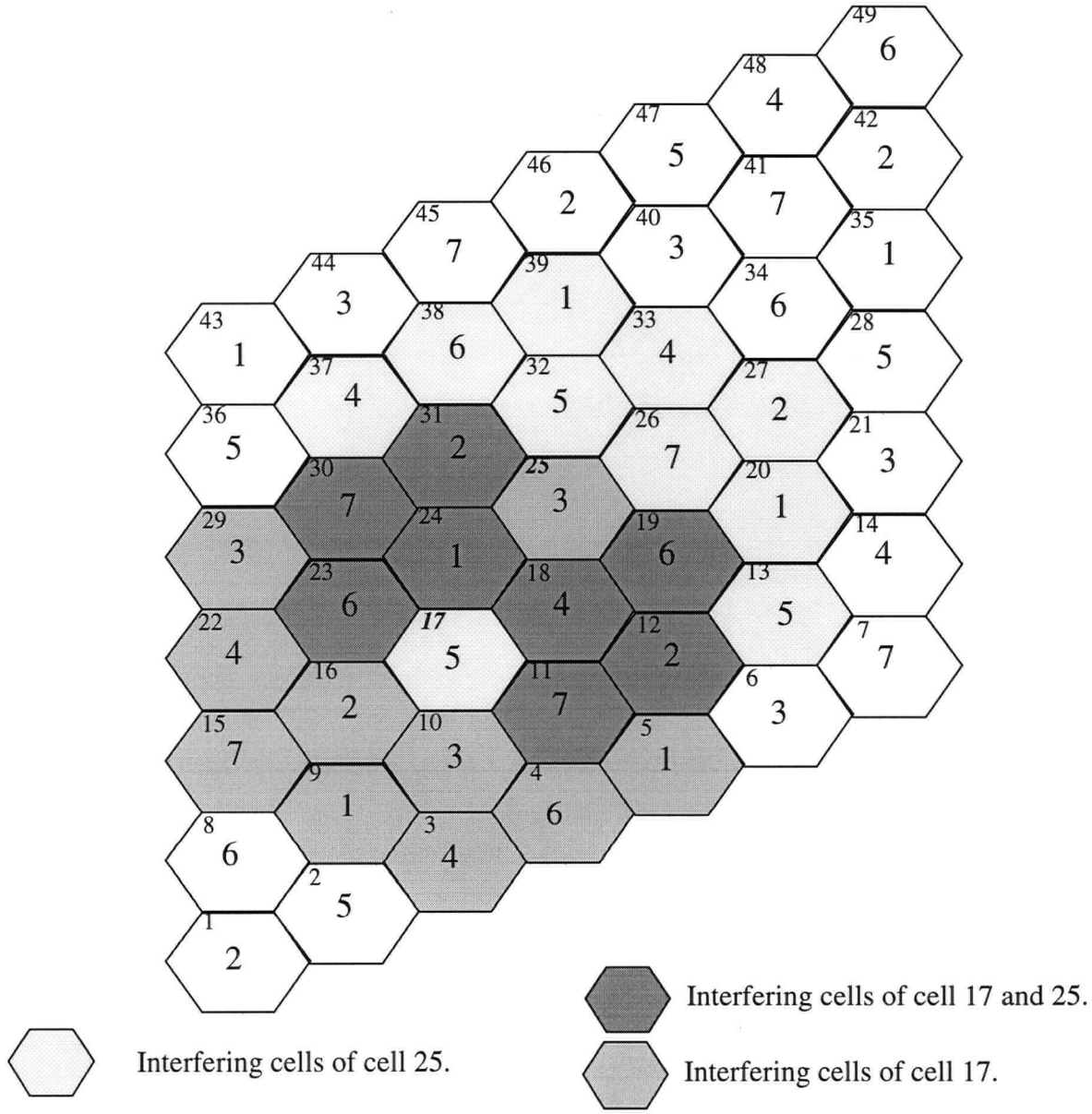

Figure 5.1 Cellular system with 49 cells for $N = 7$. The number at the center of a cell is the cluster number from 1 to 7. The number in the left upper corner is the cell number.

Table 5.1 IIT of Cell 25.

Cell No.	Channel No.									
	1	2	3	4	5	...	67	68	69	70
25		U		U						
:	:	:	:	:	:		:	:	:	:
17			U	2L	L		2L	U	U	U
:	:	:	:	:	:	...	:	:	:	:
32			L	L	L		2L	L	2L	U
33				L				L		
:	:	:	:	:	:		:	:	:	:
List of Interfering cell: 11,12,13,17,18,19,20,23,24,26,27,30,31,32,33,37,38,39										

Table 5.2 IIT of Cell 17.

Cell No.	Channel No.									
	1	2	3	4	5	...	67	68	69	70
17			U					U	U	U
3				U	U		U			
:	:	:	:	:	:		:	:	:	:
22				U		...	U			
:	:	:	:	:	:		:	:	:	:
25		U		U						
:	:	:	:	:	:		:	:	:	:
List of Interfering Cell: 3,4,5,9,10,11,12,15,16,18,19,22,23,24,25,29,30,31										

5.1.1 Channel Updating

The channel updating procedure (channel assignment, channel release or channel reassignment) is simple and involves three steps. After the BS of cell k decides to assign channel j to a call, (1) it inserts a letter U in the first row of channel j's column in its IIT, (2) it informs all its interfering cells that channel j is used in cell k; this means that a letter U is put in cell k's row and

channel j's column in each interfering cell's IIT, and (3) each interfering cell of cell k, say cell l, will inform its interfering cells e.g. cells x and y, which are not interfering cells of cell k that channel j is locked in cell l. It means that a letter L is added in the box (cell l, channel j) of cells x and y's IIT. For example, if channel 2 is used in cell 25, it will put a letter U in the box of (cell 25, channel 2) in the cell 25's IIT as shown in Table 5.1. Then, it will inform all its interfering cells that channel 2 is used by cell 25. Since cell 17 is one of the interfering cells of cell 25, a letter U is put in the box of (cell 25, channel 2) in cell 17's IIT, as shown in Table 5.2, so that cell 17 knows that channel 2 is a ***locked channel*** (in its cell) which is locked by a locking cell, cell 25. Then cell 17 compares its interfering cell set with that of cell 25. Cell 17 informs its interfering cells which are not the interfering cells of cell 25 that channel 2 is locked in cell 17. Since cell 3 is one such cell as shown in Figure 5.1, a letter L will be added in the box of (cell 17, channel 2) in cell 3's IIT.

Channel release is done following a similar three-step procedure. When the BS of cell k decides to release channel j, (1) it blanks the box of (cell k, channel j) of its IIT, (2) it informs the BS of each of its interfering cells that channel j is released in cell k, thus enabling the BS to update its IIT by blanking the box of (cell k, channel j) of each interfering cells' IIT, (3) each interfering cell, say cell l, then informs its interfering cells, e.g. cells x and y, which are not the interfering cells of cell k that channel j is no longer locked in cell l. It means that a letter L will be subtracted in the box (cell l, channel j) of cells x and y's IIT. Channel reassignment involves channel release and channel assignment.

5.2 DCA-WI Scheme

When a new call requests a channel in cell k, its BS will form an available channel list

(ACL) based on the channel information in cell k's IIT. A channel is then selected from the ACL. If the ACL is empty, the new call is blocked. The channel assignment may involve an inter-cell single channel reassignment. When a call in cell k using channel j is completed, intra-cell channel reassignment is performed in order to reduce the call blocking probability.

5.2.1 Available Channel List (ACL)

The ACL in cell k contains one of its free channel and all its locked channels with only one locking cell (i.e., channels with an empty box in the first row and exactly one box with a letter U in the channel column) in which there is at least one free channel for inter-cell single channel reassignment. For example, in Table 5.1, channel 3 is a locked channel in cell 25 with a locking cell, cell 17, in which there is a free channel, channel 1, for channel reassignment. The free channel contained in the ACL is a channel with the largest number of locked cells. If more than one such channel, a lower-numbered channel is chosen. For example, in Table 5.1, channel 5 will be chosen in the ACL although both channels 5 and 67 have 2 locked cells. The order of the channels in the ACL are determined by applying the following rules:

(i) A channel with a larger number of locked cells has a higher order; for example, in Table 5.1, the order of channel 68 is higher than that of channel 69.

(ii) In the event of a tie, a free channel has higher order than a locked channel; for example, in Table 5.1, the order of channel 5 is higher than that of channel 68. Otherwise, (in this case, they must be all locked channels),

(iii) the lower-numbered channel has higher order; for example, in Table 5.1, the order of channel 3 is higher than that of channel 69.

The ACL is used in the channel assignment strategy discussed next.

5.2.2 Channel Assignment Strategy

In DCA-WI, a channel from the ACL is selected which has the smallest value of the cost function. First, cell k calculates the cost function, $E(f)$, for the free channel f in its ACL. The cost function for the free channel is defined as

$$E(f) = I(k) - D(k, f) \tag{5.1}$$

where $D(k, f)$ is the number of locked cells for channel f in cell k's IIT and $I(k)$ is the total number of interfering cells of cell k. Then, cell k calculates the cost function value for all the locked channels in its ACL. If a locked channel j has a locking cell l (it means there is a label U in the box of (cell l, channel j) in cell k's IIT) and the call using channel j in cell l is switched to channel i which has the highest number of locked cells, then the cost function for locked channel is given by

$$E(j) = [I(k) - D(k, j) - 1] + [D(l, j) - D(l, i)]. \tag{5.2}$$

Thus, the call using channel j in cell l is switched to channel i in order to release channel j for use in cell k. In this scheme, the inter-cell single channel reassignment using $E(j)$ is based on the minimum effect on the channel availability of the interfering cells in both local and the locking cells. If more than one channel has the smallest value of E, the one which has the highest order in the ACL is selected.

Inter-cell double channel reassignment was also simulated. If no free channel or locked channel with one locking cell is available in the ACL, then find a locked channel j with two locking cells in which each locking cell must have at least one free channel for channel reassignment. Then, the call using channel j in each locking cell is switched to the free channel with the

largest number of locked cells. For simplicity, the locked channel, with two locking cells, with most number of locked cell is assigned to the call.

5.2.3 Intra-cell channel reassignment

Various intra-cell channel reassignment schemes which switch an on-going call to a released channel have been studied [28], [30]. They use the concept of channel ordering to minimize the traffic carried on the borrowed channels. In DCA-WI, the channel reassignment is based on the interference information. If channel j is released in cell k, a call in cell k using channel i which has the least number of locked cells is switched to channel j provided that the number of locked cells of channel i is smaller than that of channel j. If there is more than one such channel, the highest-numbered channel is switched. If the number of locked cells of channel i is equal to that of channel j, the call is switched to channel j provided that $j < i$. If there is more than one such channel, the highest-numbered channel is switched.

5.3 Simulation Results

The cellular system used in the simulation consists of 49 hexagonal cells as shown in Figure 5.1. A cluster size of $N = 7$ is assumed. A total of $M = 70$ channels is available in the system. New calls arrive in a cell according to a Poisson process with average arrival rate λ per cell. Call durations are exponentially distributed with a mean of $1/\mu = 3$ minutes [28]. The offered traffic (in Erlangs) to a cell is given by $\rho = \lambda/\mu$. Simulation results are presented for DCA-WI in both uniform and nonuniform traffic distributions and compared to FCA, BDCL [28], CPDCA [29] and EBCA [30] schemes. For the DCA-WI simulation results, the 99% confidence intervals are within $\pm 3\%$ of the average values shown.

The call blocking probability, P_b, averaged over all 49 cells with a uniform traffic distribution is shown in Figure 5.2. The P_b for FCA is obtained using the Erlang B formula [11]. For $P_b = 0.01$, the capacity, i.e. traffic load that can be supported by FCA is 4.5 Erlangs. The corresponding capacity values for BDCL, CPDCA, EBCA, DCA-WI and DCA-WI with double channel reassignment, DCA-WI (double), are 7.15, 7.32, 7.4, 7.56 and 7.65 respectively. These represent increases of 59%, 63%, 65%, 68% and 70% respectively over the FCA scheme. Use of inter-cell double channel reassignment yields an increase of about 2%.

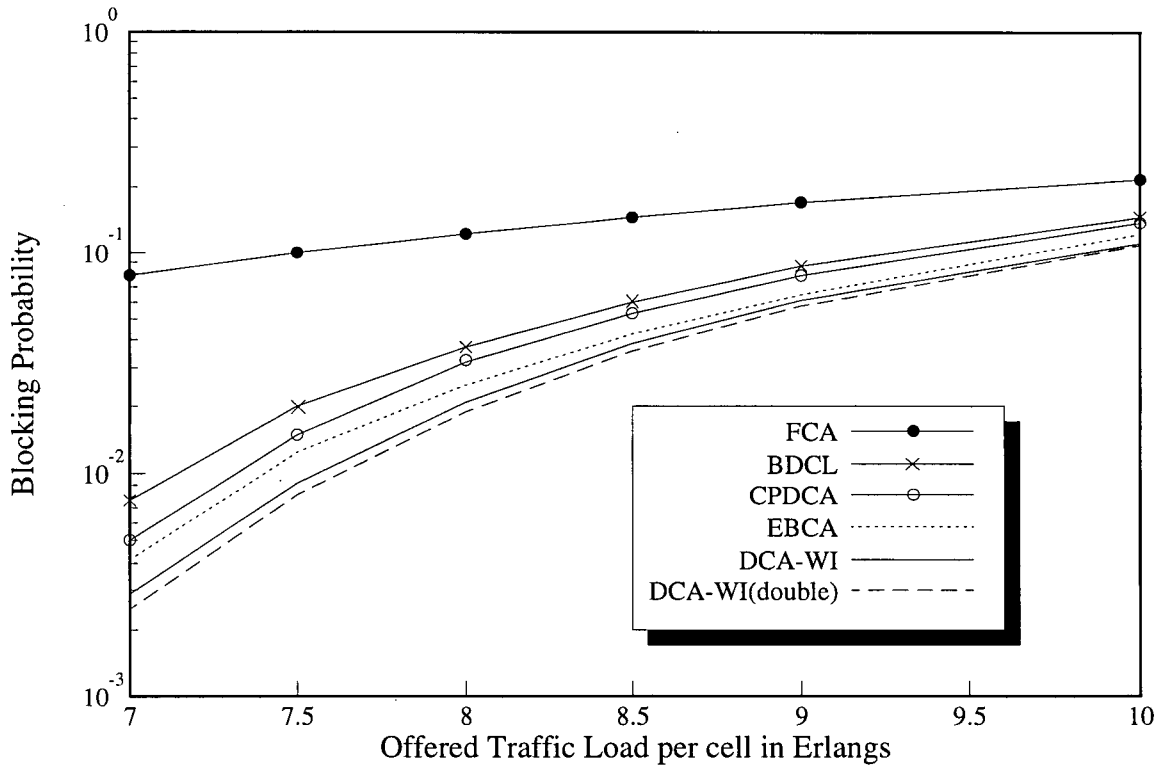

Figure 5.2 Average call blocking probability with uniform traffic distribution.

The average call blocking probability, P_c, for the central 9 cells, with 18 interfering cells, is shown in Figure 5.3. It can be seen that P_c of DCA-WI can be substantially lower than that of BDCL. The traffic loads that can be supported by BDCL, DCA-WI and DCA-WI (double) at

$P_c = 0.01$ are 6.85, 7.2 and 7.35 Erlangs respectively. A lower bound on the blocking probability, P_l, of the idealized DCA scheme obtained from the Clique Packing method [33], is also plotted in the Figure 5.3. It can be seen that the blocking probability of DCA-WI is slightly higher than the bound. For low traffic load, the blocking probability of DCA-WI with double channel reassignment is very close to the bound.

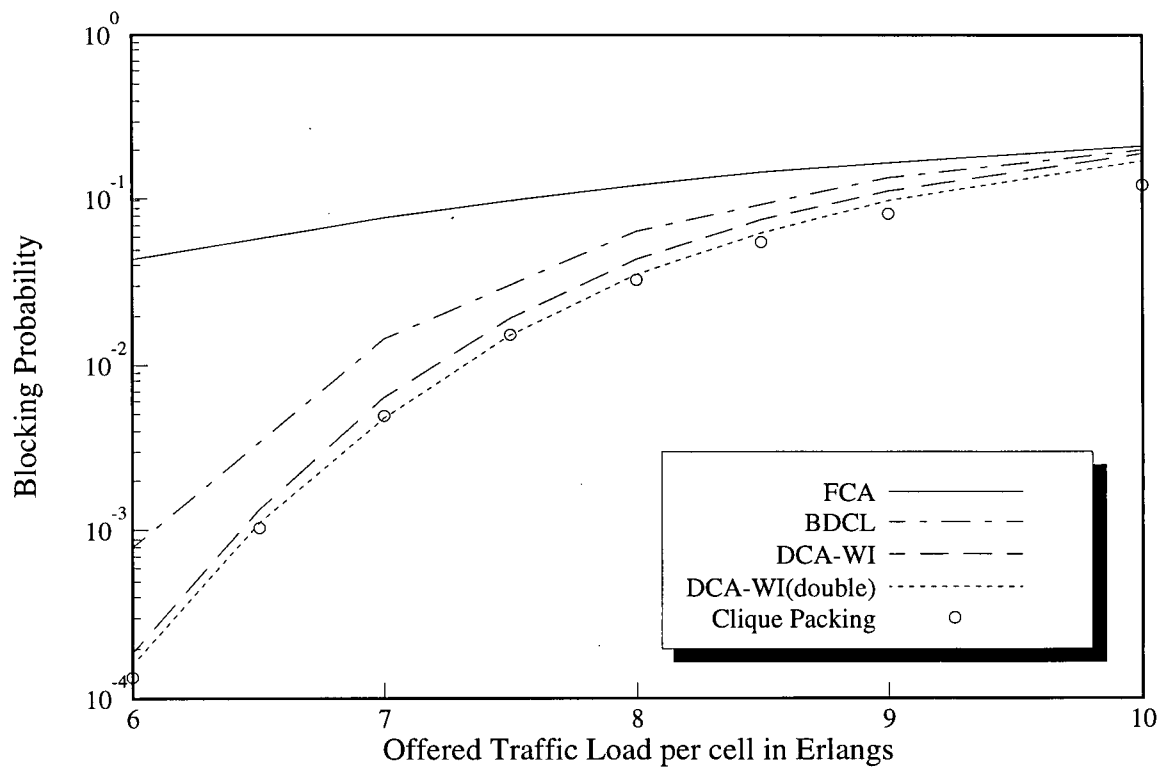

Figure 5.3 Average call blocking probability for the central 9 cells with uniform traffic distribution.

The traffic loads that can be supported at $P_c = 0.01$ for FCA, DCA-WI over central 9 cells, DCA-WI (double) over central 9 cells and Clique Packing with different values of M in uniform traffic distribution are shown in Figure 5.4. The percentage improvement in traffic load for DCA-WI over FCA decreases with M. For $M = 35$, the performance improvement is about

124% whereas for $M = 210$, the performance improvement is about 26%. The capacity of DCA-WI is slightly lower than that of the idealized DCA. With the use of inter-cell double channel reassignment, the capacity can be improved slightly, and approaches the idealized DCA limit.

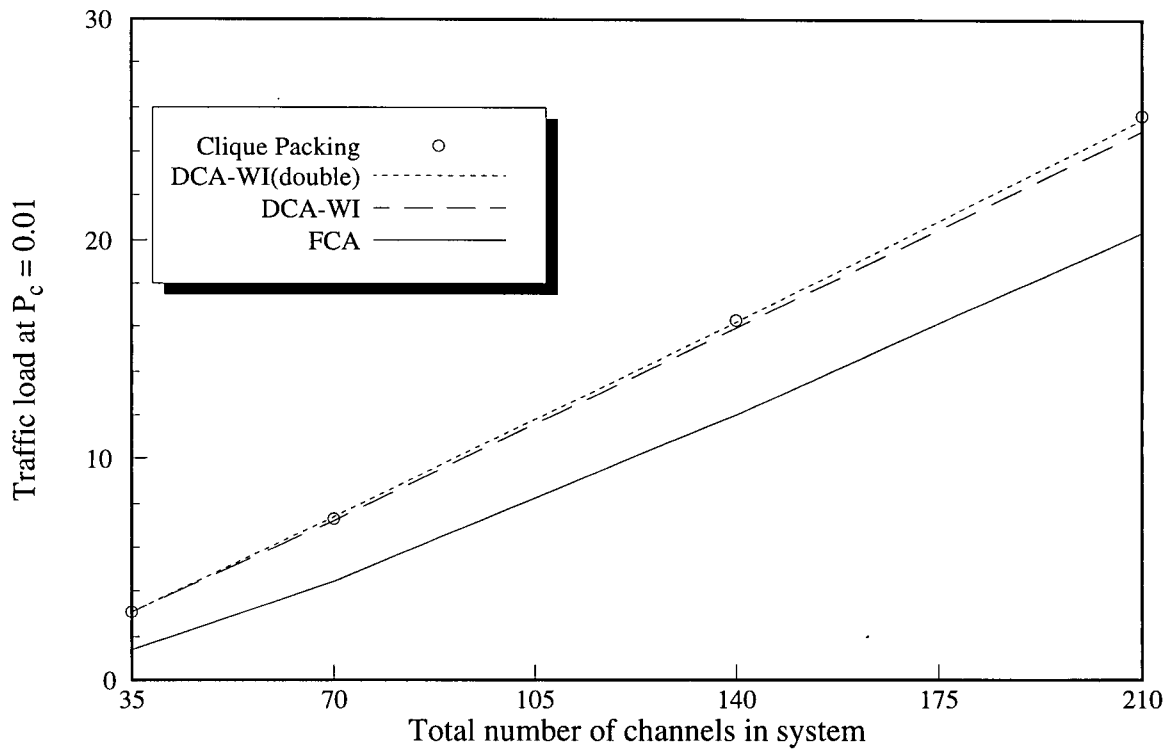

Figure 5.4 Traffic load at $P_b = 0.01$ for FCA, DCA-WI, DCA-WI(double) and idealized DCA with M in uniform traffic distribution.

Comparison of results for nonuniform traffic distributions for $M = 70$ was done using the distributions in [28, Figure 3] ("distribution A") and [29, Figure 2] ("distribution B"). The call arrival rates range from 20 to 200 calls/hour. The average offered loads over the 49 cells for distributions A and B are 4.06 and 4.59 Erlangs respectively. Figure 5.5 shows P_b of FCA, BDCL, CPDCA, DCA-WI and DCA-WI (double) with traffic distribution A. It can be seen that DCA-WI provides the lowest P_b. For $P_b = 0.01$, CPDCA and DCA-WI can carry 8% and 15% more

traffic than BDCL. Inter-cell double channel reassignment does not improve capacity by much. Figure 5.6 shows P_b of FCA, BDCL, EBCA and DCA-WI with traffic distribution B. DCA-WI provides the lowest P_b even though the P_b of EBCA is only slightly higher. The reason for the small improvement over EBCA because EBCA makes use of the information of the estimated traffic load in cells in order to assign channels to calls. But, DCA-WI does not use this information. The P_b of DCA-WI for $M = 210$ using the nonuniform traffic distribution in [27, Figure 6] ("distribution C") is shown in Figure 5.7. The per cell offered load averaged over the 49 cells for distribution C is 21.94 Erlangs. It can be seen that the P_b of DCA-WI is lower than that of BDCL and CPDCA. For the nonuniform traffic distributions considered, inter-cell double channel assignment does not improve the capacity by much.

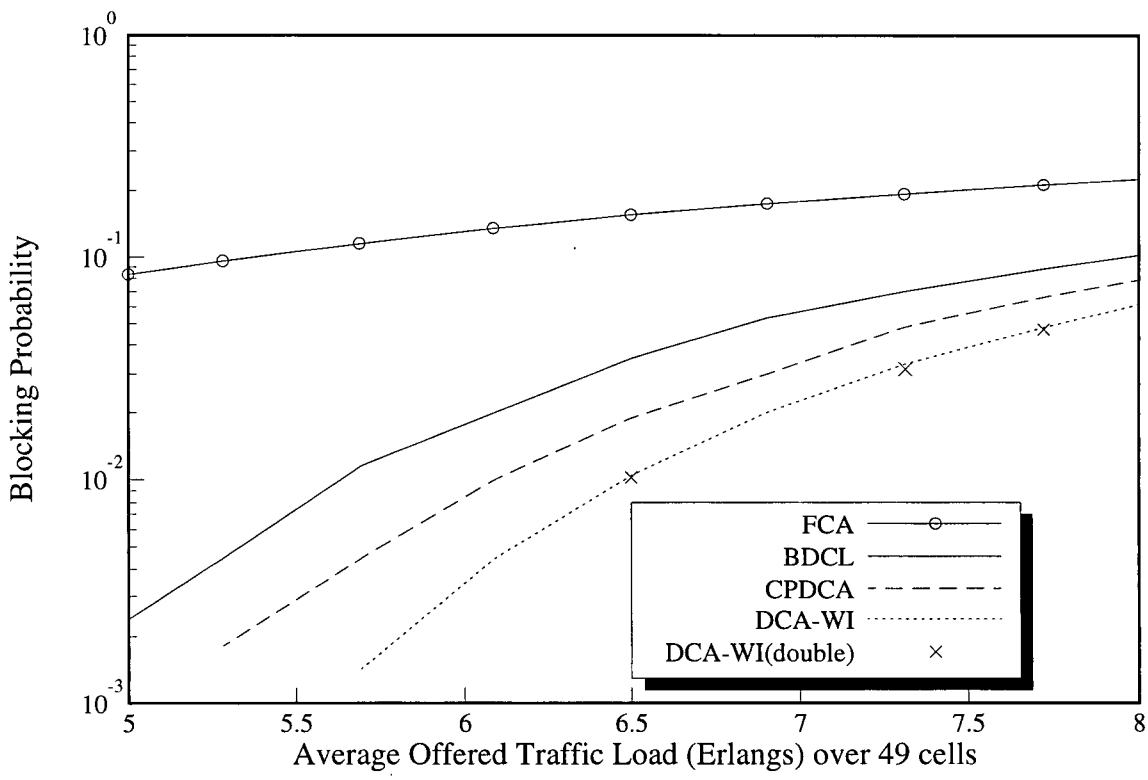

Figure 5.5 Average blocking probability with nonuniform traffic distribution A, $M = 70$.

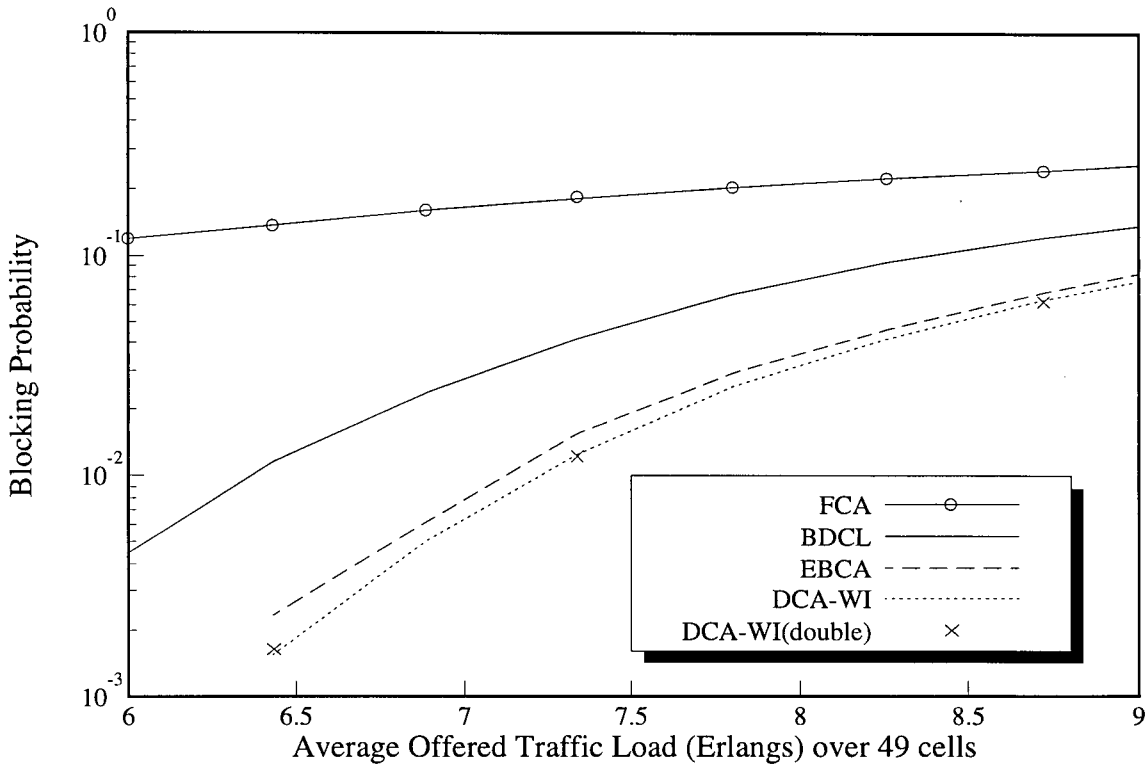

Figure 5.6 Average blocking probability with nonuniform traffic distribution B, $M = 70$.

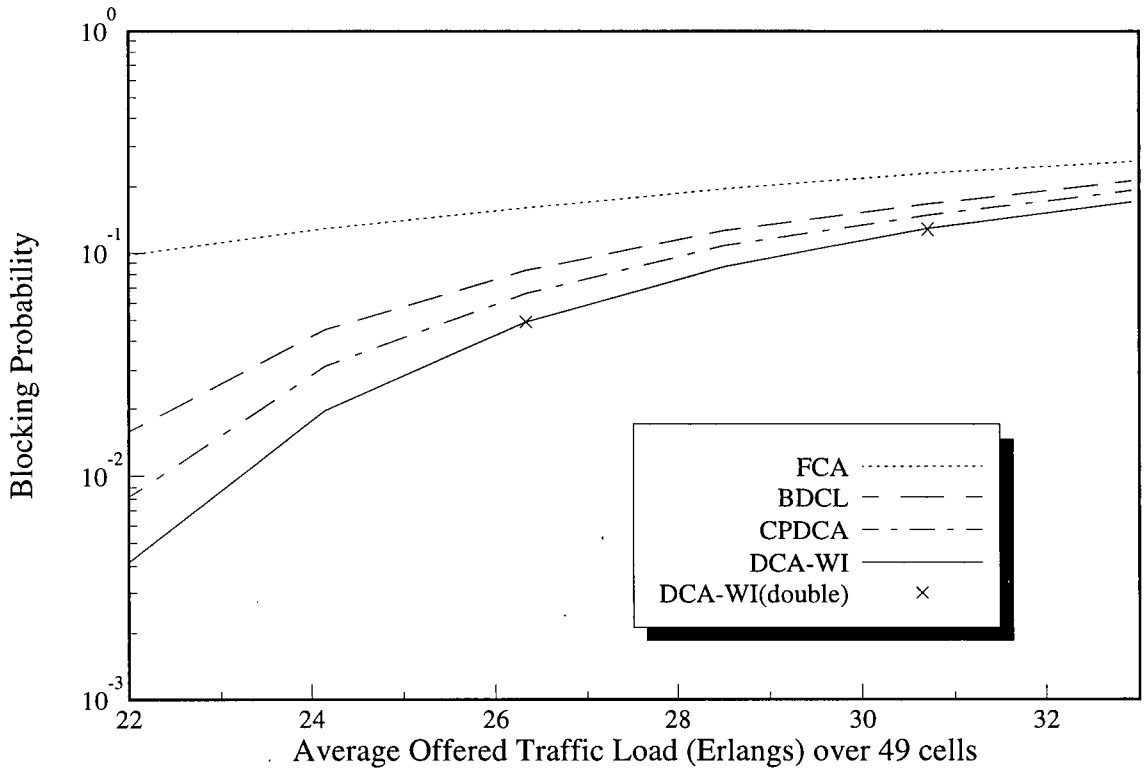

Figure 5.7 Average blocking probability with nonuniform traffic distribution C, $M = 210$.

5.4 Summary

A new channel assignment scheme, DCA-WI, was proposed. Simulation results indicate that DCA-WI outperforms existing schemes for both uniform and nonuniform spatial traffic distributions. In a 49-cell system with uniform traffic distribution, a cluster size of 7 and a total of 70 available channels, DCA-WI can carry about 70% more traffic than the conventional FCA system at a call blocking probability of 0.01. The capacity can be slightly increased with the use of inter-cell double channel reassignment. The performance of DCA-WI is very close to idealized DCA scheme using Clique Packing method regardless of the number of available channel. It was found that inter-cell double channel reassignment does not improve the system capacity for nonuniform traffic distributions.

Chapter 6 DCA for PRMA Schemes with Reassignment

In this chapter, we study and compare the performances of FCA/PRMA, FCA/PRMA++, DCA/PRMA and DCA/PRMA++ schemes for packet voice transmission in a cellular environment. Simulation results are obtained for the uplink traffic. The performance of DCA/PRMA scheme has been studied in [50]-[51]. In these studies, the DCA/PRMA scheme does not require power measurement to perform channel assignment and uses channel segregation as the DCA strategy. Firstly, we propose a technique to combine the measurement-based DCA with the PRMA protocol in which channel assignment is based on power measurements from the BS. The UT selects a channel based on the instantaneous interference power in every channel measured by the BS. This proposed scheme can employ different measurement-based DCA strategies, e.g., Autonomous Reuse Partitioning (ARP) [34], Least Interfered Channel (LIC) [36]-[37], [65] and Most Interfered Channel (MIC) [36]. In this study, we use ARP in our DCA/PRMA scheme. Secondly, we study the performance of DCA/PRMA++ scheme using various measurement-based DCA strategies, i.e., ARP, LIC and MIC. In this scheme, it is assumed that a BS is able to measure the instantaneous signal powers from all its UT's and the instantaneous interference powers from foreign UT's in every channel in order to select a channel. Thirdly, a channel reassignment (CR) method which is based on power measurements at the BS is introduced in order to reduce the number of packets lost during a talkspurt. With CR, an on-going talkspurt on a given channel is switched to another channel from the same BS if too many packets are dropped during the talkspurt due to out-of-cell interference.

In this study, we assume that the packets sent from the BS are instantaneously available to all UT's [43] and [51] i.e., processing times and the propagation delays are negligible. Except for

the FCA/PRMA without CR, it is assumed that the power measurements are available at the BS for use by other schemes in order to select a channel.

This chapter is organized as follows: An overview of FCA/PRMA and FCA/PRMA++ are provided in Section 6.1. The description of our DCA/PRMA and DCA/PRMA++ schemes are presented in Section 6.2. The channel reassignment method used to further improve the performance is given in Section 6.3. Section 6.4 presents the simulation model used in this study and discusses the performance results. The main results are summarized in Section .

6.1 Overview of FCA/PRMA and FCA/PRMA++ Schemes

In this section, the FCA/PRMA and FCA/PRMA++ schemes [50]-[52], [75] are briefly described.

6.1.1 FCA/PRMA

In an FCA/PRMA system, each cell is assigned C frequency carriers; each carrier is organized into time frames, each of which consists of N slots of duration T_s, as shown in Figure 6.1. We will refer to a given slot in a given carrier as a channel. Since a speech channel requires the allocation of one slot every frame, there is a maximum of $C \times N$ (speech) channels in each cell. The UT's recognize each channel as "available" (AV) or "reserved" (RSD) from a message that is broadcast by the BS at the end of each frame. During a talkspurt, speech packets are generated at the frame rate and buffered at the UT for transmission. No speech packets are generated during a silence period.

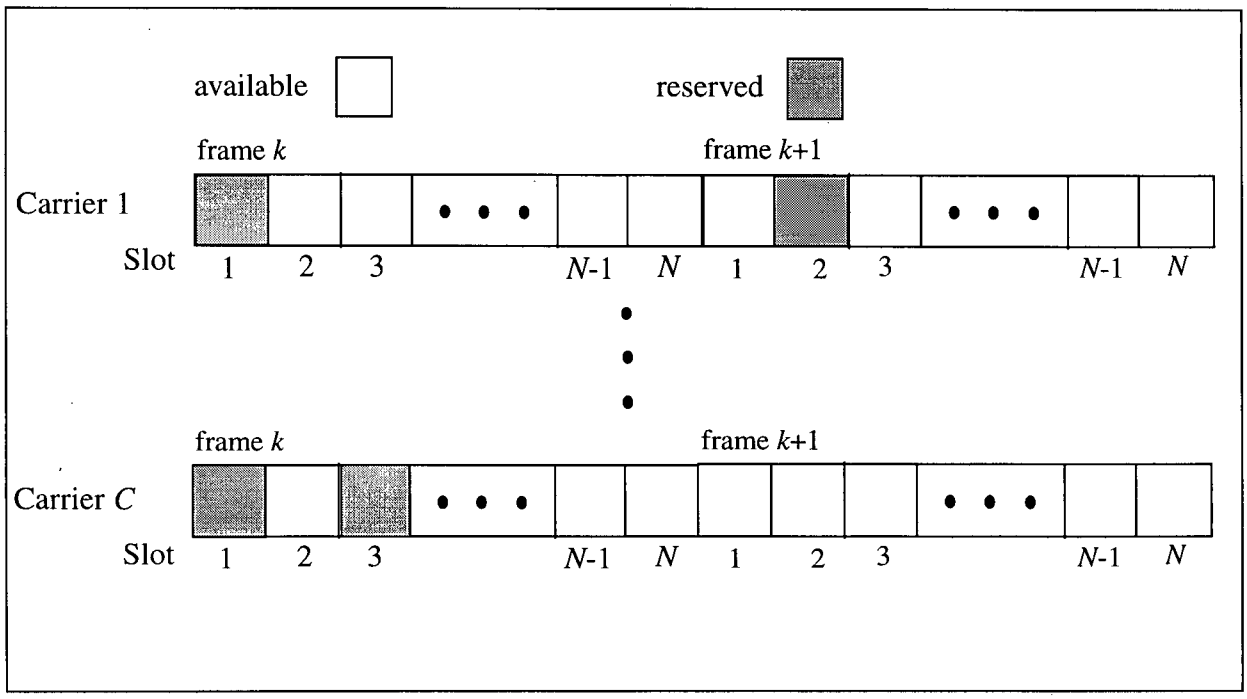

Figure 6.1 Frame structure of FCA/PRMA.

A UT **A** sends the first (oldest) unexpired packet of a talkspurt in one of the AV channels, say channel **n**, as part of a contention process. If the packet is received at the BS with an SIR greater than SIR_{min} (minimum acceptable SIR), it is assumed to be successfully decoded and at the end of the slot, the BS informs all UT's within range that channel **n** is reserved for UT **A** until the end of its current talkspurt. When the BS determines that UT **A**'s talkspurt has ended, it broadcasts that channel **n** is now AV and UT's can contend for it in the next frame. If the packet from UT **A** is not successfully decoded by the BS, UT **A** contends for the next AV channel with permission probability, p, independently of other UT's. It continues to do so until one of its packets is successfully received. The design parameter in FCA/PRMA is p.

Speech packets can only tolerate small delays. Speech packets which have been in the UT buffer longer than a maximum acceptable delay, d_{max}, are dropped resulting in "clipping" of the

speech at the beginning of the talkspurts. In our study, d_{max} is set to be twice the frame duration. The packet *dropping* probability resulting from delays of the BS successfully decoding a request for an AV channel during the contention process is given by

$$P_C = \frac{\text{number of packets dropped due to failed contention request}}{\text{total number of packets generated}}. \tag{6.1}$$

A packet transmitted by a UT in a RSD channel may still experience strong cochannel interference and be received with SIR<SIR_{min} at the BS. The packet *loss* probability due to interference [50]-[51] is given by

$$P_I = \frac{\text{number of packets received at BS with SIR}<SIR_{min}}{\text{total number of packets generated}}. \tag{6.2}$$

In this study, it is assumed that a talkspurt is interfered with if SIR<SIR_{min}.

6.1.2 FCA/PRMA++

The frame structure for FCA/PRMA++ is shown in Figure 6.2. Compared to the frame structure for FCA/PRMA, each frame now includes r_C reservation (R) slots, which are used by UT's with new talkspurts to reserve a channel on a contention basis, and $N - r_C$ information (I) slots, which can be either "available" (AV) or "reserved" (RSD). The placement of the R slots as shown in Figure 6.2 is slightly different from that of the PRMA++ protocol in [46]. There, the R slots are evenly placed within a frame because there is a delay of a few slots before a UT finds out whether its reservation attempt was successful. Since we assume no delay, the R slots can be placed anywhere within the frame; they can be placed at the end of the frame for convenience.

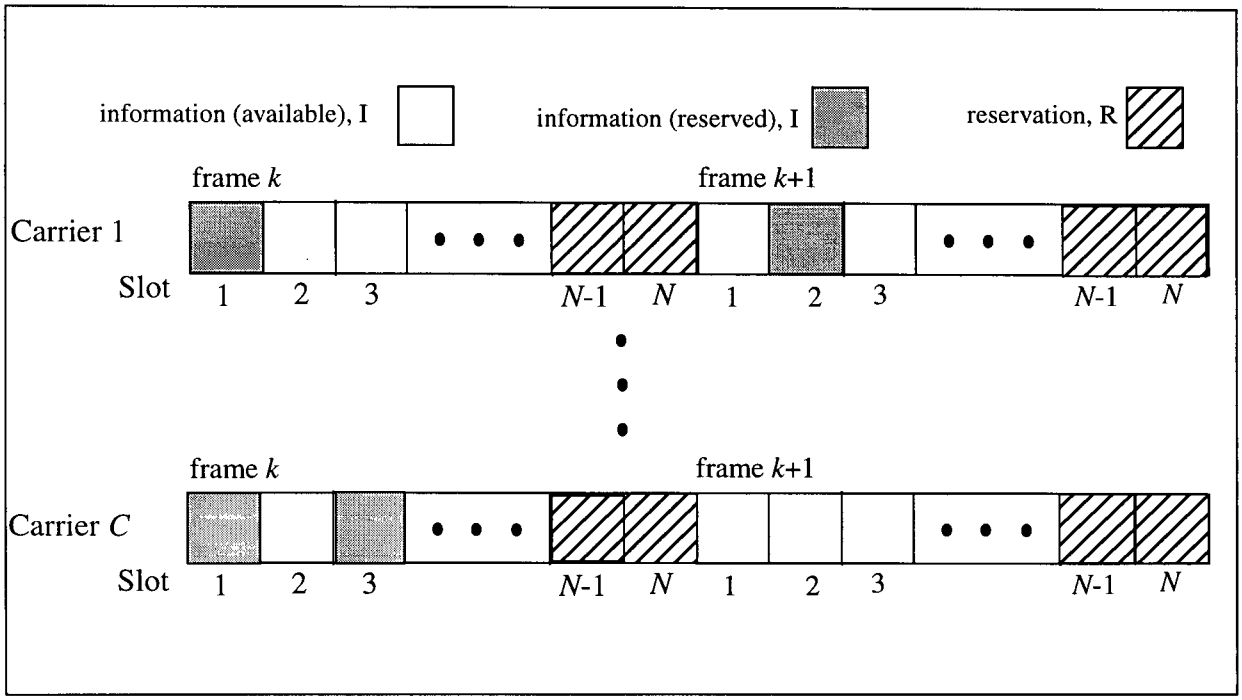

Figure 6.2 Frame structure of FCA/PRMA++.

A UT **A** with a new talkspurt sends the first unexpired packet in a R channel from one of the C carriers as a contention process. The selection of the first R channel is random if the first packet is generated before slot $N - r_C - 1$. Otherwise, the next R channel is selected. If the packet is successfully decoded by the BS, the BS broadcasts an acknowledgment (ACK) at the end of the slot and queues the request of UT **A** in its FIFO buffer. Since the BS can measure the instantaneous signal power of the UT **A** in the R channel and the instantaneous interference power of other out-of-cell UT's in all I channels, the BS can estimate the SIR of UT **A** in all I channels. At the end of each frame, the BS randomly assigns one of the AV I channels to the first UT in the buffer if the estimated SIR for that I channel is greater than SIR_{min}. This UT can then send its packets in this RSD I channel. The BS then assigns another AV I channel to the next UT in the FIFO buffer in a similar way. After assigning AV I channels to as many of the UT's in the buffer

as possible, the BS broadcasts the I channel assignment for all its UT's before the next frame starts. If a UT in the buffer cannot be assigned an I channel, due to a lack of AV channels which satisfies the SIR_{min} requirement, the UT stays in the buffer for another frame time until the next assignment. A RSD I channel reverts to AV when the BS determines that the talkspurt of the UT has ended. If the packet sent in an R channel by UT **A** is not successfully decoded by the BS, UT **A** contends again in the next R channel with permission probability, p. The design parameters in FCA/PRMA++ are p and r_C.

In addition to P_C and P_I, another performance measure of interest is the packet *dropping* probability, P_W, that a packet is dropped because the wait in the BS FIFO buffer exceeds d_{max}, i.e.

$$P_W = \frac{\text{number of packets dropped during wait in BS FIFO buffer}}{\text{total number of packets generated}}. \tag{6.3}$$

6.2 Proposed DCA/PRMA and DCA/PRMA++ Schemes

In this section, the proposed DCA/PRMA and DCA/PRMA++ schemes are described. The DCA strategy used for DCA/PRMA is ARP, whereas the DCA strategies used for DCA/PRMA++ are ARP, LIC and MIC.

6.2.1 DCA/PRMA

In a DCA/PRMA system [75], each time slot for any carrier can be used in any cell. For a total of M carriers available in the system, there are a maximum of $M \times N$ channels available in each cell as shown in Figure 6.3. Each channel is classified as AV or RSD. In this system, the BS measures the instantaneous interference power of all its AV channels. At the end of each frame,

each BS broadcasts a list of interference powers for all[1] its AV channels to its UT's. Since a UT can estimate the path loss between it and the BS, the UT can estimate its instantaneous signal power at the BS. After receiving the interference list, each UT can then estimate its received SIR at the BS for all AV channels included in the interference list in order to perform the channel assignment.

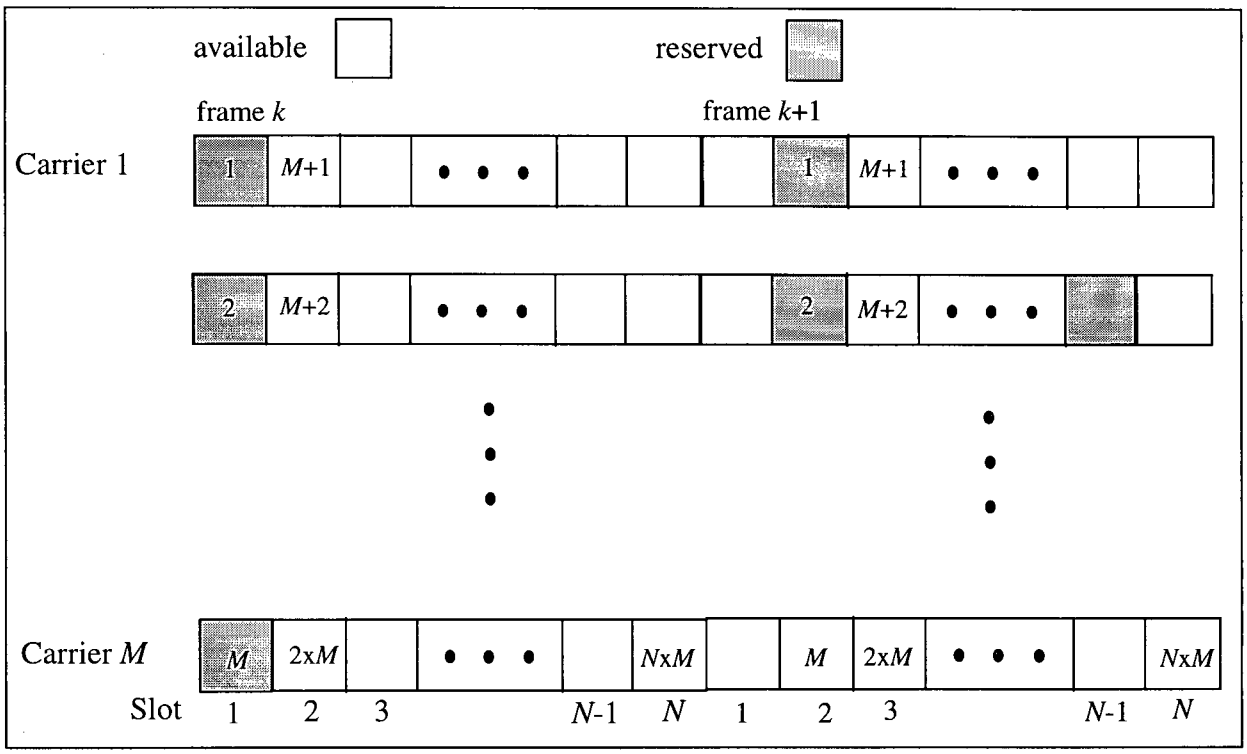

Figure 6.3 Frame structure of DCA/PRMA. The number in the center in each time slot refers to the channel number.

A UT **A** with a new talkspurt waits for the end of the current frame and listens to the interference list broadcast by its BS. The UT searches for the first AV channel, e.g., channel i in slot $j = \left\lceil \frac{i}{M} \right\rceil$, starting from the lowest numbered channel in the list for which the estimated SIR

[1] A smaller number of AV channels can be included in the interference list at the expense of some performance degradation.

is greater than SIR_{setup}, a setup threshold value which is normally greater than SIR_{min}. The UT then sends the first packet in channel i on a contention basis. If the packet is successfully decoded by the BS, the BS broadcasts an ACK at the end of slot j to inform UT's that channel i is now reserved for UT **A** until the end of the current talkspurt. When the BS determines that UT **A**'s talkspurt ends, it broadcasts that channel i is now AV. However, if the packet from UT **A** is not successfully decoded by the BS, the UT searches for the next first AV channel starting from the lowest numbered channel in slot $j+1$ and sends with permission probability p. It continues to do so until one of its packets is successfully received.

A packet might be dropped if it has been delayed longer than d_{max} and lost if the received SIR is less than SIR_{min} during transmission in a RSD channel. The performance measures used for this system are P_C and P_I, as for FCA/PRMA. The design parameters in DCA/PRMA are p and SIR_{setup}.

6.2.2 DCA/PRMA++

The frame structure for DCA/PRMA++ is shown in Figure 6.4. Compared to the frame structure for DCA/PRMA, r of the $M \times N$ channels are reservation (R) channels which are used by the UT's with new talkspurts to reserve a channel on a contention basis and $M \times N - r$ information (I) channels which can be either AV or RSD. In [52], r R channels are evenly placed in M carriers. For example, if there are M R channels, in [52] each carrier has one R channel at the beginning of a frame. In this scheme, for convenience, the r R channels are just placed at the end of the frame in one of the M carriers as shown in Figure 6.4. Simulation results shows that the performances of these two schemes are about the same as shown in Figure 6.5. In Figure 6.5, the DCA algorithm used is ARP for both schemes. The parameters, which are chosen so as to provide the overall best performance, used in the schemes are shown in Table 6.1.

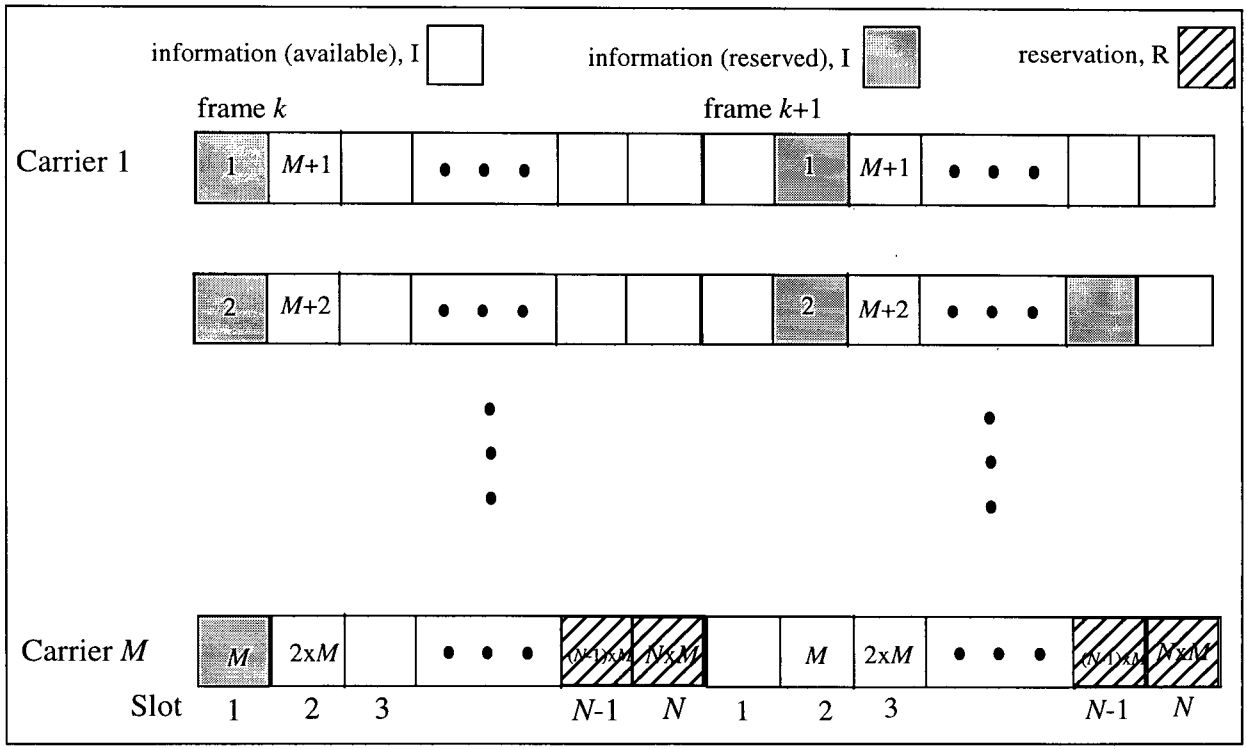

Figure 6.4 Frame structure of DCA/PRMA++. The number in the center in each time slot refers to the channel number.

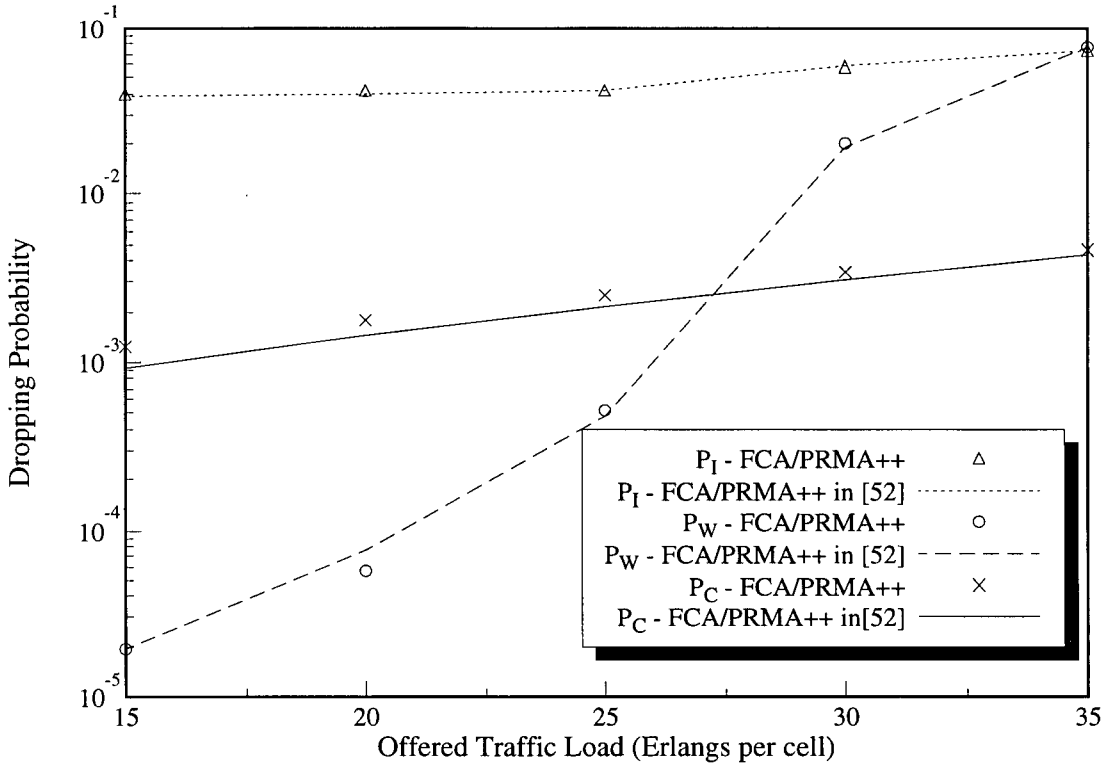

Figure 6.5 Dropping or loss probabilities for DCA/PRMA++ with no reassignment for previous scheme in [52] and our scheme.

Table 6.1 Parameters used in our FCA/PRMA++ and FCA/PRMA++ in [52].

Scheme	p	r	SIR_{setup}
DCA/PRMA++ using ARP	0.2	3	18 dB
DCA/PRMA++ in [52] using ARP	0.7	3	18 dB

In this scheme, a UT **A** with a new talkspurt sends the first unexpired packet in an R channel. The selection of the R channel is random if the first packet is generated before slot $N - r - 1$. Otherwise, the next R channel is selected. If the packet is successfully decoded by the BS, the BS broadcasts an ACK at the end of the slot and queues the request of the UT in a BS FIFO buffer. Similar to FCA/PRMA++ scheme, the BS is able to estimate the SIR for each UT in the buffer for all I channels. At the end of each frame the BS assigns the AV I channels to the UT's in the BS buffer according to different DCA strategies as follows:

(i) ARP - The BS assigns the first AV I channel, for which the estimated SIR for that channel is greater than SIR_{setup}, searching from the smallest channel number to the first UT in the buffer.

(ii) LIC - The BS assigns the AV I channel with highest SIR from the estimation, which is greater than SIR_{setup}, to the first UT in the buffer.

(iii) MIC - The BS assigns the AV I channel with lowest SIR from the estimation, which is greater than SIR_{setup}, to the first UT in the buffer.

The UT then sends its packets in its assigned RSD I channel. The BS then assigns another AV I channel to the next UT in the FIFO buffer in a similar way. After assigning AV I channels to as many of the UT's in the buffer as possible, the BS broadcasts the I channel assignment for all its UT's before the next frame starts. If UT in the buffer cannot be assigned an I channel, due to a

lack of AV channels which satisfy the SIR_{setup} requirement, the UT stays in the buffer for another frame time until the next assignment. A RSD I channel reverts to AV when the BS determines that the talkspurt of the UT has ended. If the packet sent in an R channel by UT **A** is not successfully decoded by the BS, UT **A** contends again in the next R channel with permission probability, p. Similar to FCA/PRMA++, the performance measures for this system are P_C, P_W and P_I. The design parameters in DCA/PRMA++ are p, r and SIR_{setup}.

6.3 Reassignment Method

In this section, the intracell channel reassignment for FCA/PRMA, FCA/PRMA++, DCA/PRMA and DCA/PRMA++ schemes is described. With CR, power measurements are assumed available at the BS for all four schemes. When the received SIR at the BS drops below SIR_{min} for N_L consecutive packets of a talkspurt during transmission in a RSD channel k,

(i) the BS releases channel k with release probability, p_{rel}, if channel k has just been assigned and reserved for the UT or

(ii) the BS releases channel k otherwise.

In (i), when channel k is reserved for a UT **A** at the beginning, the SIR_{min} requirement is met so that UT **A** can send its packet in channel k in the next frame without strong interference. However, this packet may be interfered with in the next frame if more than one UT's in different cells are assigned the same channel k at the same time. The motivation behind p_{rel} is to attempt to keep one UT using channel k in order to reduce intracell CR. In (ii), a talkspurt from UT **A** is interfered with in the middle if a UT **B** from different cell is assigned the same channel k. In this case, the talkspurt from UT **B** may not be interfered with such that the received SIR at the BS is still above SIR_{min}. Then, UT **A** using channel k should release channel k to avoid more dropped

packets. The choice of the value for N_L involves a trade-off. If N_L is too small, the talkspurt may require too many CR's. If N_L is too large, it may not be able to reduce the packet dropping rate. The effect of N_L is studied in Section 6.4.4.

After releasing channel k, the BS informs UT **A** not to send any additional packets in channel k and places the request of UT **A** in the BS FIFO buffer. It also broadcasts that channel k is now AV. At the end of the frame, the BS assigns another AV channel to UT **A**. For FCA/PRMA and FCA/PRMA++, the BS randomly assigns one of the AV channels with estimated SIR greater than SIR_{min} to the first UT in the FIFO buffer. For DCA/PRMA and DCA/PRMA++, the channel reassignment algorithm depends on the type of DCA strategies, i.e. ARP, LIC and MIC.

For FCA/PRMA and DCA/PRMA with no CR, no buffer is needed in the BS or no P_W is obtained. With CR, buffer is needed and thus, packets might be dropped while the requests of the UT's stored in the BS buffer are waiting too long for channel reassignment. Therefore, another performance measure of interest is P_W for FCA/PRMA and DCA/PRMA. The design parameters for CR are N_L and p_{rel}. In Section 6.4, the default values for N_L and p_{rel} are 2 and 0.5 respectively.

6.4 Simulation Model and Performance Results

The performances of the FCA/PRMA, FCA/PRMA++, DCA/PRMA and DCA/PRMA++ schemes described in sections 6.1-6.3 are studied using computer simulation. The simulated system is two-dimensional and consists of 27 hexagonal cells of radius of 600 meters with omni-directional antennas. For the case of FCA the cluster size is assumed to be 3 [51]. Results are collected from the central 3 cells to avoid edge effects. An interference-limited situation is considered so that noise is ignored. The path loss, L, between a BS and a UT is assumed to follow log-

normal statistics given by [51]:

$$L = d^{\gamma} 10^{X/10} \tag{6.4}$$

where d is the distance between the BS and the UT, $\gamma = 3.5$ is the propagation factor, and X is a zero mean Gaussian random variable with a standard deviation of 4 dB. The UT's are assumed to be stationary and the signal levels are assumed to be constant during a call. The UT is always served by the BS with the strongest received signal power.

Speech packet transmission on the uplink is simulated. The UT's are assumed to be uniformly distributed over the 27 cells. New calls arrive according to a Poisson process with arrival rate, λ, per cell. Call durations are exponentially distributed with a mean of $1/\mu = 2$ minutes. All talkspurt and silence periods are assumed to be exponentially distributed with means of 1 s and 1.35 s respectively [42]. This corresponds to an activity factor of 0.426. During talkspurts, speech packets of duration T_s are generated at the frame rate and queued in a UT buffer. The first packet in a talkspurt is generated one frame after the talkspurt has arrived in the UT. No packets are generated during silence periods. The system variables used in the simulation are summarized in Table 6.2. For FCA/PRMA and FCA/PRMA++, each BS has 1 carrier with 20 channels. For DCA/PRMA and DCA/PRMA++, each BS has 60 channels to choose from.

The duration of the simulation is in excess of 30 million slots, equivalent to 400 minutes. For most of the simulation results, the 95% confidence intervals are within $\pm 10\%$ of the average values shown. The system design parameter values, which are chosen so as to provide the overall best performance for the different schemes, are shown in Tables 6.3 - 6.5.

Table 6.2 System variable values used in the simulation.

Variables	Values	Variables	Values
Cell Radius	600 m	Packet generation rate	1 per frame
Number of cells	27	Mean talkspurt duration	1 s
Number of carriers	3	Mean silence duration	1.35 s
FCA cluster size	3	Number of slots per frame	20
Propagation factor	3.5	Frame duration	16 msec
Std. dev. of log-normal shadowing	4 dB	Minimum acceptance SIR	9 dB
Average call duration	2 mins	Maximum acceptable packet delay	32 msec

Table 6.3 System design parameters for FCA/PRMA and FCA/PRMA++ schemes.

Scheme	p	r_C	SIR_{setup}
FCA/PRMA with no reassignment	0.3	n/a	n/a
FCA/PRMA with reassignment	0.3	n/a	n/a
FCA/PRMA++ with no reassignment	0.4	2	n/a
FCA/PRMA++ with reassignment	0.4	2	n/a

Table 6.4 System design parameters for DCA/PRMA++ scheme.

Scheme	p	r	SIR_{setup}
DCA/PRMA++ using ARP with no reassignment	0.3	4	18 dB
DCA/PRMA++ using ARP with reassignment	0.3	4	15 dB
DCA/PRMA++ using LIC with no reassignment	0.3	4	12 dB
DCA/PRMA++ using LIC with reassignment	0.3	4	15 dB
DCA/PRMA++ using MIC with no reassignment	0.3	4	18 dB
DCA/PRMA++ using MIC with reassignment	0.3	4	15 dB

Table 6.5 System design parameters for DCA/PRMA scheme.

Scheme	p	r	SIR_{setup}
DCA/PRMA using ARP with no reassignment	0.3	n/a	18 dB
DCA/PRMA using ARP with reassignment	0.4	n/a	15 dB

6.4.1 Results for Schemes with No Channel Reassignment (CR)

The dropping and loss probabilities of FCA/PRMA and FCA/PRMA++ with no reassignment are shown in Figure 6.6. In Figure 6.6, the packet loss probability, P_I, due to strong interference is quite high even at low traffic load, ρ. This is because once a talkspurt is interfered with, the rest of the talkspurt will likely be continuously affected if no channel reassignment is performed resulting in a high P_I. It can be seen that P_I for FCA/PRMA++ is slightly higher than that for FCA/PRMA; this is because with PRMA++ there are only 18 channels which can be reserved for packet transmission. At light traffic load, P_C for FCA/PRMA is lower because not many channels are being reserved for packet transmission by UT's and hence there are more AV channels for contention. But for FCA/PRMA++, there are only $r_C = 2$ channels for contention. Conversely, P_C for FCA/PRMA is higher at high traffic loads because many channels are reserved and cannot be used for contention. For FCA/PRMA with no CR as well as DCA/PRMA with no CR, there is no P_W. In general, the total packet failure probability, $P_T = P_C + P_W + P_I$, for FCA/PRMA++ is higher than that for FCA/PRMA.

The dropping or loss probabilities of DCA/PRMA++ with no reassignment using different DCA strategies, ARP, LIC and MIC, are shown in Figure 6.7. The P_C for all DCA algorithms are almost the same because they all have the same value of r as shown in Table 6.4. The P_C increases slightly with ρ because the number of R channels which is chosen to be 4 is sufficient to handle the reservation traffic during the contention process. For $\rho < 20$, the P_W for MIC is lowest whereas the P_W for LIC is highest. In MIC, a channel with a lowest SIR > SIR_{setup} is selected, and thus the reuse distances between different UT's using the same channel are smaller. Therefore, more UT's can be assigned channels. In LIC, a channel with a highest SIR > SIR_{setup} is selected and thus, the distances between different UT's using the same channel are normally

larger, resulting in fewer UT's being assigned channels. As ρ increases, P_W increases because the number of UT's in the buffer requesting for channel assignment increases. The P_I for MIC and ARP is more or less independent of ρ, with MIC having the highest P_I. In MIC, a channel is selected with the SIR difference, SIR_{diff}, at initial setup which is the difference between the estimated SIR at initial setup and SIR_{min}, as low as possible and therefore, packets sending in this channel can be easily interfered with by out-of-cell UT's. For light loads, the P_I for LIC is lowest because channel are selected with maximum SIR_{diff} and thus the packets sending in these channels are least likely to be interfered with. As ρ increases, P_I for LIC increases because SIR_{diff} decreases with ρ due to many UT's using the channels. In general, the P_T of ARP is better than the other two algorithms.

The dropping and loss probabilities of DCA/PRMA and DCA/PRMA++ with no reassignment using ARP are shown in Figure 6.8. For both schemes, P_I increases slowly with ρ. Similar to the observations from Figure 6.6, it can be seen that (1) P_I is quite high, (2) P_I for DCA/PRMA++ is higher than that for DCA/PRMA and (3) P_C for DCA/PRMA is lower at light traffic loads and higher at heavy traffic loads than for DCA/PRMA++. The reason is the same as mentioned previously for FCA. In general, the performance of DCA/PRMA is better than that of DCA/PRMA++.

The total packet failure probabilities, P_T, for FCA/PRMA, FCA/PRMA++, DCA/PRMA using ARP and DCA/PRMA++ using ARP with no CR are plotted in Figure 6.9. It can be seen that the P_T for PRMA++ is higher than that for PRMA. The P_T for DCA/PRMA and DCA/PRMA++ are higher than FCA/PRMA and FCA/PRMA++, except for traffic loads around 25 Erlangs. For $\rho < 25$, the P_T for DCA/PRMA and DCA/PRMA++ do not vary much because P_I

for both schemes do not change much with ρ as shown in Figure 6.8. For $\rho > 25$, P_T increases due to the significant increase in P_C for PRMA and P_W for PRMA++ as shown in Figure 6.8. If we set the maximum acceptable value for P_T at 0.01 in order to provide reasonable speech quality [42]-[43], the capacity that can be supported for FCA/PRMA and FCA/PRMA++ is less than 15 Erlangs. It can be seen that DCA/PRMA and DCA/PRMA++ cannot meet this requirement even at relatively low ρ as shown in the figure. In [51], it was found that the capacity of DCA/PRMA at $P_T \approx 0.06$ for $P_C \approx 0.01$ and $P_I \approx 0.05$ is about the same as that of FCA/PRMA. The same conclusion is reached for both PRMA and PRMA++ schemes if we use $P_T \approx 0.06$ as shown in Figure 6.9.

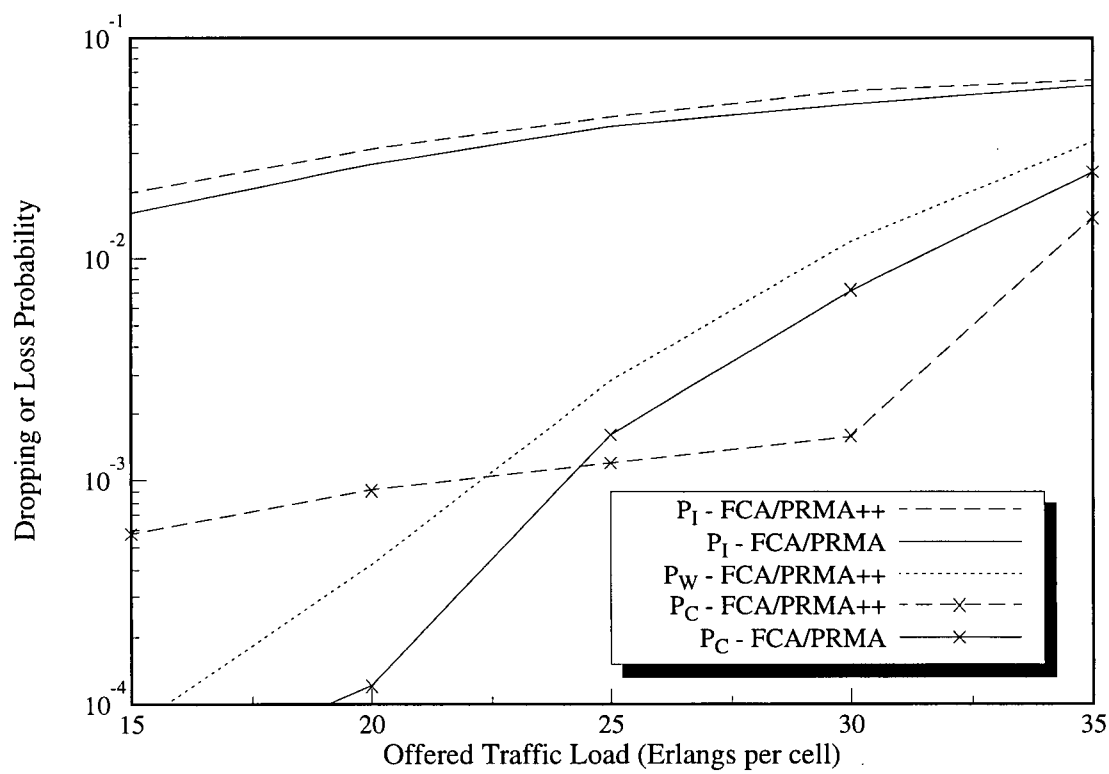

Figure 6.6 Dropping or loss probabilities for FCA/PRMA and FCA/PRMA++ with no reassignment.

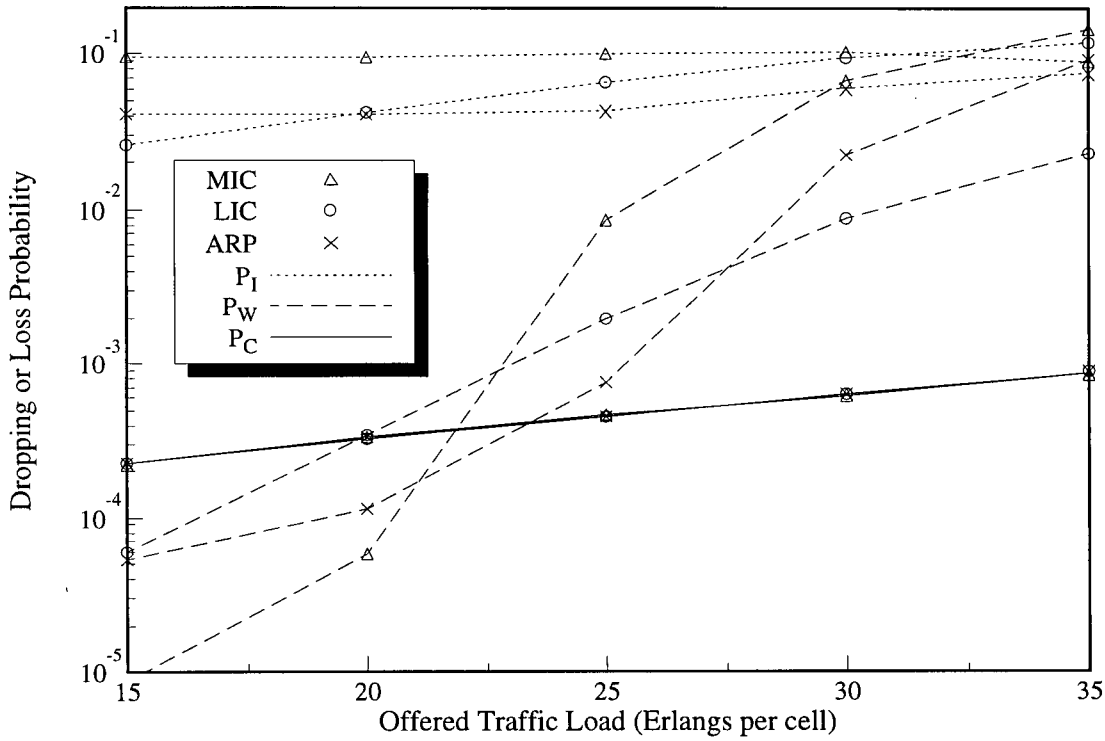

Figure 6.7 Dropping probabilities for DCA/PRMA++ with no reassignment using ARP, LIC and MIC.

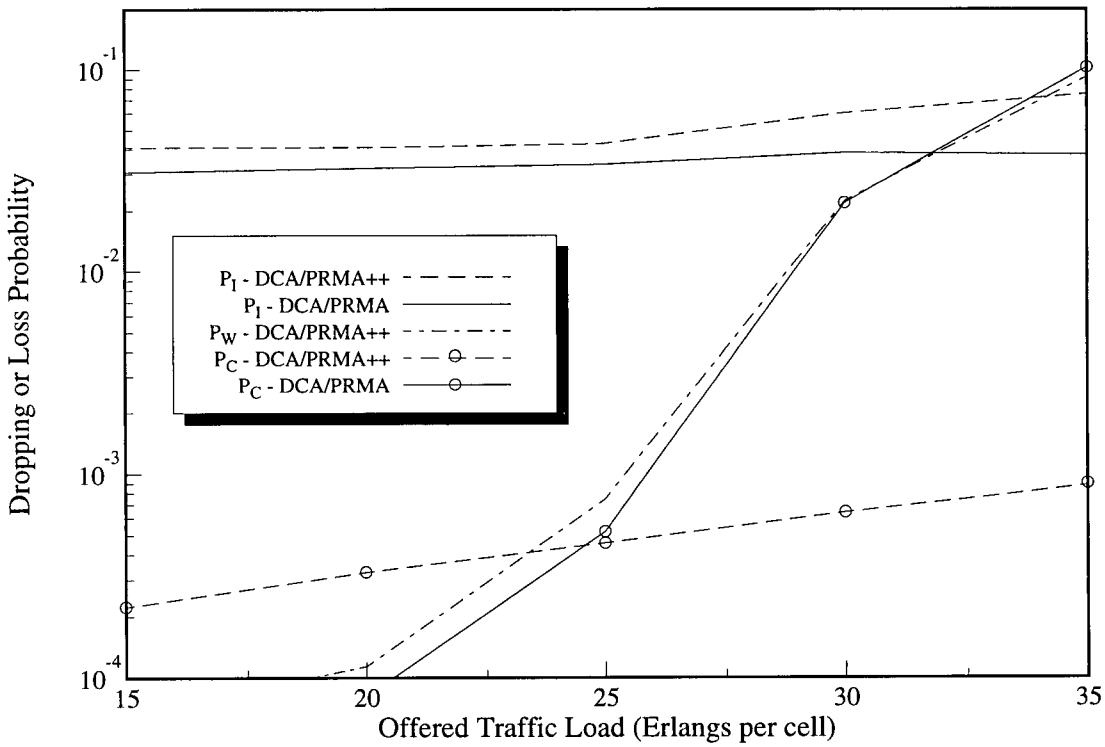

Figure 6.8 Dropping probabilities of DCA/PRMA and DCA/PRMA++ with no reassignment and using ARP.

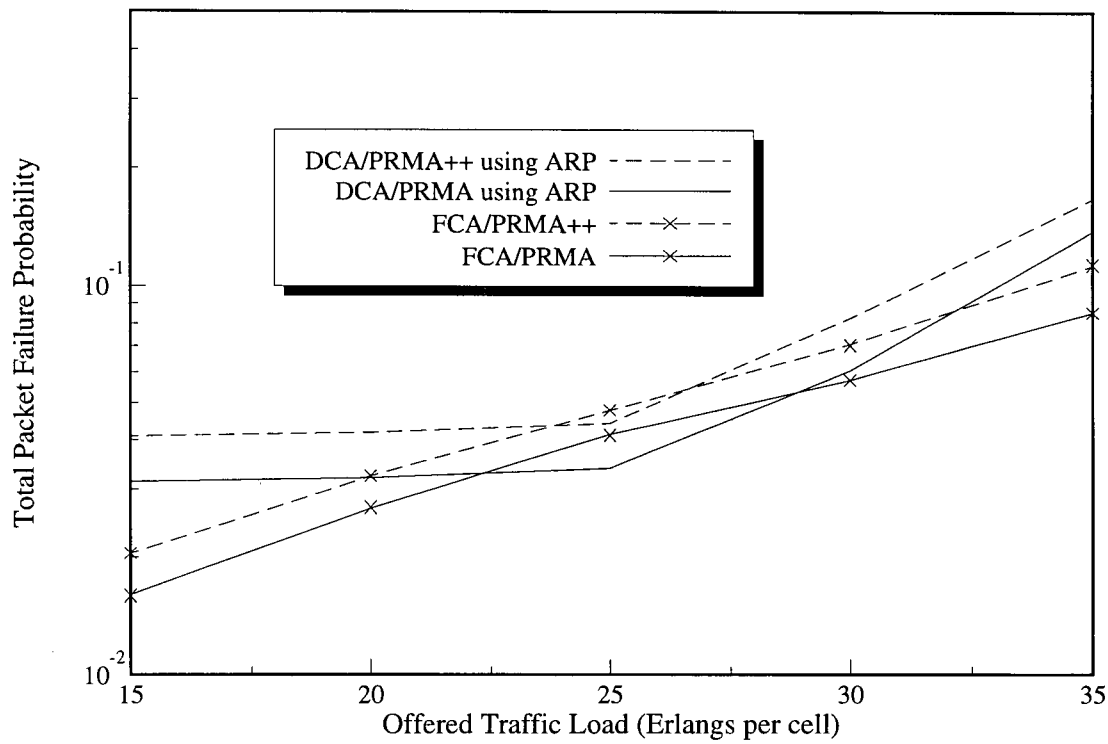

Figure 6.9 Total packet failure probabilities for all four schemes with no reassignment.

6.4.2 Results for Schemes with Channel Reassignment (CR)

The dropping and loss probabilities of FCA/PRMA and FCA/PRMA++ with reassignment are shown in Figure 6.10. Compared to Figure 6.6, P_C are similar in both figures since it is not affected by reassignments whereas P_I is substantially lower. This is because with reassignment a talkspurt which starts experiencing high interference can be reassigned to another channel to avoid continuous packet loss. Also, P_W for PRMA++ is slightly higher because more requests waits in the buffer due to CR. It can be seen that P_I for FCA/PRMA and FCA/PRMA++ with reassignment are comparable, but with no reassignment FCA/PRMA++ has a higher P_I than FCA/PRMA. Also, P_W for FCA/PRMA++ is higher than that for FCA/PRMA; this is because with PRMA++ there are only 18 channels which can be used for channel assignment for packet transmission whereas there are 20 channels in PRMA system.

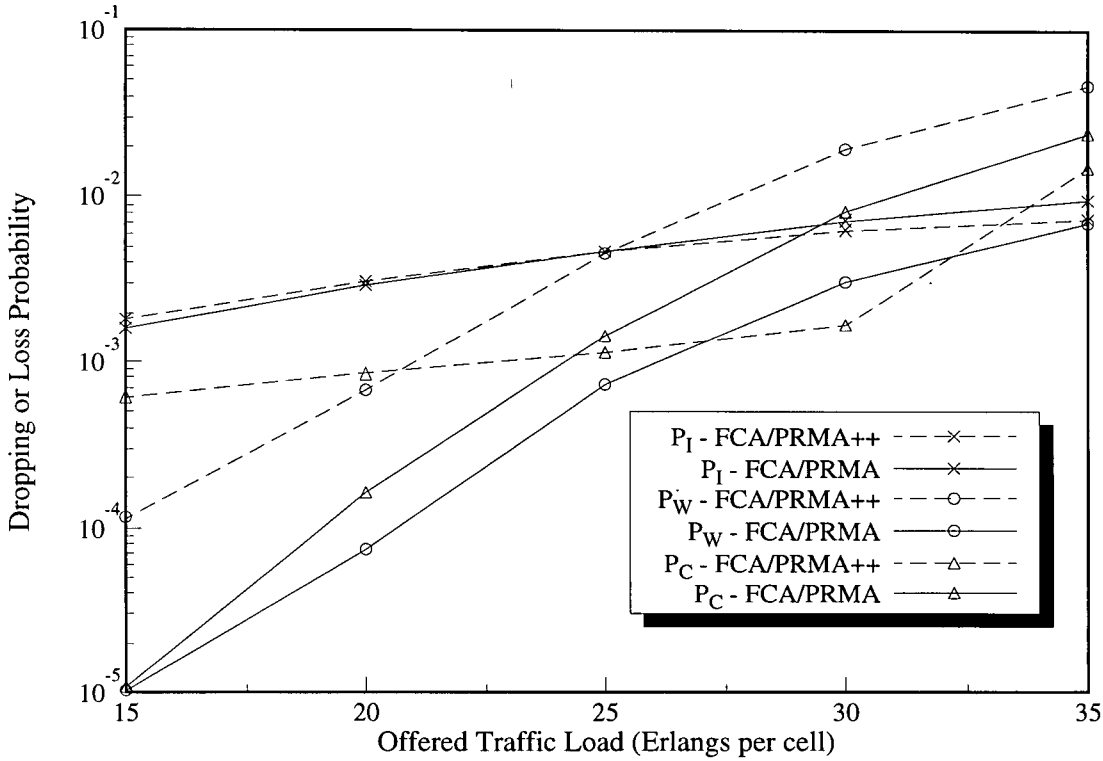

Figure 6.10 Dropping or loss probabilities for FCA/PRMA and FCA/PRMA++ with reassignment.

The dropping and loss probabilities of DCA/PRMA++ with reassignment using ARP, LIC and MIC are shown in Figure 6.11. For $\rho > 21$, ARP has the lowest P_W whereas with no CR as shown in Figure 6.7, LIC has the lowest P_W for $\rho > 27$. With no CR, the SIR_{setup} = 12 dB used in LIC is much lower than that in ARP, SIR_{setup} = 18 dB, as shown in Table 6.4. Therefore, the UT can be easily assigned a RSD channel at the expense of increasing P_I as shown in Figure 6.7. With CR, the SIR_{setup} values used are the same for all three algorithms and ARP outperforms other algorithms because it can form a "reuse partitioning" pattern. The P_T of ARP is better than those of the other two algorithms. The dropping and loss probabilities of DCA/PRMA and DCA/PRMA++ with CR using ARP are shown in Figure 6.12. It can be seen that P_I can be reduced substantially by using CR. Similar to the observations from Figure 6.10, P_I for DCA/PRMA and DCA/PRMA++ are comparable and P_W for DCA/PRMA++ is higher than that for DCA/PRMA.

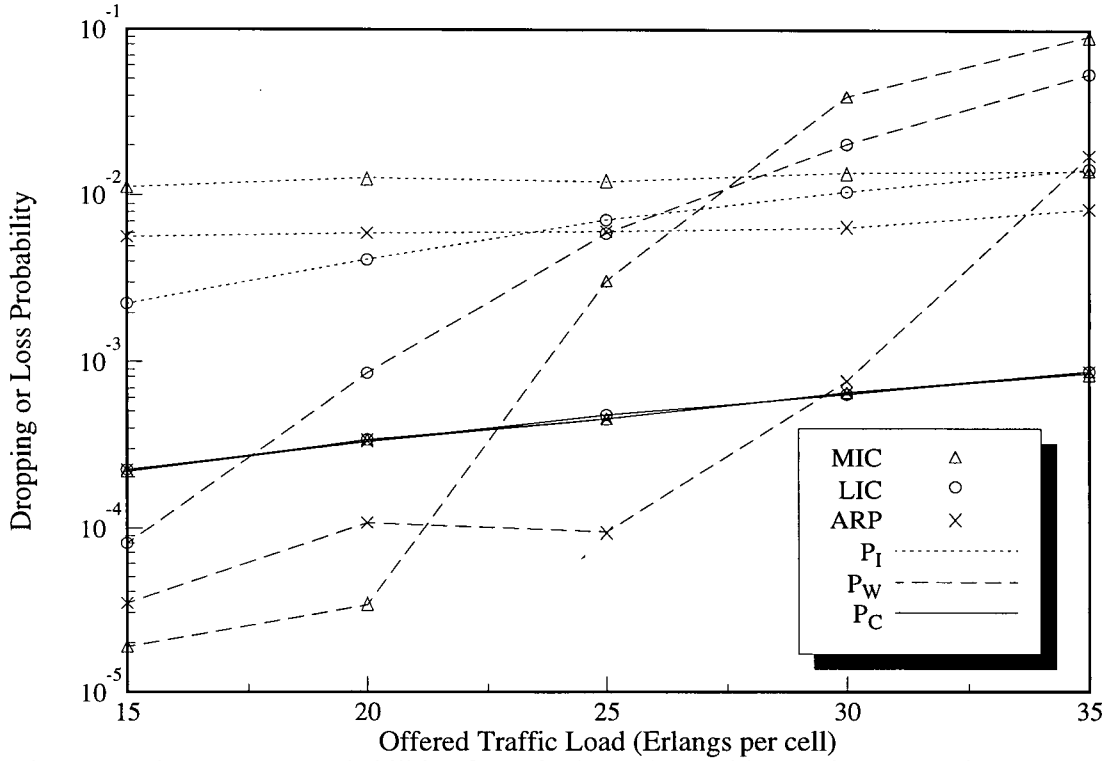

Figure 6.11 Dropping or Loss probabilities for DCA/PRMA++ with reassignment using ARP, LIC and MIC.

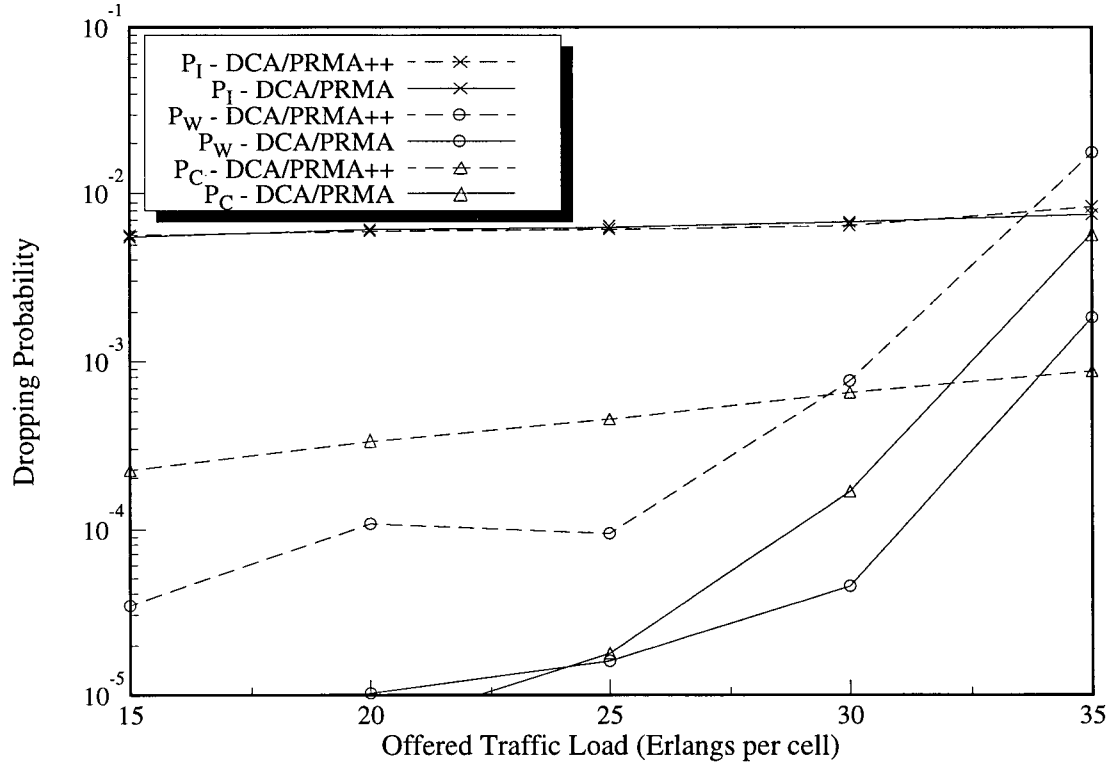

Figure 6.12 Dropping or loss probabilities of DCA/PRMA and DCA/PRMA++ with reassignment using ARP.

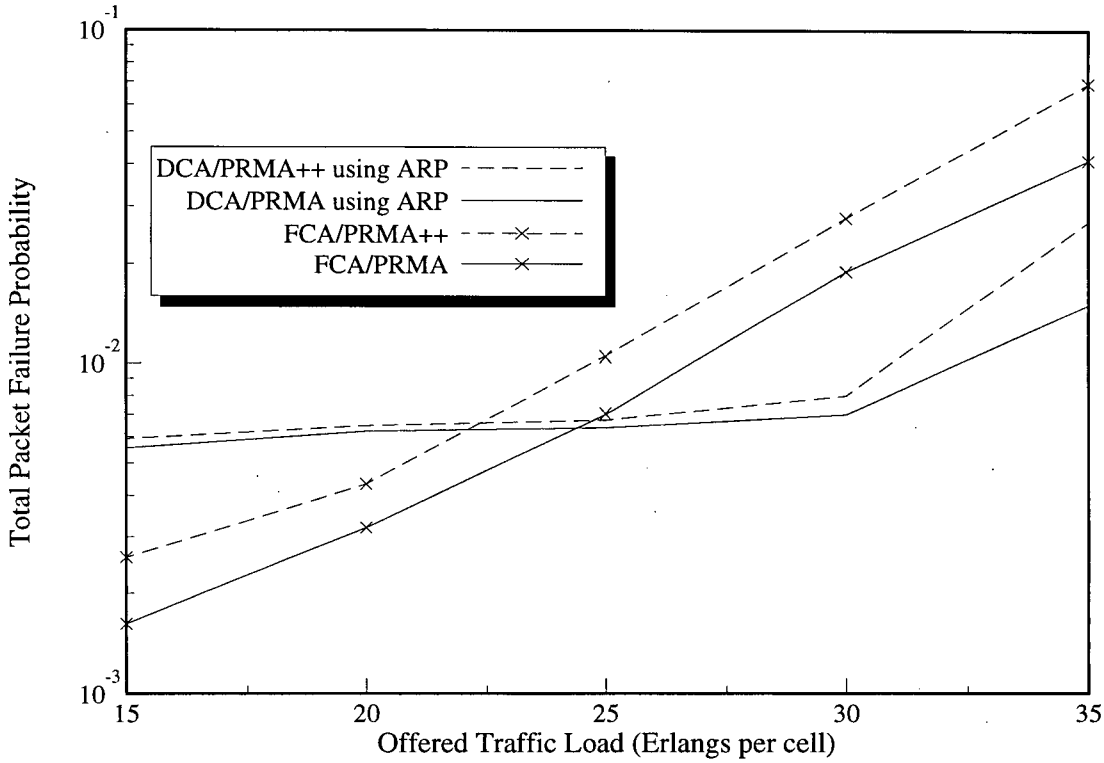

Figure 6.13 Total packet failure probabilities for all four schemes with reassignment.

The total packet failure probability, P_T, for FCA/PRMA, FCA/PRMA++, DCA/PRMA using ARP and DCA/PRMA++ using ARP with CR are plotted in Figure 6.13. The P_T for DCA/PRMA using ARP and DCA/PRMA++ using ARP are almost constant for $\rho < 30$ because P_I does not vary much with ρ as shown in Figure 6.12. For $\rho > 30$, the P_T for the DCA schemes increase due to increases in P_C and P_W as shown in Figure 6.12. For light loads, FCA/PRMA and FCA/PRMA++ perform better than DCA/PRMA and DCA/PRMA++. This is because the distances among UT's using the same channel are closer in DCA. Therefore, the talkspurts will be easily interfered with out-of-cell UT's. For FCA, the probability of the talkspurts being interfered with increases with ρ because more co-channel cells use the same channel. At high loads, the performance of FCA is worse than DCA because the reuse distance of FCA is generally larger than that of DCA. At $P_T \approx 0.01$, the capacities for FCA/PRMA++, FCA/PRMA, DCA/PRMA++

and DCA/PRMA are 25, 27, 31 and 32.5 Erlangs respectively. The capacity for FCA with CR can be improved by about 80% compared to that for FCA with no CR as shown in Figure 6.9. An additional 25% increase in capacity can be obtained with DCA In general, PRMA performs better than PRMA++ with FCA or DCA because PRMA has more number of channels to carry information.

In the above results, perfect power measurements are assumed to be available so that the BS is able to measure the instantaneous desired signal power and interference power in every channel in order to make a channel assignment. In reality, power measurement errors are inevitable. To study the effect of imperfect power measurements, we model the error to be Gaussian distributed with zero mean and $\sigma = 10\ \%$. The results show that P_C, P_W and P_I in all four schemes are about the same compared to those with perfect power measurement except that P_I for FCA/PRMA++ is about 25% higher. This is because for FCA/PRMA++, power measurement is required in the contention process and CR process whereas for FCA/PRMA, power measurement is required only in the CR process. Even though, for DCA/PRMA and DCA/PRMA++, power measurement is required in the contention process and CR process, the SIR_{setup} is several dB's higher than the SIR_{min}. This lessens the effect of error measurements on P_I. The P_T for all four schemes is about the same compared to those with perfect power measurement except that P_T for FCA/PRMA++ is slightly higher. The capacities for all schemes at $P_T = 0.01$ still remain about the same. With imperfect power measurement, the average number of CR per call is increased by about 10% for FCA/PRMA and FCA/PRMA++. This is because no SIR_{setup} is used for CR process in FCA schemes.

Other results for all four schemes with CR are presented in Sections 6.4.3-6.4.5. The DCA

algorithm used for PRMA and PRMA++ is ARP.

6.4.3 Number of Channel Reassignments and Reservation Access Delay

The cumulative distribution function (CDF) of the number, N_{cr}, of channel reassignments per call at $\rho = 30$ Erlangs is shown in Figure 6.14. It can be seen that the probability that $N_{cr} = 0$ for DCA is lower than that for FCA. This is because in DCA the distance between two calls using the same channel is usually shorter than the minimum reuse distance in FCA. Therefore, the calls are more easily interfered with and require more CR's. The CDF of FCA (or DCA) with PRMA and PRMA++ is about the same.

The average values of N_{cr}, $\overline{N_{cr}}$, per call at different traffic loads are plotted in Figure 6.15. For $\rho < 30$, the DCA schemes require more CR's than the FCA schemes due to shorter reuse distances. The $\overline{N_{cr}}$ for DCA increases slowly with ρ whereas the $\overline{N_{cr}}$ for FCA increases rapidly. This is because in DCA the reuse distance between the same channel always keeps to be minimum at any load. However, in FCA, the number of cochannel cells using the same channel increases as ρ increases. Therefore, the talkspurt will be interfered with more easily with ρ and require more CR's. The $\overline{N_{cr}}$ for PRMA++ is higher than that for PRMA because the number of channels used for information packets in PRMA++ is less than that in PRMA. For traffic loads corresponding to $P_T \approx 0.01$ (see Figure 6.13), the $\overline{N_{cr}}$ for FCA/PRMA++, FCA/PRMA, DCA/PRMA++ and DCA/PRMA are 6.9, 6.6, 9.7 and 8.2. The $\overline{N_{cr}}$ for DCA/PRMA++ is higher than other schemes due to less number of information channels.

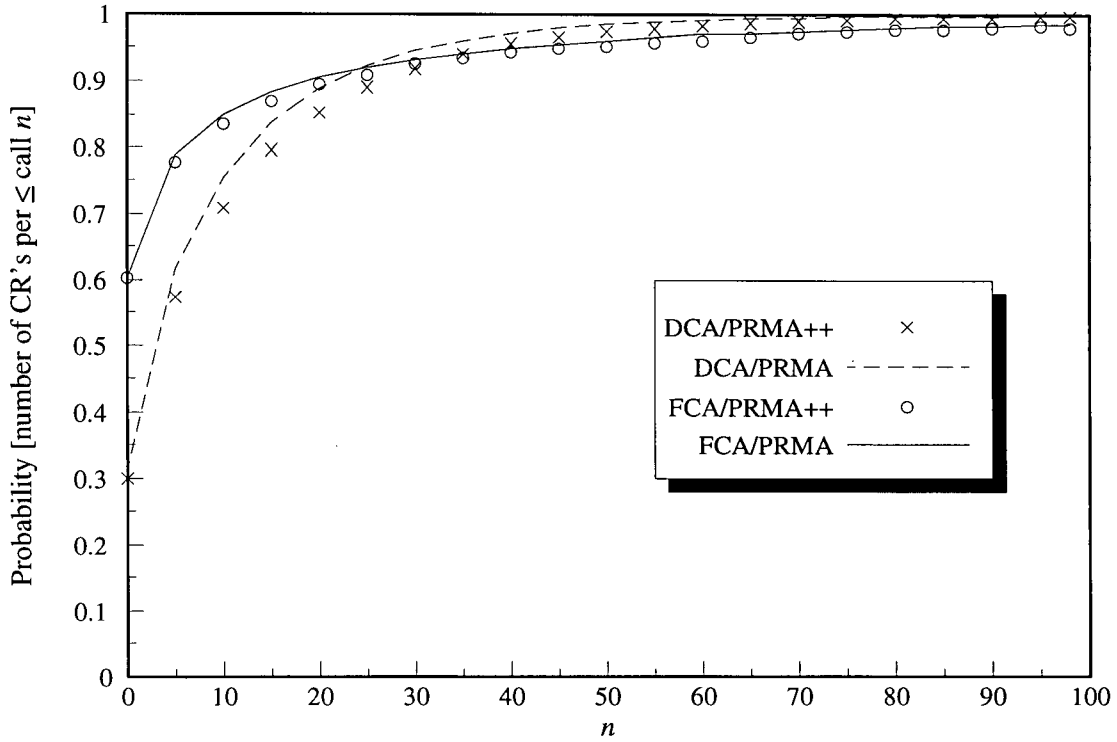

Figure 6.14 CDF of the number of CR per call for all schemes at $\rho = 30$ Erlangs.

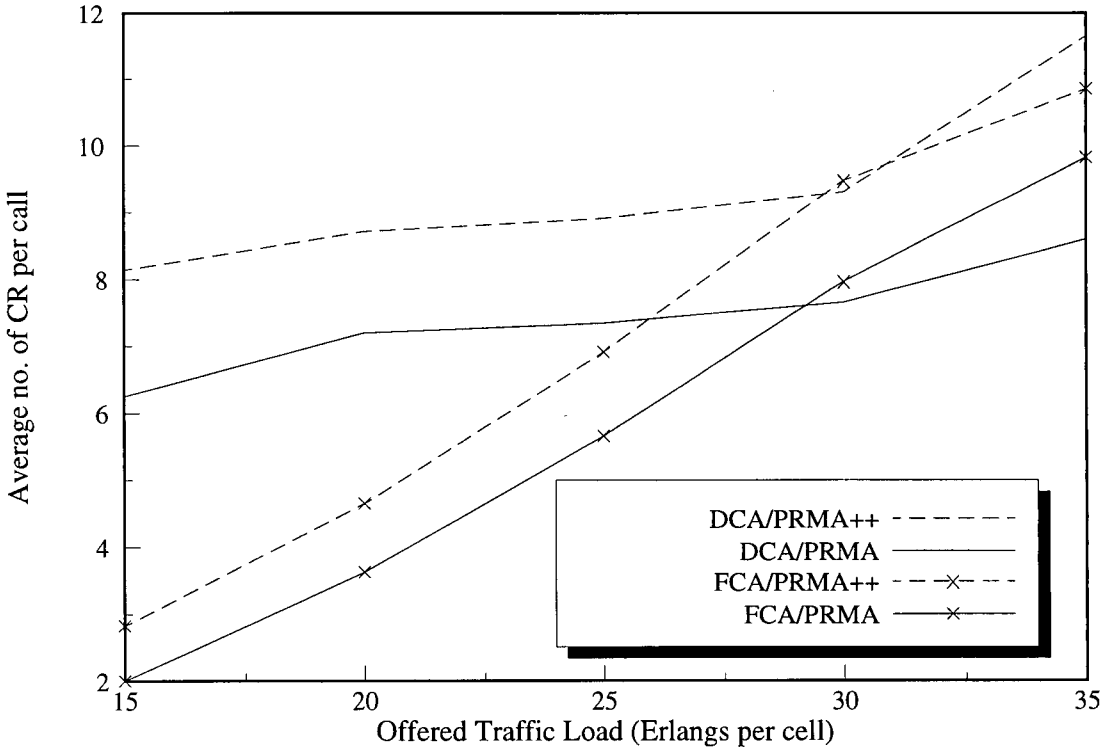

Figure 6.15 Average number of channel reassignment per call.

The CDF of the reservation access delay, D_r, per talkspurt at $\rho = 30$ Erlangs is shown in Figure 6.16. The reservation access delay, D_r, is defined as the time interval between the complete generation of the first packet in a talkspurt at the UT and the time that the first packet is successfully received at the BS during the contention process. In the figure, it can be seen that the reservation access delay in FCA/PRMA is smallest. For FCA/PRMA, about 80% of the talkspurts have their first packets received successfully by the BS within 5 msec. The corresponding figures are about 30% for both FCA/PRMA++ and DCA/PRMA++ and 10% for DCA/PRMA. In FCA/PRMA scheme, once the first packet is generated, the UT can send the packet in *next* available slot. However, in the other schemes, a newly generated packet has to wait for a short period of time. In DCA/PRMA scheme, the newly generated packet cannot be sent until the interference list is received at the end of the frame. In PRMA++ schemes, the newly generated packet is sent in the specified R channels which are placed at the end of the frame.

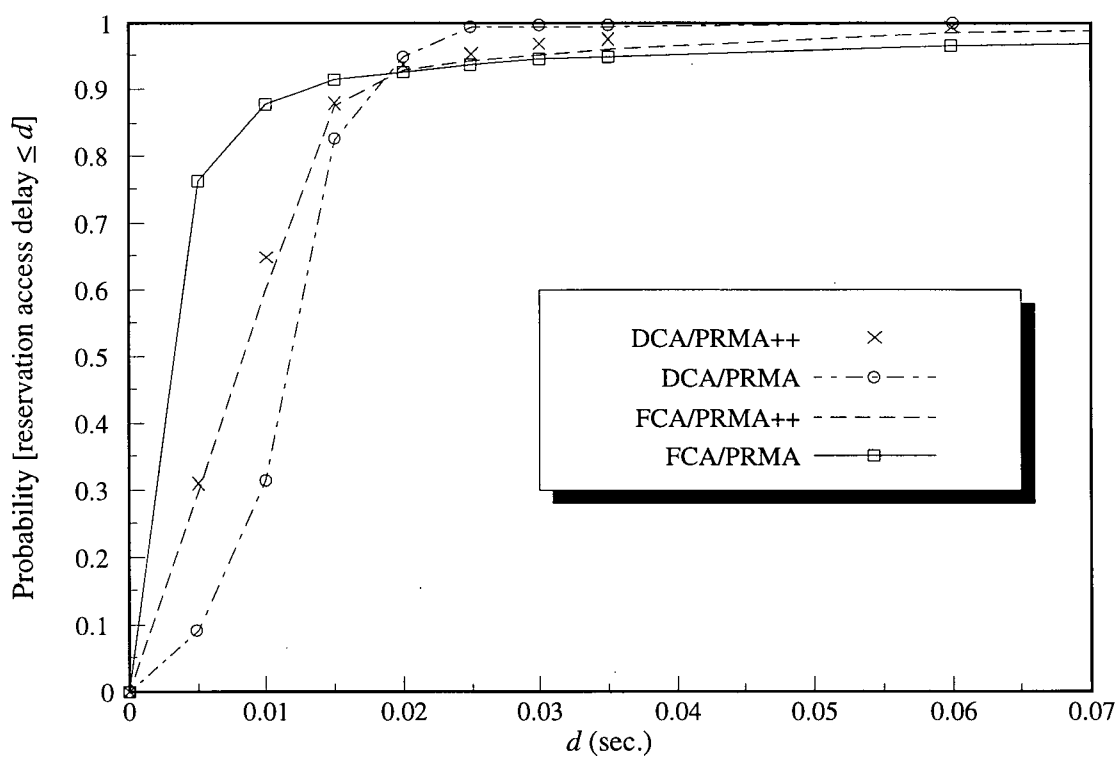

Figure 6.16 The CDF of reservation access delay per talkspurt at $\rho = 30$ Erlangs.

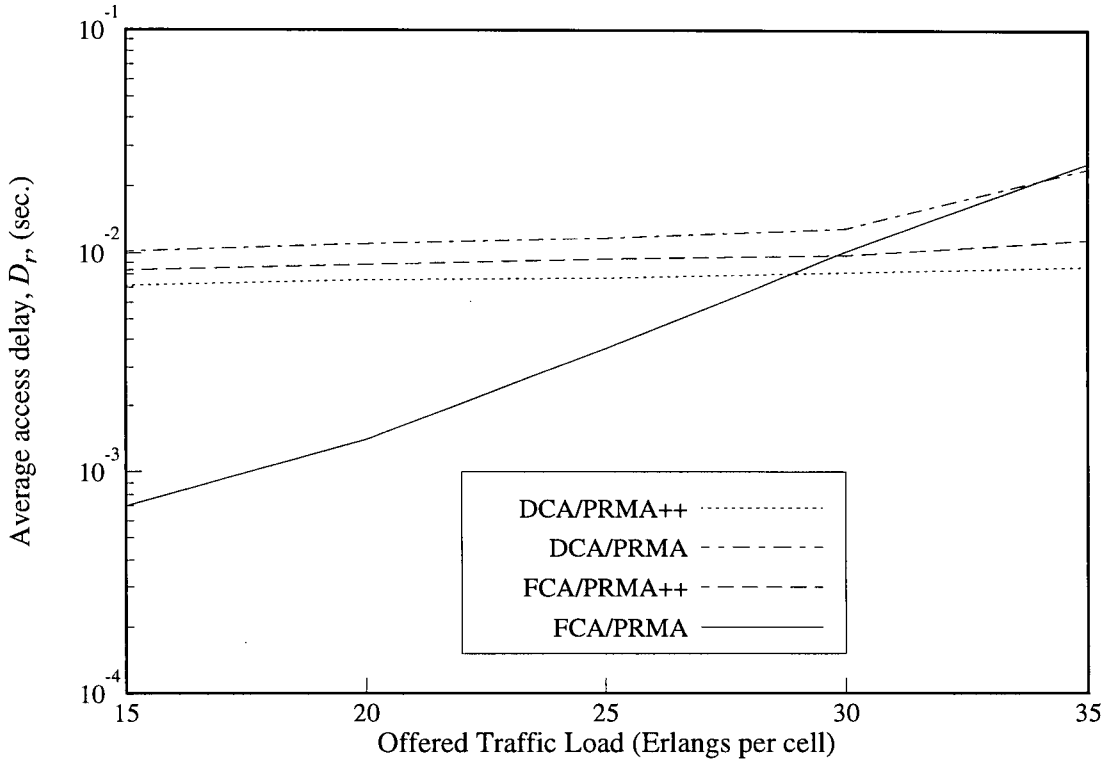

Figure 6.17 Average reservation access delay per talkspurt.

The average access delay, $\overline{D_r}$, is shown in Figure 6.17. It can be seen that the $\overline{D_r}$ of DCA/PRMA is highest because the UT's need to wait for the interference list broadcast from the BS at the end of the frame before sending the first packet in the next frame. For $\rho < 29$, the $\overline{D_r}$ of FCA/PRMA is lowest and increases with ρ. For $\rho > 30$, the $\overline{D_r}$ for FCA/PRMA and DCA/PRMA increase because many UT's attempt to send their packets in the AV channels to contend for reservation. At high loads, the $\overline{D_r}$ for FCA/PRMA becomes higher than that for DCA/PRMA because there are more possible channels (60) used for contending for a RSD channel in DCA/PRMA. In FCA/PRMA++ and DCA/PRMA++, $\overline{D_r}$ increases very slowly because there are enough R channels for contention process. The $\overline{D_r}$ for FCA/PRMA++ is higher than that for DCA/PRMA++ because in FCA/PRMA++ there are two R channels whereas in DCA/PRMA++ there are four R channels. In FCA/PRMA++, if a UT cannot get the reserved channel within these

2 R channels, the UT needs to wait for another frame time to make another attempt. For traffic loads corresponding to $P_T \approx 0.01$ (see Figure 6.13), the $\overline{D_r}$ for FCA/PRMA++, FCA/PRMA, DCA/PRMA++ and DCA/PRMA are 9.3, 6.3, 8.4, 18.5 msec.

6.4.4 Effect of N_L

The effects of the number, N_L, of consecutive packets lost before CR are shown in Figure 6.18 (a) and (b) respectively for FCA/PRMA and DCA/PRMA with CR. In both figures, the N_L value has little effect on P_W and P_C because N_L mainly affects the number of packets lost during their transmission in the RSD channels. Hence, P_I increases with N_L. This can be explained by the following example. If $N_L = 1$, each interfered talkspurt will undergo CR after one packet is lost whereas if $N_L = 2$, each interfered talkspurt will undergo CR after two packets are lost. This explains why the P_I for $N_L = 2$ is about twice of that for $N_L = 1$. Similar observations are obtained for FCA/PRMA++ and DCA/PRMA++ with CR as shown in Figure 6.19 (a) and (b) respectively.

The total packet failure probability, P_T, for PRMA and PRMA++ with different values of N_L is shown in Figure 6.20 (a) and (b) respectively. The increase in P_T with N_L is due to P_I increasing with N_L as shown in Figures 6.18 and 6.19. As ρ increases, P_T curves for different values of N_L become closer because as shown in Figures 6.18 and 6.19 $P_C + P_W$ is close for different N_L and its value becomes higher than P_I for high ρ. At $P_T \approx 0.01$, the capacities for FCA/PRMA++, FCA/PRMA, DCA/PRMA++ and DCA/PRMA with different values of P_I are shown in Table 6.6. It can be seen that the capacities decrease with N_L. The effect of N_L on the capacity at $P_T \approx 0.01$ for FCA is less than that for DCA. For DCA, the capacity is reduced by about 50% when N_L is increased from 2 to 4. This is because the number of CR's per talkspurt in DCA is higher than in FCA and thus, the number of packet lost increases with N_L.

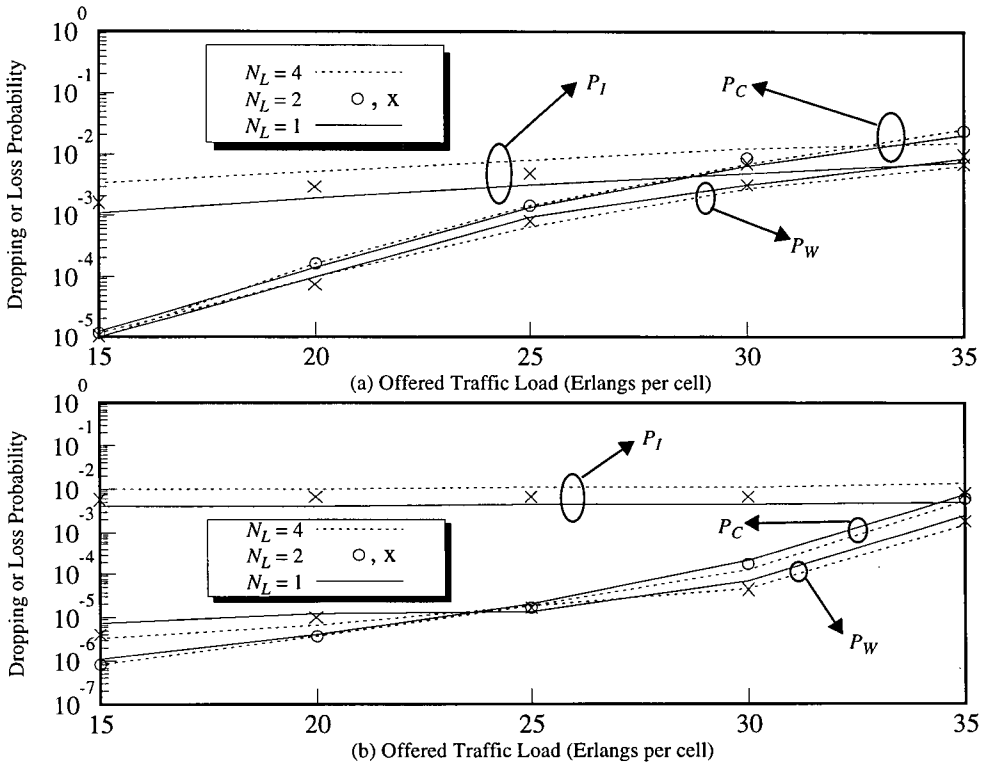

Figure 6.18 Dropping or loss probability with different N_L values for (a) FCA/PRMA and (b) DCA/PRMA.

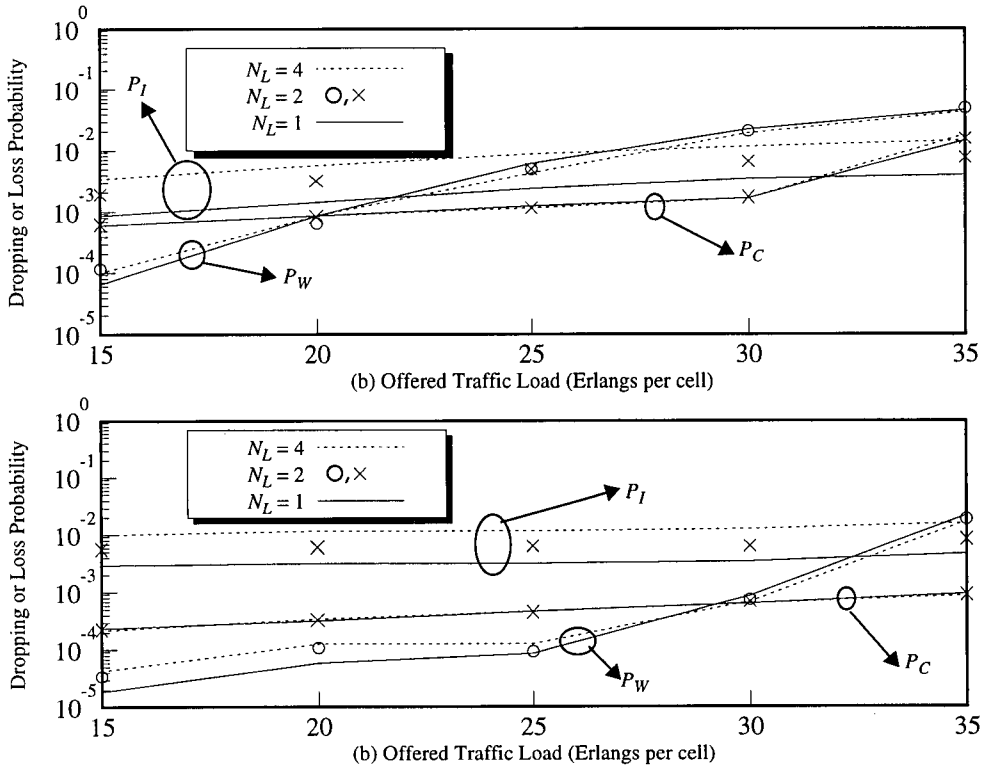

Figure 6.19 Dropping or loss probability with different N_L values for (a) FCA/PRMA++ and (b) DCA/PRMA++.

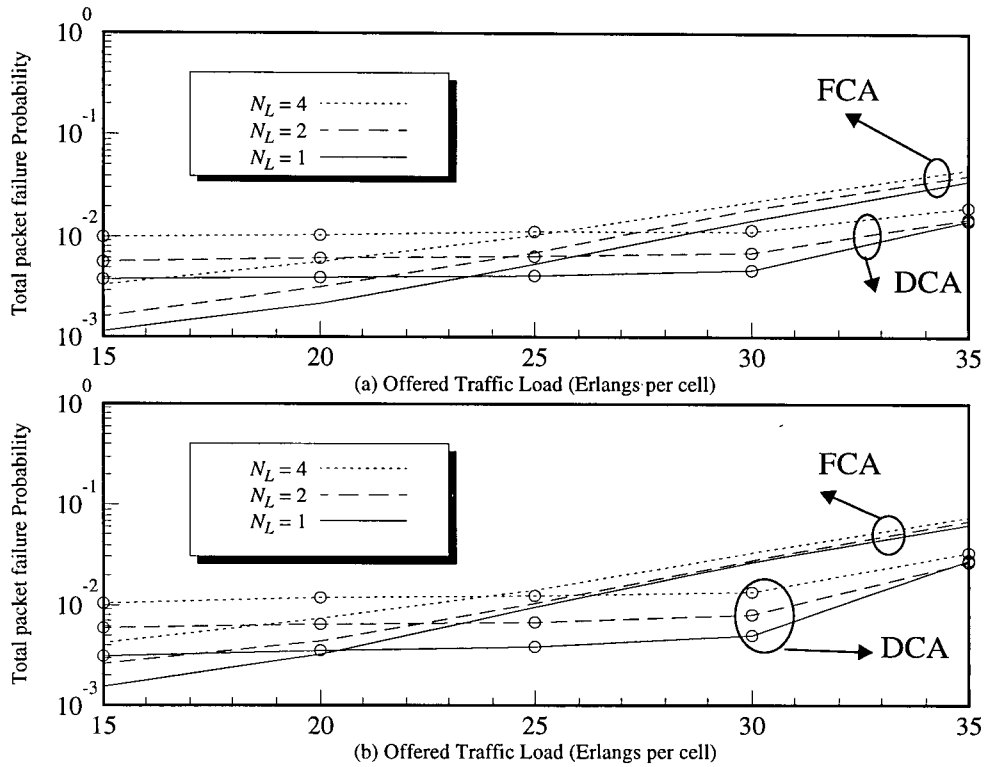

Figure 6.20 Total packet failure probability with different N_L values for (a) PRMA and (b) PRMA++.

Table 6.6 Capacity (Erlangs) at $P_T \approx 0.01$ for different values of N_L.

N_L	**FCA/PRMA**	**FCA/PRMA++**	**DCA/PRMA**	**DCA/PRMA++**
1	28.3	25.5	33.5	32.2
2	27	25	32.5	31
4	25	22.5	15	15

The $\overline{N_{cr}}$ for PRMA and PRMA++ with different values of N_L are shown in Figure 6.21 (a) and (b) respectively. The $\overline{N_{cr}}$ values decrease with N_L because each talkspurt is less likely to undergo CR. For traffic loads corresponding to $P_T \approx 0.01$, the $\overline{N_{cr}}$ for all schemes are shown in Table 6.7. The effect of N_L on $\overline{D_r}$ was also studied. It was found that the $\overline{D_r}$ does not change much with N_L in all schemes.

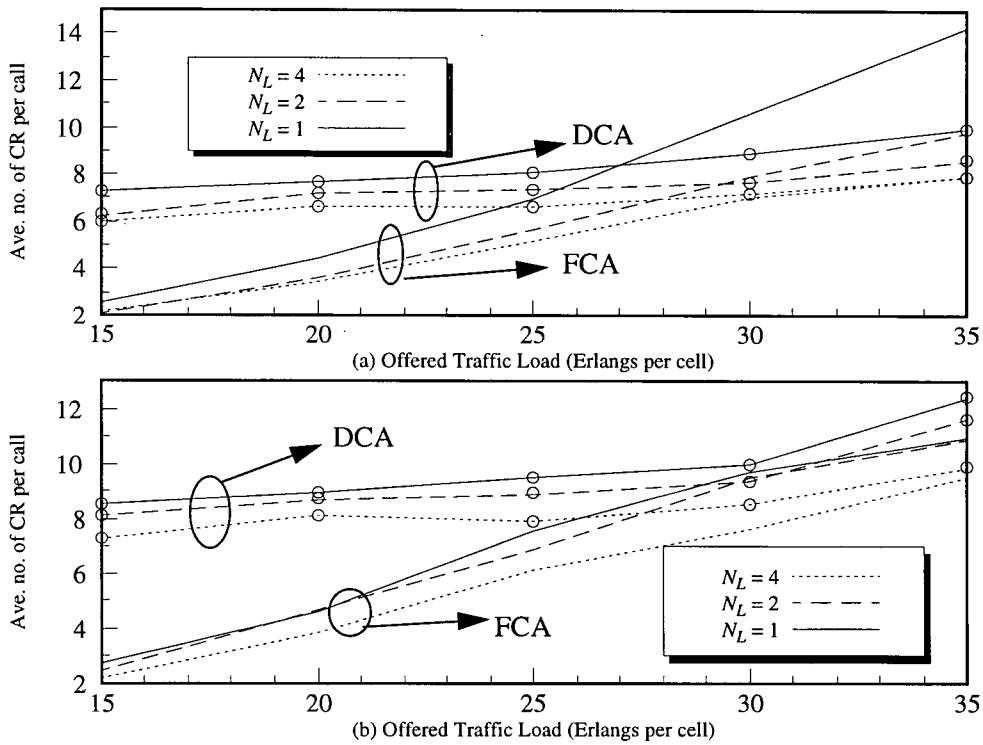

Figure 6.21 Average number of channel reassignments per call with different N_L for (a) PRMA and (b) PRMA++.

Table 6.7 Number of CR for traffic loads corresponding to $P_T \approx 0.01$ with different values of N_L.

N_L	**FCA/PRMA**	**FCA/PRMA++**	**DCA/PRMA**	**DCA/PRMA++**
1	9.3	7.8	8.3	11.0
2	6.6	6.9	8.1	9.7
4	5.2	5.0	5.9	7.3

6.4.5 Effect of Call Setup Time Threshold

In the above results, it is assumed that every new call in the system is accepted so that no new calls are blocked [50]-[53]. However, at high traffic loads, new calls should not always be accepted because of adverse effects on existing calls [76]. In this section, the effect of a call setup time is studied. It is assumed that a new call is blocked if the new call cannot be accepted by the

BS within a maximum call setup time, T_{set}, which is set to 5 seconds in this study. When a new call arrives at the UT, the UT sends its *admission* packet to the BS using the same procedures described for the four schemes in Sections 6.1-6.2, except that the permission probability, p, is replaced by the new call permission probability, p_N. If the *admission* packet can be correctly received at the BS within T_{set}, the new call is accepted. Otherwise, the new call is blocked and lost.

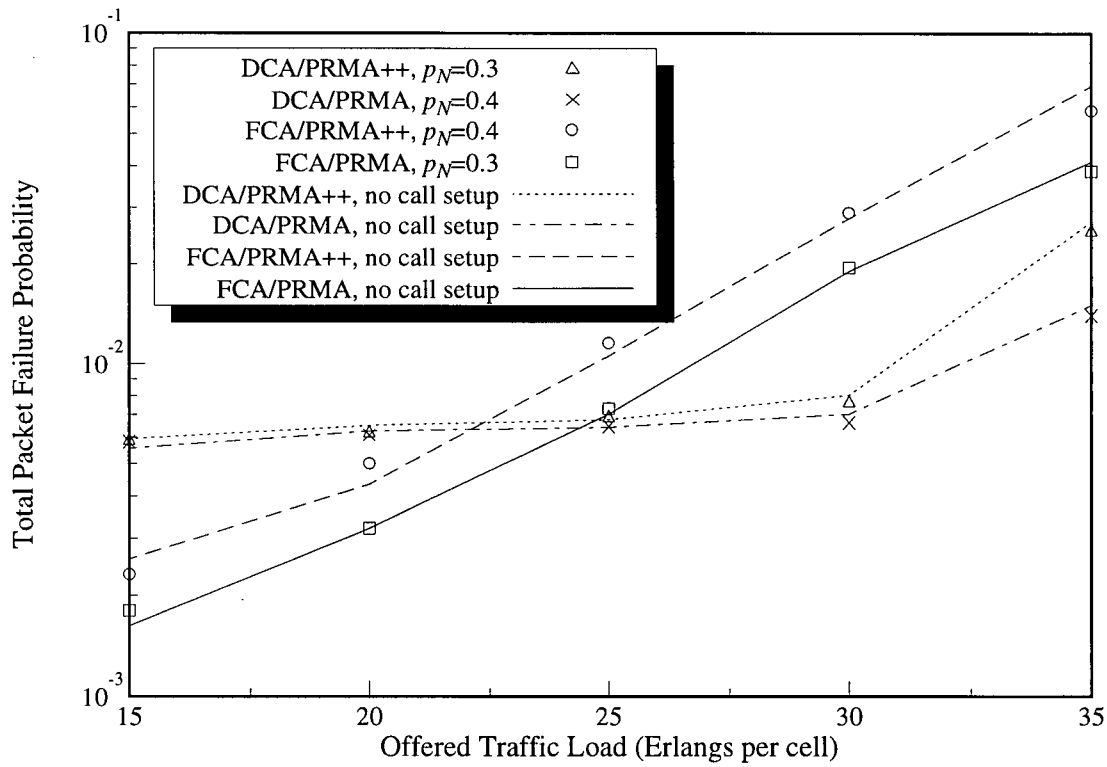

Figure 6.22 Total packet failure probability with call setup time.

The P_T of all four schemes with call setup time threshold for $p_N = p$ are shown in Figure 6.22. The results for P_T without call setup are also included for comparison. It can be seen that P_T is not affected by the call setup time threshold for $\rho \leq 30$. At $\rho = 35$, the use of call setup results in a slightly lower P_T. The new call blocking probabilities, P_b, of all four schemes

are zero for $\rho \leq 30$. At $\rho = 35$, the P_b of all four schemes are quite small, less than 0.1%. As p_N decreases, the number of accepted new calls is reduced thereby lessening the impact on existing calls. Therefore, P_T can be decreased at the expense of a larger P_b by lowering p_N.

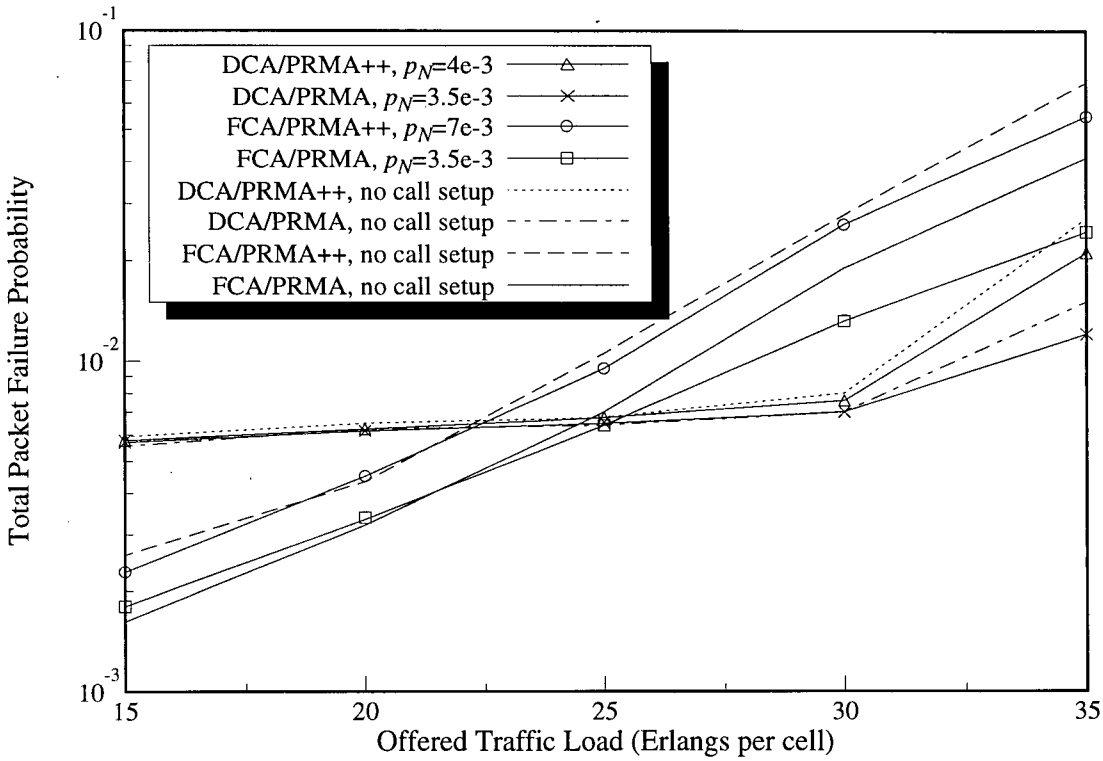

Figure 6.23 Total packet failure probability with optimum p_N.

The P_T with optimum p_N values are shown in Figure 6.23. The optimum p_N values provide the highest capacity at $P_T \approx 0.01$ and $P_b \approx 0.01$. For low loads, the P_T with and without call setup are about the same. This is because there are not many new calls arriving to the system and there are sufficient number of AV channels to accept the new calls. For $\rho > 30$, the P_T with call setup is lower than that without call setup. The P_b values with optimum p_N are shown in Figure 6.24. The P_b for PRMA schemes increases rapidly for $\rho > 30$ because at such high loads

many UT's send their packets to the AV channels to contend for a reservation, thereby increasing the number of collisions and blocked calls. The P_b for PRMA++ increases more slowly because a sufficient number of R channels is allocated for the contention process. The capacities and P_b for all four schemes with optimum p_N corresponding to $P_T \approx 0.01$ are shown in Table 6.8. Compared to Table 6.6, the capacities are increased slightly at the expense of blocking new calls.

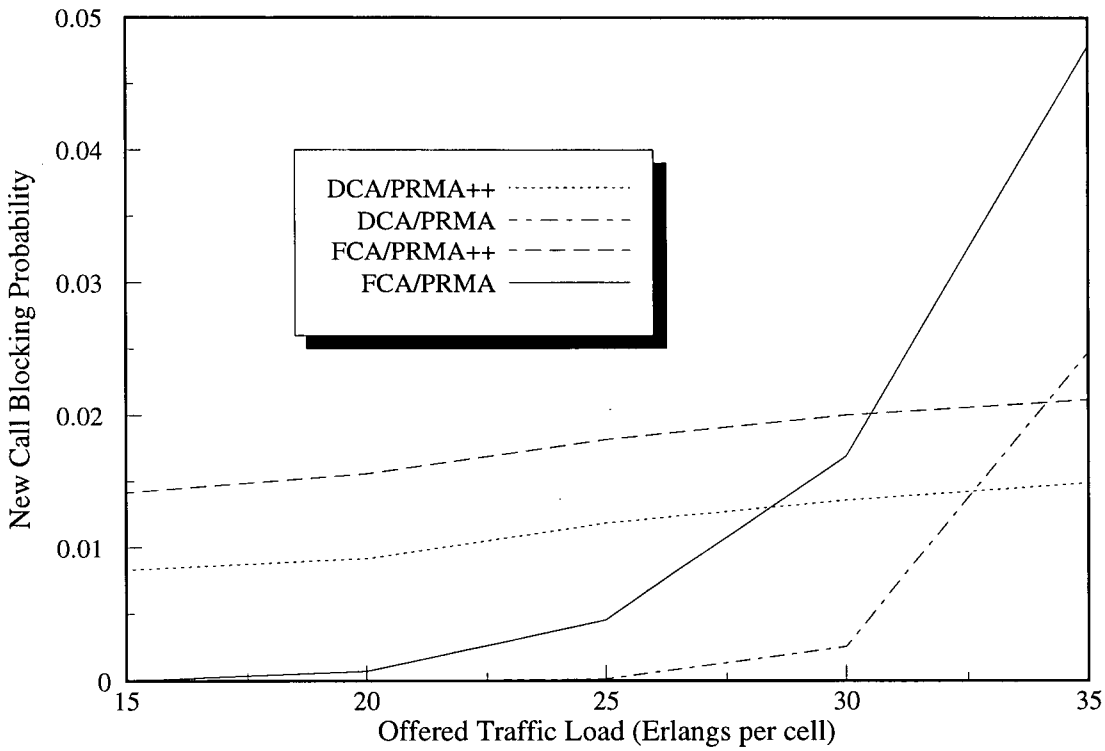

Figure 6.24 New call blocking with optimum p_N.

Table 6.8 Capacities and P_b for all four schemes with optimum P_N corresponding to $P_T \approx 0.01$.

	FCA/PRMA	**FCA/PRMA++**	**DCA/PRMA**	**DCA/PRMA++**
Capacity	28 Erlangs	25.3 Erlangs	33.3 Erlangs	31.5 Erlangs
P_b	0.012	0.018	0.017	0.014

6.5 Conclusions

The performances of FCA or DCA used in conjunction with PRMA or PRMA++ in packet-switched voice cellular systems were studied using computer simulations. The measurement-based DCA schemes were considered to cope with the highly unpredictable and time-varying microcellular environment. First, a measurement-based DCA with the use of PRMA is proposed. Second, the performance of DCA/PRMA++ using different types of measurement-based DCA strategies was studied. Third, a channel reassignment scheme is introduced in order to improve the capacity. It was found that the capacity of PRMA is higher than that of PRMA++ with either FCA or DCA. With no channel reassignment, the total packet failure probability for all four schemes is quite high due to the high packet loss probabilities for talkspurts which experience high interference. With channel reassignment, the packet loss probability due to talkspurts which encounter high interference can be reduced significantly. The capacity for FCA with channel reassignment at a 1% total packet failure probability can be increased by about 80% compared to that for FCA with no channel reassignment. An additional 25% increase in capacity can be obtained by using DCA. The number of channel reassignment per call for DCA/PRMA++ is highest for traffic loads corresponding to $P_T \approx 0.01$. The reservation access delay for DCA/PRMA is highest for traffic loads corresponding to $P_T \approx 0.01$. We also studied the effect of call setup time threshold in terms of call blocking probability.

Chapter 7 Conclusions

This chapter summarizes the main contributions of this thesis. Some suggestions for future work are also given.

7.1 Main Contributions

The focus of this research work is to study the performances of various types of channel assignment schemes for use in cellular communications systems. The performance of improved fixed channel assignment (FCA) schemes using reuse partitioning (RP) is studied first.

- In Chapter 3, the analysis for an n-region basic RP scheme with no channel rearrangement (NCR) using FCA for stationary users is presented. A Markov chain model is developed to evaluate the call blocking probability in each region. A *modified* n-region RP scheme with optimal channel rearrangement (OCR) or single channel rearrangement (SCR) is then introduced. A closed-form expression for the call blocking probability for n-region RP scheme with OCR is derived. Results show that a 2, 3 and 4-region RP scheme with OCR can improve the system capacity by about 25%, 36% and 43% compared to a conventional FCA system without RP. The effects of allowing no, single or optimal channel rearrangement are studied. As expected, RP with OCR provides the best performance. The performance difference between SCR and OCR is quite small indicating that SCR is a good choice for the RP system. The performance difference between the NCR and OCR schemes increases slightly with n. For $n = 2$, the capacity of RP with NCR is about same as that with OCR. For $n = 4$, the capacity of RP with NCR is about 5% less than that of RP with OCR. Finally, numerical results

for a 2-region RP system are compared with simulation results for slowly moving users for different mobility models in order to determine the range of parameters over which the assumption of stationary users is valid.

- In Chapter 4, the impact of mobile users on a 2-region RP using FCA (FRP) system with prioritized handoff is studied. A 2-dimensional Markov chain model is obtained to evaluate the call blocking and dropping probabilities. With no channels reserved for handoffs, the call blocking and dropping probabilities can be approximated using a product form solution. The analytic results are verified using simulation for different mobility models. With stationary users, the capacity can be increased by about 30% compared to conventional FCA. With mobile users, the capacities for both FRP and FCA decrease with average handoff rates. Also, the capacity improvement of FRP relative to FCA is reduced as the average handoff rates increase. The results show that more channels should be assigned to the outer region as average handoff rates increase. It is found that even though prioritized handoff can reduce the call dropping probability, in some cases it may also degrade the capacity. The choice of the number of channels to be reserved for handoffs which maximizes the capacity is also examined.

In these analyses, a regular hexagonal cell pattern with equal cell size is assumed. For irregular and different cell sizes, it is expected that RP can still perform better than conventional FCA. This is because RP allows an increase in the total number of channels available in each cell.

Then a new cell-based distributed dynamic channel assignment scheme to improve capacity is proposed and compared with previous DCA schemes.

- In Chapter 5, a new distributed channel assignment scheme, namely DCA with interference information (DCA-WI), is proposed. In DCA-WI, the channel to be used in a cell is selected by the local BS based on information provided by its interference information table. The channel assignment strategy attempts to minimize the effect on the availability of channels in interfering cells. Inter-cell and intra-cell channel reassignment are introduced to further reduce the call blocking probability. Simulation results indicate that DCA-WI outperforms previously proposed schemes for both uniform and nonuniform spatial traffic distributions. In a 49-cell system with uniform traffic distribution, a cluster size of 7 and a total of 70 available channels, DCA-WI with inter-cell single channel reassignment can carry about 70% more traffic than the conventional FCA system at a call blocking probability of 0.01. The capacity can be slightly increased with the use of inter-cell double channel reassignment. The performance of DCA-WI is close to that of the idealized DCA scheme using the Clique Packing method. It is found that inter-cell double channel reassignment does not improve the system capacity for nonuniform traffic distributions.

The above studied channel assignment schemes can be used in *current* circuit-switched TDMA systems, i.e., IS-136 and GSM, to improve their system capacity. To support bursty traffic, third-generation cellular communication systems will employ packet-switching technology. The final aspect of this research is to propose and evaluate the performance of measurement-based DCA with the use of packet reservation multiple access (PRMA) schemes in future packet-switched TDMA cellular systems.

- In Chapter 6, the performances of FCA or DCA used in conjunction with PRMA or PRMA++, i.e., FCA/PRMA, FCA/PRMA++, DCA/PRMA and DCA/PRMA++, in packet-switched cellular systems are studied for packet voice transmission. The measurement-based, DCA/PRMA and DCA/PRMA++, schemes, are considered to cope with the highly unpredictable and time-varying microcellular environment. Firstly, we propose a new DCA/PRMA scheme in which channel assignment is based on power measurements from the BS. Secondly, we study the performance of DCA/PRMA++ using various measurement-based DCA strategies, i.e., ARP, LIC and MIC. Thirdly, a channel reassignment (CR) scheme is introduced in order to improve the capacity; this reassignment reduces the number of packets lost during a talkspurt which experiences high interference. The capacity for FCA with CR at a 1% total packet failure probability can be increased by about 80% compared to that for FCA with no CR. An additional 25% increase in capacity can be obtained by using DCA.

7.2 Suggestions for Future Work

Among the related topics for further study are the following:

- Third-generation cellular communication systems use hierarchical cell structures (HCS) [7] which consist of overlaying macrocells on top of smaller microcells to increase the system capacity. In this suggestion, we can use a cell with 2 concentric regions as a macrocell and a regular one region cell as a microcell in a FCA system as shown in Figure 7.1. Therefore, fast mobile users can be assigned to 2-region RP macrocells in order to increase the capacity whereas slow mobile users are assigned to mi-

crocell. In this HCS, the 2-region cell used as a macrocell can still provide a reasonably good improvement because the outgoing handoff rate is small due to the large macrocell.

- The effect of mobile users in the DCA-WI scheme can be studied. The performance of reserved channels for handoffs only to improve the capacity can be considered.
- The DCA-WI scheme can be combined with RP (DRP) in an attempt to further improve the capacity as shown in Figure 7.2. In this scheme, the total number of available channels can be divided into two sets, inner and outer channels. Inner calls which find no free inner region channels can be assigned to the outer region channels.
- The effect of mobile users on the performance of the measurement-based DCA/PRMA and DCA/PRMA++ schemes can be studied. The inclusion of data and other traffic in addition to voice can be considered.

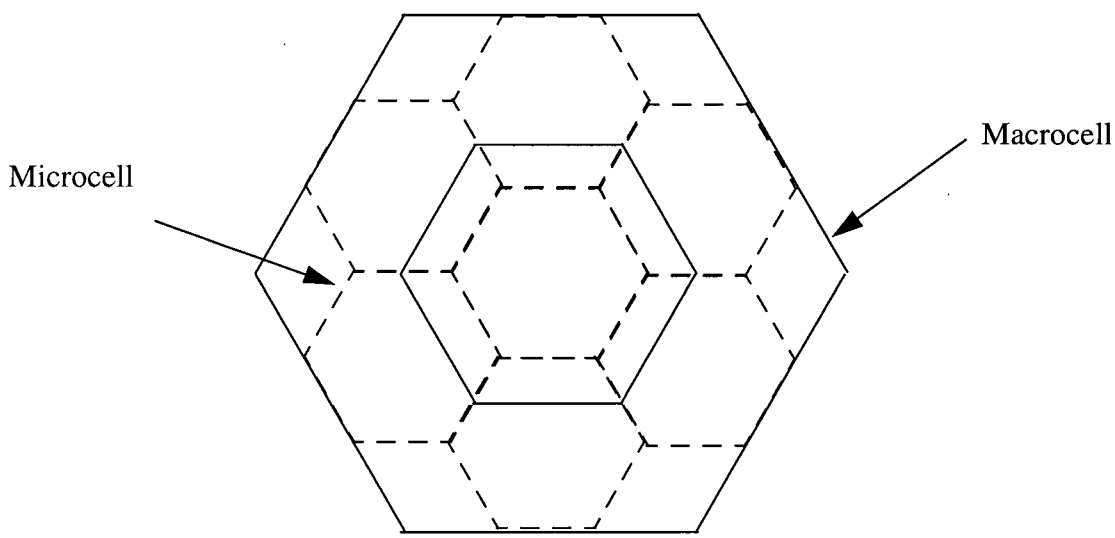

Figure 7.1 Hierarchical cell structures with 2-region cell overlaying one-region cells.

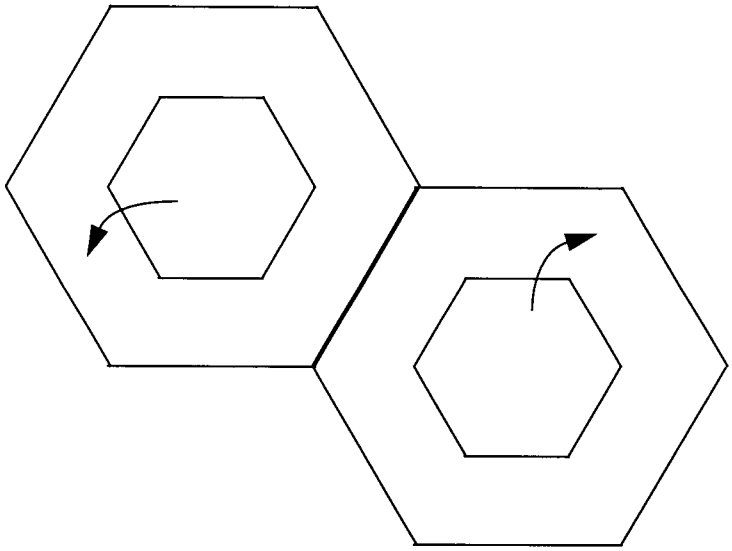

Figure 7.2 Cell structure of DRP.

Glossary

α	- Grade of Service parameter
γ	- Propagation factor
ρ	- Traffic load
A-slot	- Acknowledgment Slot
ACK	- Acknowledgment
ACL	- Available Channel List
AMPS	- Advanced Mobile Phone Service
ARP	- Autonomous RP
ATDMA	- Advanced TDMA
AV	- Available
BCO	- Borrowing with Channel-Ordering
BDCL	- Borrowing with Directional Channel-Locking
BS	- Base Station
C_i	- Number of channels assigned to region i
C_{opt}	- Optimum number of reserved channels
CBA	- Channel Borrowing Assignment
CBWL	- Channel Borrowing Without Locking
CDCA	- Centralized DCA
CDMA	- Code Division Multiple Access
CR	- Channel Reassignment
d_{max}	- Maximum acceptable delay
d_i	- Reuse distance for region i
D	- Minimum co-channel reuse distance
D_r	- Reservation access delay

$\overline{D_r}$	- Average reservation access delay
DCA	- Dynamic Channel Assignment
DCA-WI	- DCA with interference information
DCA-WI (double)	- DCA-WI with double channel rearrangement
DCA/PRMA	- DCA with PRMA scheme
DDCA	- Distributed DCA
FCA	- Fixed Channel Assignment
FCA/PRMA	- FCA with PRMA scheme
FDD	- Frequency-Division Duplexing
FDMA	- Frequency Division Multiple Access
FRP	- RP using FCA
FRU	- Flexible Reuse
GSM	- Global System for Mobile Communications
H_n	- Handoff activity
I-slot	- Information Slot
IIT	- Interference Information Table
IMT-2000	- International Mobile Telecommunications 2000
L	- Path loss
LIC	- Least Interfered Channel
MCS	- Mobile Communication Systems
MIC	- Most Interfered Channel
MP	- Maximum Packing
MS	- Mobile Station
MSIR	- Maximum SIR
N_{cr}	- Number of channel rearrangement per call
$\overline{N_{cr}}$	- Average number of channel rearrangement per call

N_i	- Cluster size for region i
N_L	- Number of consecutive packets lost before CR
NC	- Nominal Channel
NCR	- No Channel Rearrangement
NCS	- Nominal Channel Set
NMT	- Nordic Mobile Telephone System
OCR	- Optimal Channel Rearrangement
OV	- Overflow
p_{rel}	- Release probability
P_C	- Probability of packet dropped due to failed contention process
P_I	- Probability of packet lost due to strong interference
P_T	- Total packet failure probability
P_W	- Probability of packet dropped due to waiting too long in the BS buffer
P_{nc}	- Noncompleted call probability
PRMA	- Packet Reservation Multiple Access
r_i	- Radius for region i
R-slot	- Reservation Slot
RP	- Reuse Partitioning
RSD	- Reserved
SIR_{diff}	- SIR difference between the estimated SIR at initial setup and SIR_{min}
SIR_{min}	- Minimum acceptable SIR
SIR_{setup}	- SIR setup threshold
SCR	- Single Channel Rearrangement
SIR	- Signal-to-Interference Power Ratio

T_{set}	- Call setup time
TACS	- Total Access Communications System
TDD	- Time-Division Duplexing
TDMA	- Time Division Multiple Access
UMTS	- Universal Mobile Telecommunications System
UT	- User Terminal
UTRA	- UMTS Terrestrial Radio Access
UWC-136	- Universal Wireless Communications-136
$\overline{V}$	- Mean speed of the mobile station
WCDMA	- Wideband CDMA
WTDMA	- Wideband TDMA

Bibliography

[1] J. Gibson, *The Communications Handbook*: CRC Press, 1997.

[2] UMTS Forum, "A regulartory framework for UMTS," Rep. 1, June 26, 1997.

[3] E. Nikula, A. Toskala, E. Dahlman, L. Girard and A. Klein, "FRAMES multiple access for UMTS and IMT-2000," *IEEE Pers. Commun.*, vol. 5, no. 2, pp. 16-24, April 1998.

[4] K. Balachandran, R. Ejzak, S. Nanda, S. Vitebskiy and S. Seth, "GPRS-136: high-rate packet data service for North American TDMA digital cellular systems," *IEEE Pers. Commun.*, vol. 6, no. 3, pp. 34-47, June 1999.

[5] M. Zeng, A. Annamalai and V. Bhargava, "Recent advances in cellular wireless communications," *IEEE Commun. Mag.*, vol.37, no. 9, pp. 128-138, Sept. 1999.

[6] P. Chaudhury, W. Mohr and S. Onoe, "The 3GPP proposal for IMT-2000," *IEEE Commun. Mag.*, vol.37, no. 12, pp. 72-81, Dec. 1999.

[7] T. Ojanpera and R. Prasad, "An overview of air interface multiple access for IMT-2000/ UMTS," *IEEE Commun. Mag.*, vol.36, no. 9, pp. 82-95, Sept. 1998.

[8] R. Steele and M. Nofal, "Teletraffic performance of microcellular personal communication networks," *Proc. IEE*, Part I, no. 4, pp. 448-461, 1992.

[9] R. Steele, "Microcellular Radio Communications," *The Communications Handbook*: CRC Press, 1997, pp. 1160 - 1174.

[10] S. Nanda, "Teletraffic models for urban and suburban microcells: cell sizes and handoff rates," *IEEE Trans. on Veh. Technol.*, vol. 42, no. 4, pp. 673-682, Nov. 1993.

[11] W.C.Y Lee, *Mobile Cellular Communication Systems*, 2nd ed. New York: McGraw-Hill, 1995.

[12] I. Katzela and M. Naghshineh, "Channel assignment schemes for cellular mobile telecommunication systems: a comprehensive survey," *IEEE Pers. Commun.*, vol. 3, no. 3, pp. 10-31, June 1996.

[13] N. Sollenberger, N. Seshadri and R. Cox, "The evolution of IS-136 TDMA for Third-Generation Wireless Services," *IEEE Pers. Commun.*, vol. 6, no. 3, pp. 8-18, June 1999.

[14] C. Mihailescu, X. Lagrange and Ph. Godlewski, "Locally centralized dynamic resource allocation algorithm for the UMTS in Manhattan environment," in *Proc. of IEEE Pers., Indoor and Mobile Radio Commun. Symposium*, Boston, USA, Sept. 1998.

[15] C. Mihailescu, X. Lagrange and Ph. Godlewski, "Dynamic resource allocation for UMTS TD-CDMA systems," in *Proc. of the 3rd European Pers. Commun.*, Paris, France, March 1999.

[16] S. W. Halpern, "Reuse partitioning in cellular systems", in *Proc. of IEEE Veh. Technol. Conf.,* Toronto, Canada, pp. 322-327, May 1983.

[17] K. Sallberg, B. Stavenow and B. Eklundh, "Hybrid assignment and reuse partitioning in a cellular mobile radio telephone system", in *Proc. of IEEE Veh. Technol. Conf.,* Tampa, Florida, USA, pp. 405-411, June 1987.

[18] T. Salvalaggio, "On the application of reuse-partitioning", in *Proc. of IEEE Veh. Technol. Conf.,* Philadelphia, PA, USA, pp. 182-185, 1988.

[19] A. Pattavina, S. Quadri and V. Trecordi, "Spectral efficiency improvement of enhanced assignment techniques in cellular networks", in *Proc. of IEEE GLOBECOM '96*, London, UK, vol. 2, pp. 1031-1035, Nov 1996.

[20] S. Papavassiliou, L. Tassiulas and P. Tandon, "Meeting QOS requirements in a cellular network with reuse partitioning", *IEEE J. on Selected Areas in Comm.*, vol. 12, no. 8, pp. 1389-

1400, October 1994.

[21] J. Choi and J.A. Silvester, "A Fair-Optimal channel borrowing scheme in multiservice cellular networks with reuse partitioning", in *Proc. of IEEE Int. Conf. Universal Pers. Commun.*, Florence, Italy, pp. 261-265, Oct. 1998.

[22] J. Zander and M. Frodigh, "Capacity allocation and channel assignment in cellular radio system using reuse partitioning", *Electronics Letters*, vol. 28, no. 5, pp. 438-440, February 1992.

[23] D. Goodman, S. Grandhi and V. Vijayan, "Distributed dynamic channel assignment schemes," in *Proc. of IEEE Veh. Technol. Conf.*, pp. 532-535, 1993.

[24] P. H. J. Chong and C. Leung, "Performance analysis of reuse partitioning in cellular systems," in *Proc. of IEEE Pacific Rim Conf. on Commun., Computers and Signal Processing*, Victoria, Canada, pp. 213-216, Aug. 1999.

[25] D. Bertsekas and R. Gallager, *Data Networks*, 2nd ed. New Jersey: Prentice-Hall, 1992.

[26] T. Chu and S. Rappaport, "Overlapping coverage with reuse partitioning in cellular communications systems," *IEEE Trans. Veh. Technol.*, vol. 46, no. 1, pp. 41-54, Feb. 1997.

[27] P. H. J. Chong and C. Leung, "Performance analysis of reuse partitioning with mobile users," in *Proc. of IEEE Int. Conf. on Commun.*, Vancouver, BC, Canada, vol. 3, pp. 1852-1858, June 6-10, 1999.

[28] M. Zhang and T. Yum, "Comparisons of channel assignment strategies in cellular mobile telephone systems," *IEEE Trans. Veh. Technol.*, vol. 38, no. 4, pp. 211-215, Nov. 1989.

[29] K. Yeung and T. Yum, "Compact pattern based dynamic channel assignment for cellular mobile systems," *IEEE Trans. Veh. Technol.*, vol. 43, no. 4, pp. 892-896, Nov. 1994.

[30] K. Chang, J. Kim, C. Yim and S. Kim, "An efficient borrowing channel assignment scheme

for cellular mobile systems," *IEEE Trans. Veh. Technol.*, vol. 57, no. 2, pp. 602-608, May 1998.

[31] P. H. J. Chong and C. Leung, "A new channel borrowing scheme with interference information for cellular systems," in *Proc. of IEEE Veh. Technol. Conf.*, Houston, TX, USA, vol. 1, pp. 20-24, May 16-19, 1999.

[32] P. Raymond, "Performance analysis of cellular networks," *IEEE Trans. on. Commun.*, vol. 39, no. 12, pp. 1787-1793, Dec. 1991.

[33] K. Nakano, M. Sengoku, S. Shinoda and T. Abe, "Clique packing in cellular mobile communication systems," in *Proc. of IEEE Int. Conf. Universal Pers. Commun.*, pp. 71-75, Nov. 1995.

[34] T. Kanai, "Autonomous reuse partitioning in cellular systems," in *Proc. of IEEE Veh. Technol. Conf.*, vol. 42, pp. 782-785, May 1992.

[35] J. Chuang, "Performance issues and algorithms for dynamic channel assignment," *IEEE J. Select. Areas Commun.*, pp. 955-963, Aug. 1993.

[36] M. Cheng and J. Chuang, "Performance evaluation of distributed measurement-based dynamic channel assignment in local wireless communications," *IEEE J. Select. Areas Commun.*, pp. 698-710, May 1996.

[37] A. Law and L. Lopes, "Effects of channel history on choice of DCA algorithm within DECT," in *Proc. of IEEE Veh. Technol. Conf.*, pp. 1669-1673, May 1997.

[38] J. Chuang and N. Sollenberger, "Spectrum resource allocation for wireless packet access with application to advanced cellular internet service," *IEEE J. on Selected Areas in Comm.*, vol. 16, no. 6, pp. 820-829, Aug. 1998.

[39] M. Cheng and L. Chang, "Comparison of two dynamic channel assignment schemes under

packet data traffic," in *Proc of IEEE Veh. Technol. Conf.*, Ottawa, Canada, vol. 3, pp. 1765-1769, May 1998.

[40] W. Tsuchiya and H. Morikawa, "Downlink channel assignment algorithms for packet-based wireless TDMA/FDMA networks," in *Proc. of IEEE Pers. Indoor and Mobile Radio Commun. Symposium*, vol. 3, pp. 1202-1206, Oct. 1996.

[41] T.S. Rappaport, *Wireless Communications*. New Jersey: Prentice-Hall, 1996.

[42] D. Goodman, R. Valenzuela, K. Gayliard and B. Ramamurthi, "Packet reservation multiple access for local wireless communications," *IEEE Trans. Commun.*, vol. 37, pp. 885-890, Aug. 1989.

[43] R. Fantacci and F. Innocenti, "Performance evaluation of a modified PRMA protocol for joint voice and data packet wireless networks," *IEEE Trans. Commun.*, vol. 47, pp. 1837-1848, Dec. 1999.

[44] D. Goodman and S. Wei, "Efficiency of packet reservation multiple access," *IEEE Trans. Veh. Technol.*, vol. 40, no. 1, pp. 170-176, Feb. 1991.

[45] S. Nanda, "Stability evaluation and design of the PRMA joint voice data system," *IEEE Trans. Commun.*, vol. 42, pp. 2092-2104, May 1994.

[46] A. Urie, "Advanced TDMA mobile access," in *Proc. of IEEE Int. Conf. Universal Pers. Commun.*, Ottawa, Canada, vol. 1, pp. 392-396, Oct. 1993.

[47] J. DeVile, "A Reservation based multiple access scheme for a future universal mobile telecommunications system," in *Proc. of IEE Conf. on Mobile and Pers. Commun.*, London, UK, pp. 210-215, Dec. 1993.

[48] J. Dunlop, J. Irvine, D. Robertson and P. Cosimini, "Performance of a statistically multiplexed access mechanism for a TDMA radio interface," *IEEE Pers. Commun.*, vol. 2, no. 3,

pp. 56-64, June 1995.

[49] J. Dunlop, P. Cosimini and D. Robertson, "Optimization of packet access mechanisms for advanced time division multiple access," in *Proc. of IEE Conf. on Mobile Pers. Commun.*, Brighton, UK, pp. 13-15, Dec. 1993.

[50] M. Frullone, G. Riva, P. Grazioso and C. Carciofi, "Performance analysis of channel segregation in cellular environment with PRMA," *IEICE Trans. Fundamentals*, vol. E78-A, no. 7, July 1995.

[51] M. Frullone, G. Riva, P. Grazioso and C. Carciofi, "PRMA performance in cellular environments with self-adaptive channel allocation strategies," *IEEE Trans. Veh. Technol.*, vol. 45, pp. 657-665, Nov. 1996.

[52] T. Benkner and K. David, "Autonomous slot assignment schemes for PRMA++ third generation TDMA systems," in *Proc. of IEEE Sym. Commun. Veh. Technol. Benelux*, Eindhoven, Neth., pp. 13-19, 1995.

[53] T. Uehara, T. Seto and Y. Akaiwa, "A dynamic channel assignment method for voice packet transmission cellular system," in *Proc. of IEEE Veh. Technol. Conf.*, Houston, TX, pp 2000-2004, May 1999.

[54] M. Zhang and T. Yum, "The nonuniform compact pattern allocation algorithm for cellular mobile systems," *IEEE Trans. Veh. Technol.*, vol. 40, pp. 387-391, 1991.

[55] W. Tuttlebee, "Cordless personal communications," *IEEE Commun. Mag.*, pp. 42-53, Dec 1992.

[56] D. Cox and D. Reudink, "Dynamic channel assignment in two-dimensional large scale mobile radio systems," *Bell Syst. Technol. J.*, pp. 1611-1629, Sept. 1972.

[57] D. Cox and D. Reudink, "A comparison of some channel assignment strategies in large-scale

mobile communication systems," *IEEE Trans. Commun.*, vol. COM-20, pp. 190-195, Apr. 1972.

[58] T. Kahwa and N. Georganes, "A hybrid channel assignment scheme in large-scale cellular-structured mobile communication systems," *IEEE Trans. Commun.*, vol. Com-26, pp. 432-438, Apr. 1978.

[59] D. Everitt and N. Macfadyen, "Analysis of multicellular mobile radiotelephone systems with loss," *British Telecom. Technol. J.*, vol. 1, no. 2, pp. 37-45, 1983.

[60] D. Dimitrijevic and J. Vucetic, "Design and performance analysis of the algorithms for channel allocation in cellular networks," *IEEE Trans. Veh. Technol.*, vol. 42, no. 4, pp. 526-534, Nov, 1993.

[61] C. I and P. Chao, "Local packing - Distributed dynamic channel allocation at cellular base station," in *Proc of IEEE GLOBECOM* '93, pp.293-301, 1993.

[62] E. Del Re, R. Fantacci and G. Giambene, "Handover and dynamic channel allocation techniques in mobile cellular networks," *IEEE Trans. Veh. Technol.*, vol. 44, no. 2, pp. 229-237, May, 1995.

[63] R. Nettleton and G. Schloemer, "A high capacity assignment method for cellular mobile telephone systems," in *Proc. of IEEE Veh. Technol. Conf.*, pp. 359-367, 1989.

[64] S. Onoe and S. Yasuda, "Flexible reuse for dynamic channel assignment in mobile radio systems," in *Proc. of IEEE Int. Conf. on Commun.*, pp. 472-476, June 1989.

[65] M. Serizawa and D. Goodman, "Instability and deadlock of distributed channel allocation," in *Proc. of IEEE Veh. Technol. Conf.*, pp. 528-531, 1993.

[66] Y. Akaiwa and H. Andoh, "Channel Segregation-A self-organized dynamic channel allocation method: application to TDMA/FDMA microcellular system," *IEEE J. on Sel. Areas in*

Comm., vol. 11, no. 6, pp. 949-954, Aug. 1993.

[67] H. Furukawa and Y. Akaiwa, "Self-organized reuse partitioning, a dynamic channel assignment method in cellular system," in *Proc. of IEEE Veh. Technol. Conf.*, pp. 524-527, May 1993.

[68] Y. Yeh and S. Schwartz, "Outage probability in mobile telephony due to multiple log-normal interferers," *IEEE Trans. Commun.*, vol. Com-32, pp. 380-388, Apr. 1984.

[69] F. Blecher, "Advanced mobile phone service," *IEEE Trans. Veh. Technol.*, vol. VT-29, pp. 238-244, May 1980.

[70] D. Cox, "Wireless network access for personal communications," *IEEE Comm. Mag.*, pp. 96-115, Dec., 1992.

[71] L. Anderson, "A simulation study of some dynamic channel assignment algorithm in a high capacity mobile telecommunication system," *IEEE Trans. Veh. Technol.*, vol. VT-22, no. 4, pp. 210-217, Nov. 1973.

[72] S. Elnoubi, R. Singh and S. Gupta, "A new frequency channel assignment in high capacity mobile communication systems," *IEEE Trans. Veh. Technol.*, vol. VT-31, no. 3, pp. 125-131, Aug. 1982.

[73] H. Jiang and S. Rappaport, "CBWL: A new channel assignment and sharing method for cellular communication systems," *IEEE Trans. Veh. Technol.*, vol. 43, no. 2, pp. 313-322, May 1994.

[74] A. Tanenbaum, *Computer Networks*. Englewood Cliffs, NJ: Prentice-Hall, 1981.

[75] M. Frullone, G. Falciasecca, P. Grazioso, G. Riva and A. Serra, "On the performance of packet reservation multiple access with fixed and dynamic channel allocation," *IEEE Trans. Veh. Technol.*, vol. 42, no. 1, pp. 78-86, Feb. 1993.

[76] W. Wong, "Packet reservation multiple access in a metropolitan microcellular radio environment," *IEEE J. Select. Areas Commun.*, vol. 11, no. 6, pp. 918-925, Aug. 1993.

[77] W. Wong, "Dynamic allocation of packet reservation multiple access carriers," *IEEE Trans. Veh. Technol.*, vol. 42, no. 4, pp. 385-392, Nov. 1993.

[78] F. Priscoli, G. Picciano and F. Sestini, "Dynamic carrier allocation in a PRMA cellular network," in *Proc. of IEEE GLOBECOM '95*, Singapore, vol. 2, pp. 1157-1161, Nov. 1995.

[79] F. Priscoli, "Basic issues on dynamic allocation of PRMA carriers," in *Proc. of IEEE Int. Conf. on Commun.*, Seattle, WA, pp. 428-432, June, 1995.

[80] S. Nanda and D. Goodman, "Dynamic resource acquisition: Distributed carrier allocation for TDMA cellular systems," in *Proc. of IEEE GLOBECOM '91*, pp. 883-889, 1991.

[81] H. Furukawa and A. Yoshihiko, "A self-organized reuse-partitioning dynamic channel assignment scheme with quality power control," in *Proc. of IEEE Pers. Indoor and Mobile Radio Commun. Conf.*, Toronto, Canada, vol. 2, pp. 562-566, 1995.

[82] R. Guerin, "Channel occupancy time distribution in a cellular radio system," *IEEE Trans. Veh. Technol.*, vol. VT-35, pp. 89-99, Aug. 1987.

[83] R. Thomas, H. Gilbert and G. Mazziotto, "Influence of the movement of the mobile station on the performance of a radio cellular network," in *Proc. of 3rd Nordic Seminar*, Copenhagen, Paper 9.4, Sept. 1988.

[84] H. Xie and D. Goodman, "Mobility models and biased sampling problem," *in Proc. of IEEE Int. Conf. Universal Pers. Commun.*, Ottawa, Canada, pp. 803-807, 1993.

[85] L. Kleinrock, *Queueing Systems*, vol 1: Theory. New York: John Wiley & Sons, 1975.

[86] D. Hong and S. Rappaport, "Traffic model and performance analysis for cellular mobile radio telephone systems with prioritized and nonprioritized handoff procedures," *IEEE Trans.*

Vech. Technol., vol. VT-35, no. 3, pp. 77-92, Aug. 1986.

[87] H. Xie and S. Kuek, "Priority handoff analysis," in *Proc. of IEEE Veh. Technol. Conf.*, pp. 855-858, 1993.

[88] K. Yeung and S. Nanda, "Channel management in microcell/macrocell cellular radio systems," *IEEE Trans. Vech. Technol.,* vol. 45, no. 4, pp. 601-612, Nov. 1996.

[89] T. Chu and S. Rappaport, "Overlapping coverage and channel rearrangement in microcellular communication systems," *IEE-Proc.-Commun.*, vol. 142, no. 5, pp. 323-332, Oct 1995.

[90] C. Baugh, E. Laborde, V. Pandey and V. Varma, "Personal access communications system: fixed wireless local loop and mobile configurations and services," *Proceedings of the IEEE*, vol. 86, no. 7, July 1998.

[91] M. Zonoozi and P. Dassanayake, "User mobility modeling and characterization of mobility patterns," *IEEE J. on Sel. Areas in Comm.*, vol. 15, no. 7, pp. 1239-1252, Sept. 1997.

[92] M. Rajaratnam and F. Takawira, "Hand-off traffic modelling in cellular networks," in *Proc. of IEEE GLOBECOM '97*, Phoenix, Arizona, pp. 131-137, Nov. 1997.

[93] M. Zonoozi, P. Dassanayake and M. Faulkner, "Effect of mobility on the traffic analysis in cellular mobile networks," in *Proc. of IEEE Int. Conf. Networks & Info. Eng.*, Singapore, pp. 407-410, July 1995.

[94] P. Orlik and S. Rappaport, "A model for teletraffic performance and channel holding time characterization in wireless cellular communication with general session and dwell time distributions," *IEEE J. on Sel. Areas in Comm.*, vol. 16, no. 5, pp. 788-803, June 1998.

[95] C. Jedrzycki and V. C. M. Leung, "Probability distribution of channel holding time in cellular telephony systems," in *Proc. of IEEE Veh. Technol. Conf.*, Atlanta, Georgia, pp. 247-251, May 1996.

[96] J. Sanchez, F. Barcelo and J. Jordan, "Inter-arrival time distribution for channel arrivals in cellular telephony," *Electronics Letter*, vol. 34, no. 2, pp. 146-147, 1998.

[97] S. Kuek and W. Wong, "Ordered dynamic channel assignment scheme with reassignment in highway microcells," *IEEE Trans. Vech. Technol.*, vol. 41, no. 3, pp. 271-277, Aug. 1992.

[98] J. Engel and M. Peritsky, "Statistically-Optimum dynamic server assignment in systems with interfering servers," *IEEE Trans. Vech. Technol.*, Vol. VT-22, no. 4, pp. 203-209, Aug. 1973.